

T L
508
A21
113
REF

THE CAA VHF OMNIRANGE

By
H C Hurley, S R Anderson
and H F Keary

Electronics Division

Technical Development Report No 113



CIVIL AERONAUTICS ADMINISTRATION
TECHNICAL DEVELOPMENT AND
EVALUATION CENTER
INDIANAPOLIS, INDIANA

June 1950

1387

Call Library

TABLE OF CONTENTS

	Page
SUMMARY	1
INTRODUCTION	1
GROUND STATION EQUIPMENT	2
AIRBORNE EQUIPMENT	29
OMNIRANGE OPERATIONAL CHARACTERISTICS	50
CONCLUSIONS	62

Manuscript received, January 1949

THE CAA VHF OMNIRANGE

SUMMARY

This report describes the development of a VHF omnirange system operating in the frequency band of 112 to 118 Mc. The range furnishes magnetic bearing information with respect to the range station and provides definite track guidance between the station and any point within its service area.

The omnirange produces two 30 cps signals, one is constant in phase and independent of the aircraft's position, and the other varies in relative phase directly in accordance with the magnetic bearing of the aircraft from the station. A phase-measuring device in the receiver enables the pilot to determine his magnetic bearing with respect to the station and to select and fly a range course on any desired magnetic bearing.

The accuracy of the system in operation at the CAA Technical Development and Evaluation Center, Indianapolis, Indiana, including the receiver plus ground equipment is approximately $\pm 1.5^\circ$. The ground equipment has been in continuous operation for more than three years.

The VHF omnirange has been selected as part of the common Civil-Military System, Transition Program as recommended by the Radio Technical Commission for Aeronautics, report on Air Traffic Control prepared by Special Committee 31.

INTRODUCTION

In planning a system of airways to provide a means of navigation for all aircraft, and to provide facilities for the separation and maintenance of a continuous flow of a large volume of traffic, it becomes apparent that radio ranges defining courses of tracks in only a few directions are not adequate to the task.

There are as many as six air routes converging on some of our air terminals under present operations, and it is likely that this number will be greatly exceeded under anticipated conditions of an expanded air commerce. To serve adequately such terminals with two-course ranges or four-course ranges would require such a multiplicity of stations as to be obviously impractical.

The CAA has carried out the development of two-course visual, two-course aural VHF ranges in accordance with recommendations made by the RTCA in the summer of 1939. Development was completed early in 1942, but the conversion of the airways to VHF range operation was interrupted by the war. Just prior to 1945, however, the conversion program was resumed on a limited scale with the establishment of the Chicago-New York VHF airway. Simultaneously, the CAA had been working on the development of a VHF omnidirectional radio range, along the principles proposed by Dr. D. G. C. Luck of RCA, at the Kansas City meeting of the RTCA in the summer of 1939. Progress on this development had taken such a promising turn that two-course VHF ranges were rapidly superseded by omnidirectional VHF ranges, more commonly referred to as omniranges.

The general principle of the omnirange dates back to Lee de Forest, who proposed rotating a radio beam keyed to identify the sectors forming the 360° sweep of the beam.¹ Another omnirange was developed, using a rotating beam, but with a nondirectional signal transmitted each time the beam passed through North.² The beam rotated clockwise so that the time interval between the omnisignal and the beam alignment with the observer, measured by means of a stop watch, would be a measure of the observer's azimuth. A practical form of this type of range was developed in England by rotating a loop antenna.³ Later this rotation was accomplished electrically.⁴ Others proposed purely

¹U. S. Patent No. 833,034, 1906.

²J. Zenneck (Trans. Seelig) "Wireless Telegraphy," McGraw-Hill, New York 1915, p. 368.

³T. H. Gill and N. F. S. Hecht, "Rotating Loop Radio Transmitters and Their Applications to Direction-Finding and Navigation," Jour. Inst. Elect. Engr., Vol. 66, 1928, p. 256.

⁴H. A. Thomas, "A Method of Exciting the Aerial System of a Rotating Radio Beacon," Jour. Inst. Elec. Engr., Vol. 77, 1935, p. 285.

electrical means of rotating a field pattern for use in an omnirange ^{5, 6, 7} The omnirange developed by the Radio Corporation of America was described in a paper by D G C Luck ⁸ In a paper ⁹ presented before the RTCA annual meeting, January 1945, D M Stuart, Director, Office of Technical Development, described an early model of the CAA omnirange

The present omnirange has elements in common with other types of radio ranges and direction finding systems, and represents a refinement in practice rather than a fundamental departure in principle It may be likened to the standard four-course aural radio range with a means provided for precisely determining the ratio of the two signals at any point, and thereby the azimuth from the station at any point, rather than at points lying only on certain specific courses where the signal ratio is unity

The antenna system is the familiar arrangement of five radiating elements located at the corners and the center of a square, which is so widely employed in direction finding and radio range systems Opposite pairs of antennas are operated 180° out of phase, and the electrical spacing between the elements is small compared to the wavelength, so that a figure-of-eight field pattern results This field pattern is rotated, so to speak, by means of a capacity goniometer which is driven by a synchronous motor at 1,800 rpm The rotating goniometer acts as a balanced modulator, eliminating the carrier frequency, and supplying sideband energy at carrier frequency ± 30 cps to the two antenna pairs Since the entire field is, in effect, rotated once for each rotation of the goniometer, it is

obvious that each direction in space will have a certain phase of the rotational frequency associated with it, and that this phase will change degree for degree with a change in azimuth relative to the station If then we have a signal supplying a 30 cps voltage of reference phase which is independent of azimuth, we can determine a azimuth from the station by comparing the phase of the two 30 cps signals

The purpose of this report is to present a detailed technical description of the latest CAA omnirange system and to indicate what improvements have been made over the earlier model

GROUND STATION EQUIPMENT

General

A block diagram of the essential components of the ground station transmitting equipment is shown in Fig 1 A conventional VHF transmitter has its final stage amplitude modulated by a subcarrier and simultaneous voice The subcarrier itself is frequency modulated at 30 cps The output from the final stage is fed to the center antenna of the 5-loop array and also to the input of the modulation eliminator A goniometer functions as a mechanical sideband generator and delivers 30 cps sideband energy to its output circuits Output No 1 of the goniometer delivers 30 cps sideband energy of 0° audio phase to one pair of diagonally opposite loop antennas Output No 2 of the goniometer feeds 30 cps sideband energy of 90° audio phase to a second pair of diagonally opposite loops The four antennas are arranged in the form of a square around the center loop antenna and fed in such a manner as to produce two figure-of-eight field patterns The two figure-of-eight patterns are in both space and time phase quadrature and can be visualized as a single figure-of-eight pattern with a positive lobe and negative lobe rotating at an audio rate of 30 cps, which, produces amplitude modulation (in space) of the main rf carrier, transmitted from the center antenna This energy, when detected in a suitably designed receiver, is known as the "variable phase" signal The 30 cps signal produced in the receiver from the frequency modulated subcarrier is termed the "reference phase" signal The purpose of the subcarrier modulation is to provide a means of discrim-

⁵P H Evans and J W Grieg, U S Patent No 1,933,248, 1933

⁶J W Grieg, U S Patent No 1,988,006, 1935

⁷G H Brown and D G C Luck, U S Patent No 2,112,824, 1938

⁸D G C Luck, "An Omnidirectional Radio-Range System," Part I, RCA Review, Vol VI, No 1, July 1941, Part II, RCA Review, Vol VI, No 3, January 1942

⁹D M Stuart, "The Omnidirectional Range " Presented before the RTCA Annual Meeting, January 1945, and later published in Aero Digest, June 15, 1945

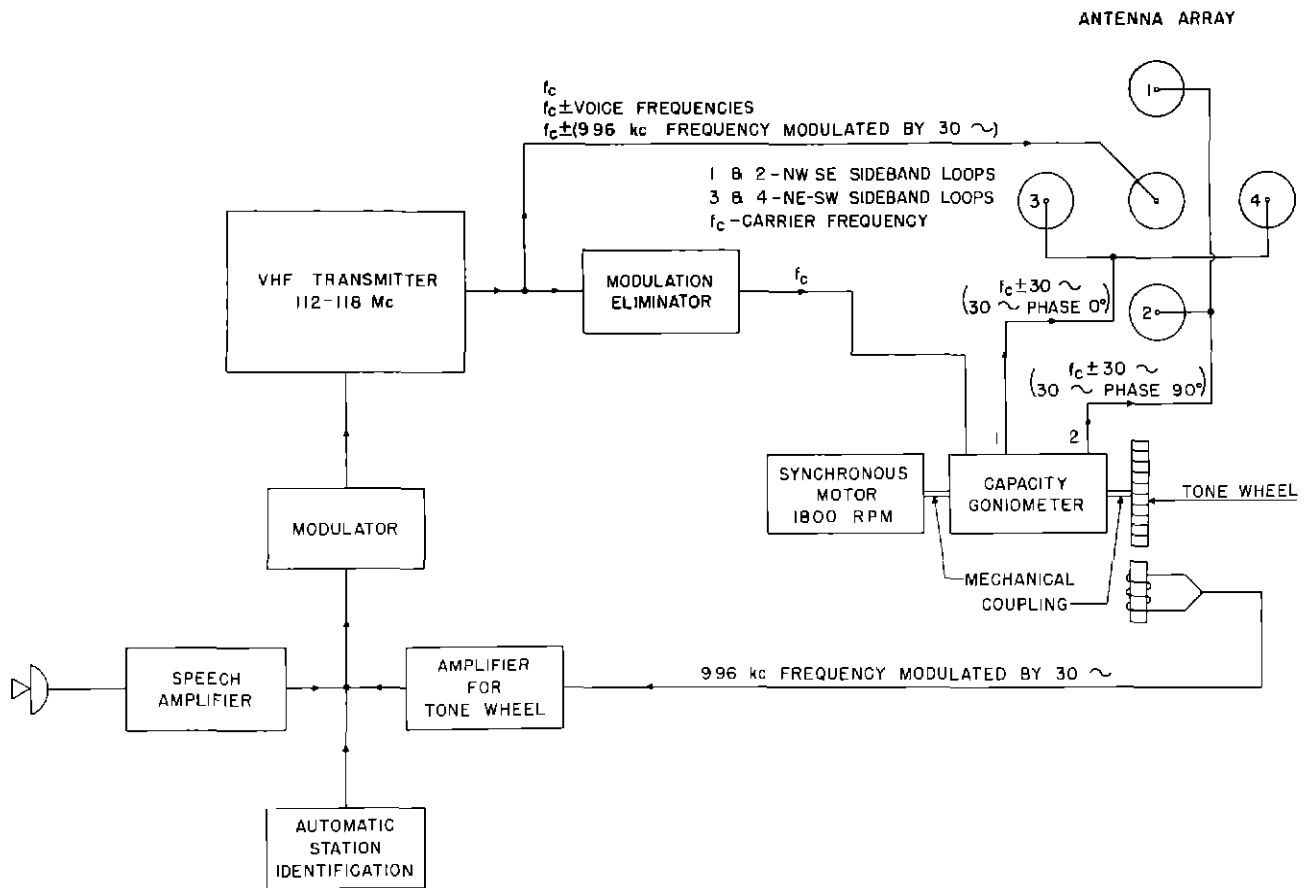


Fig 1 Block Diagram of VHF Omnidirectional Transmitting Equipment

inating between the two 30 cps voltages in the receiver

Fig 2 is a view of a CAA omnidirectional ground facility using a 30-foot tower. The antenna array is located inside the cylindrical housing on the tower. The transmitters and associated equipment located in the building on the ground are shown in Fig 3. Approximately half the equipment is "standby" to permit maintenance while providing continuous service.

Antenna Array

The polarization most desirable for an omnidirectional operating in the 100 Mc region of the radio spectrum was determined by experiment. The first CAA omnidirectional was intended to produce horizontal polarization. However, the difficulties encountered with an antenna array designed for this purpose led to the design and testing of two simpler vertically polarized arrays.¹⁰ An improved horizontally polarized array also was developed and

carefully flight tested during 1945.¹¹ All three arrays were tested at the same site, under identical conditions, using the same aircraft. The two vertically polarized arrays produced approximately the same amount of scalloping,¹² while the horizontally polarized array produced approximately one-fourth as much

¹⁰S. R. Anderson and H. F. Keary, "Comparison Flight Tests Between Omnidirectional Radio Range Antenna Arrays," CAA Unpublished Memorandum, December 19, 1944.

¹¹S. R. Anderson and H. F. Keary, "Six-loop Omnidirectional Radio Range Flight Tests," CAA Unpublished Memorandum, May 15, 1945.

¹²Scalloping is defined as the amplitude of the course deviation indicator's fluctuations due to the effect of reflections from trees, buildings, wires, the earth's surface, etc.

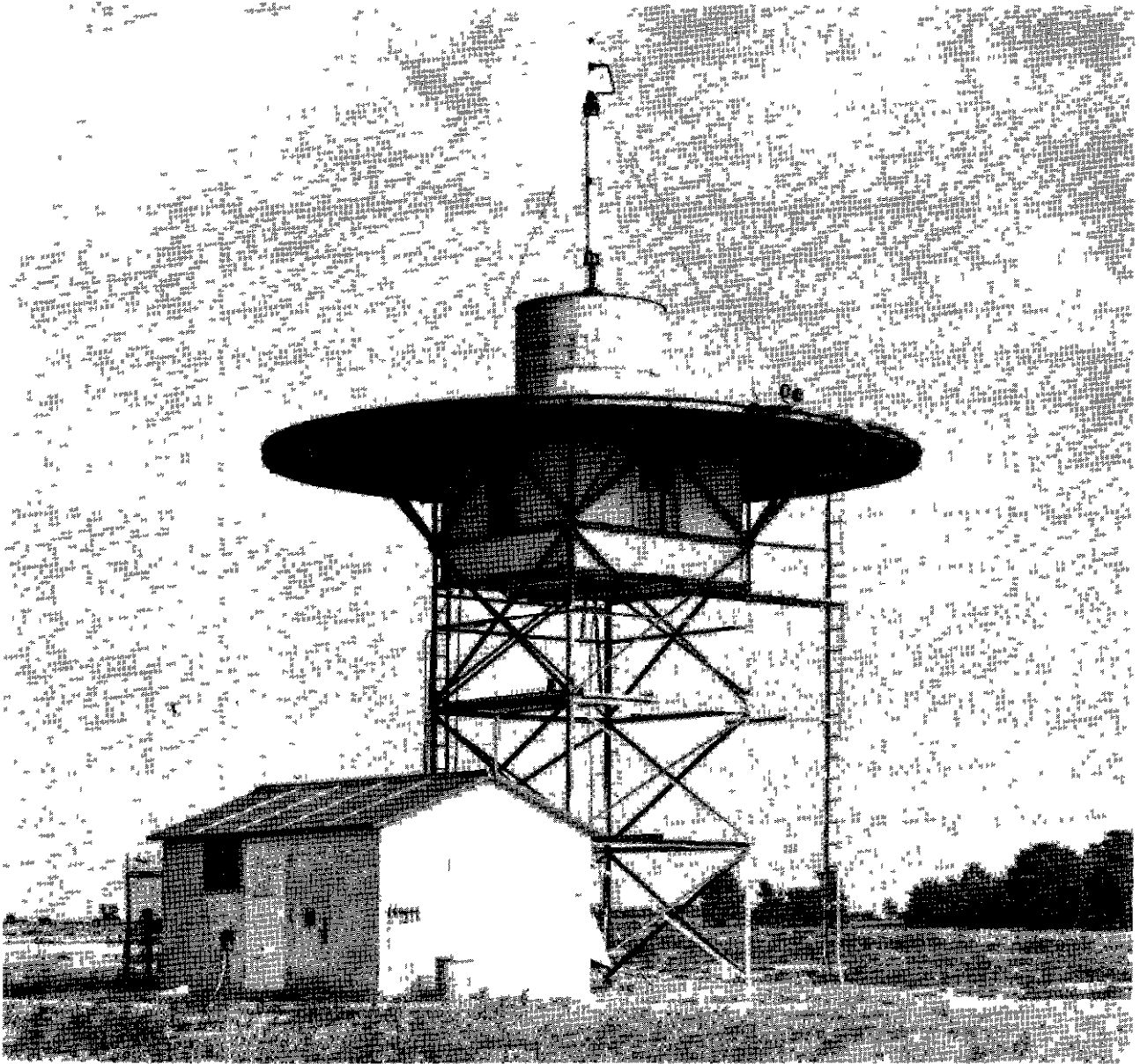


Fig 2 Omnirange Ground Facility

scalloping as either of the vertically polarized arrays. The maximum amount of scalloping was $\pm 3^\circ$ for the vertically polarized arrays and $\pm 0.7^\circ$ for the horizontally polarized array. The site used for these tests was considered to be better than average. Trees probably caused the scalloping which was observed.

The polarization used in the present omnirange system is horizontal, as a result of conclusions drawn from the early comparison tests. The arrangement of the loop radiators is shown in Fig 4. The approximate shape of the horizontal plane field pat-

terns produced by the antenna array is illustrated in Fig 5. The pair of antennas with currents I_1 produces the figure-of-eight pattern E_{SB1} . Similarly, the pair of antennas with currents I_2 produces the pattern E_{SB2} . It can be shown that, in free space, the electric field intensity is represented by

$$E_{SB1} = \left[\frac{K_1}{r} e^{-jGr} I_B \sin \theta \sin (Gb \cos \theta) \sin \rho t \sin (GS \sin \phi \sin \theta) \right] \quad (1)$$

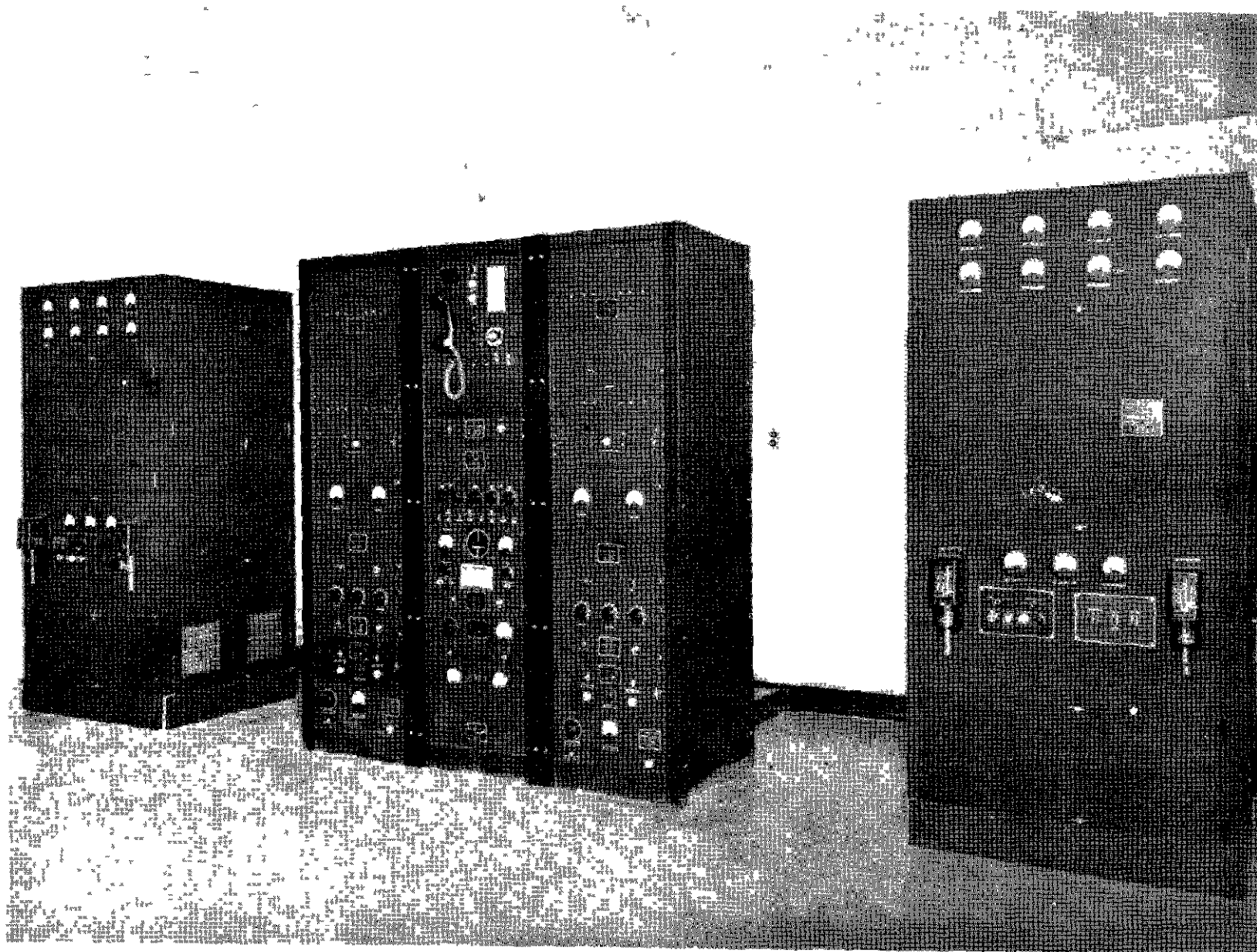
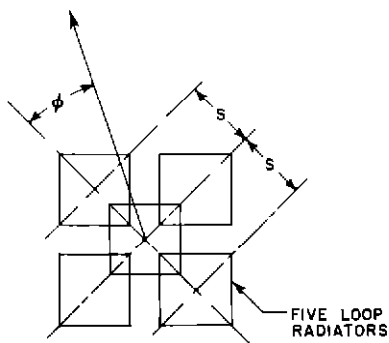


Fig 3 Omnirange Transmitting Equipment



$S = 16'$
 $b = 48'$
 $h = 63 \frac{3}{8}'$

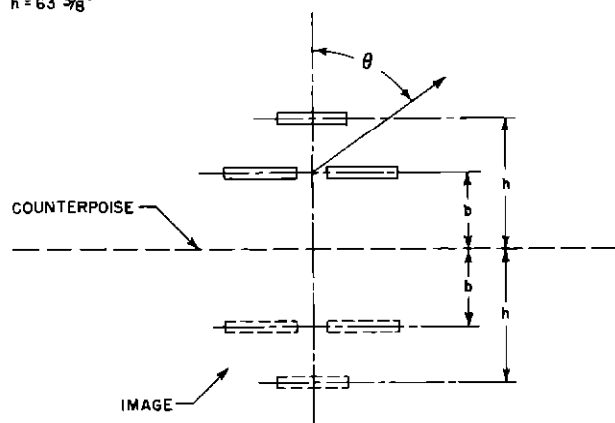


Fig 4 Mechanical Layout of Omnirange Antenna Array

similarly

$$E_{SB2} = \left[\frac{K_1}{r} e^{-jGr} I_B \sin \theta \sin (Gb \cos \theta) \cos \rho t \sin (Gs \cos \phi \sin \theta) \right] \quad (2)$$

where

$$G = \frac{2\pi}{\lambda}$$

$\frac{\rho}{2\pi}$ = modulation frequency (variable phase signal)

K_1 = a constant determined by the units

t = time

r = distance from the radiating system to the receiver

λ = wavelength of the carrier

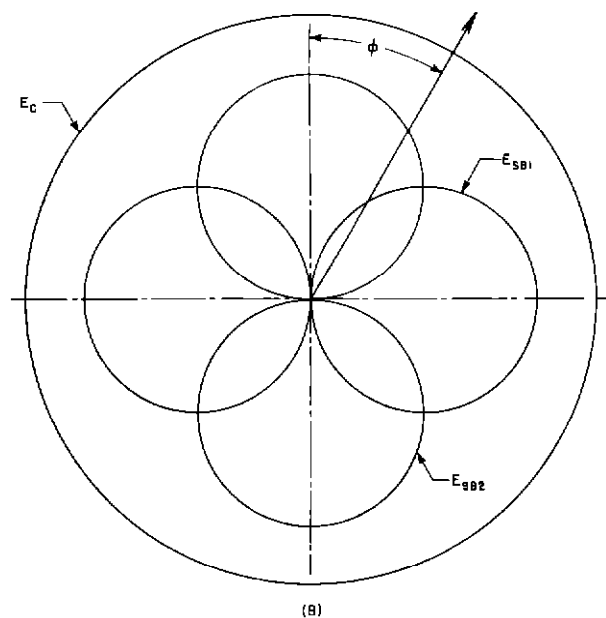
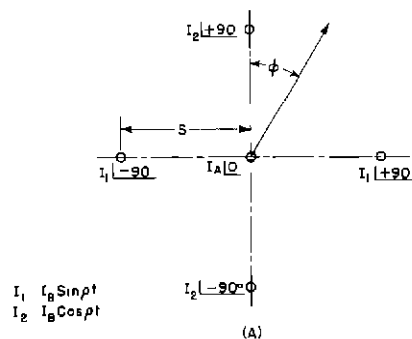


Fig 5 Currents of Radiators and Theoretical Horizontal Plane Field Patterns

h, s, b, ϕ and θ are shown in Fig 4

I_A = maximum rms current in the carrier antenna

I_B = maximum rms current in each sideband antenna

The center antenna produces the circular pattern of Fig 5(B), which is expressed by

$$E_C = \frac{-K_1}{r} I_A e^{-jGr} \sin \theta \sin (Gh \cos \theta) \quad (3)$$

The electric field intensity in the vicinity of the aircraft due to all five antennas is the resultant of the fields produced by each di-

agonal pair of antennas and the center antenna as follows

$$E_t = E_c + E_{SB1} + E_{SB2} \quad (4)$$

$$E_t = \frac{-K_1}{r} e^{-jGr} \sin \theta \left\{ I_A \sin (Gh \cos \theta) - \frac{I_B \sin (Gb \cos \theta) \sqrt{\sin^2 (GS \cos \phi \sin \theta) + \sin^2 (GS \sin \phi \sin \theta)}}{\cos (\rho t - B)} \right\} \quad (5)$$

$$B = \arctan \left[\frac{\sin (GS \sin \phi \sin \theta)}{\sin (GS \cos \phi \sin \theta)} \right] \quad (6)$$

$$M = \left\{ \frac{I_B \sin (Gb \cos \theta)}{I_A \sin (Gh \cos \theta)} \frac{\sqrt{\sin^2 (GS \cos \phi \sin \theta) + \sin^2 (GS \sin \phi \sin \theta)}}{\cos (\rho t - B)} \right\} \quad (7)$$

Equation (5) may be rewritten

$$E_t = \frac{-K_1}{r} e^{-jGr} \sin \theta I_A \sin (Gh \cos \theta) \left\{ 1 - M \cos (\rho t - B) \right\} \quad (8)$$

Equation (8) is an expression of an amplitude modulated wave, the modulation frequency of which is $\frac{\rho}{2\pi}$. The most significant characteristic about this amplitude modulated wave is the phase angle of the modulation frequency B , which varies with ϕ according to equation (6)

If $GS \rightarrow 0$

$$B = \arctan \left[\frac{GS \sin \phi \sin \theta}{GS \cos \phi \sin \theta} \right] = \phi \quad (9)$$

Hence for small values of GS , a measure of electrical phase angle is a direct measure of azimuth angle. The modulation percentage of the amplitude modulated wave is equal to $|M| \times 100$. From equation (7) it can be seen that the variable phase modulation percentage is a function of the position of the aircraft. Fig. 6 shows how the variable phase modulation percentage varies with vertical angle and bearing angle. The dashed curves are for parameters used on the CAA VHF omnirange array at the present time. Fig. 7 is a plot of $B-\phi$, using equation (6) for the present antenna array. The terms "course

errors", "errors" or the equivalent as used throughout this report refer to deviation from the correct reading, and are not to be confused with observational or random errors.

The diagonal spacing between each pair of sideband antennas is 32 in. Each sideband antenna is mounted on top of a pedestal 48 in. above the counterpoise. The carrier antenna also is supported by a pedestal 63 3/8 in. above the counterpoise. The spacing between adjacent sideband antenna sides is 3 in. and the sideband antennas are symmetrically disposed around the carrier antenna. It is important that the sideband antennas be properly oriented with respect to each other and to the carrier antenna. A template is usually provided to accomplish this purpose. The five pedestals supporting the loop antennas are mounted on a circular base plate 40 in. in diameter. The base plate can be rotated through a 360° angle.

Three rf receptacles are mounted directly under each loop transposition, see Fig. 8. Two of the receptacles are connected directly to the transposition. Rf power is fed to the loop antennas through Type RG 8/U solid dielectric coaxial cable. Since the loop antenna is a balanced circuit, it is necessary to convert from unbalanced to balanced line in order to feed the loop in the proper manner. The conversion is accomplished by the use of a 180° section of RG 8/U unbalanced line.

Diagonally opposite pairs of sideband antennas are connected through 350° lengths of RG 8/U cable and excited 180° out of phase. This line length was found to be optimum at 115 Mc for minimum parasitic currents in the sideband antennas, induced therein by the center antenna. The 180° phase relation is obtained by reversing the connections at the transposition in one loop antenna of each diagonal pair. One pair of sideband loops is fed from the goniometer output No. 1 and the second pair of sideband antennas from output No. 2. The center carrier antenna is fed directly from the transmitter output stage by RG 8/U coaxial cable.

Tests conducted to determine the operating characteristics of the VHF loop antennas included field measurements to obtain the horizontal plane patterns, impedance measurements to ascertain impedance matching requirements, rf current measurements to determine current distribution and balance around the periphery of the loop, and measurements of parasitic currents due to inter-

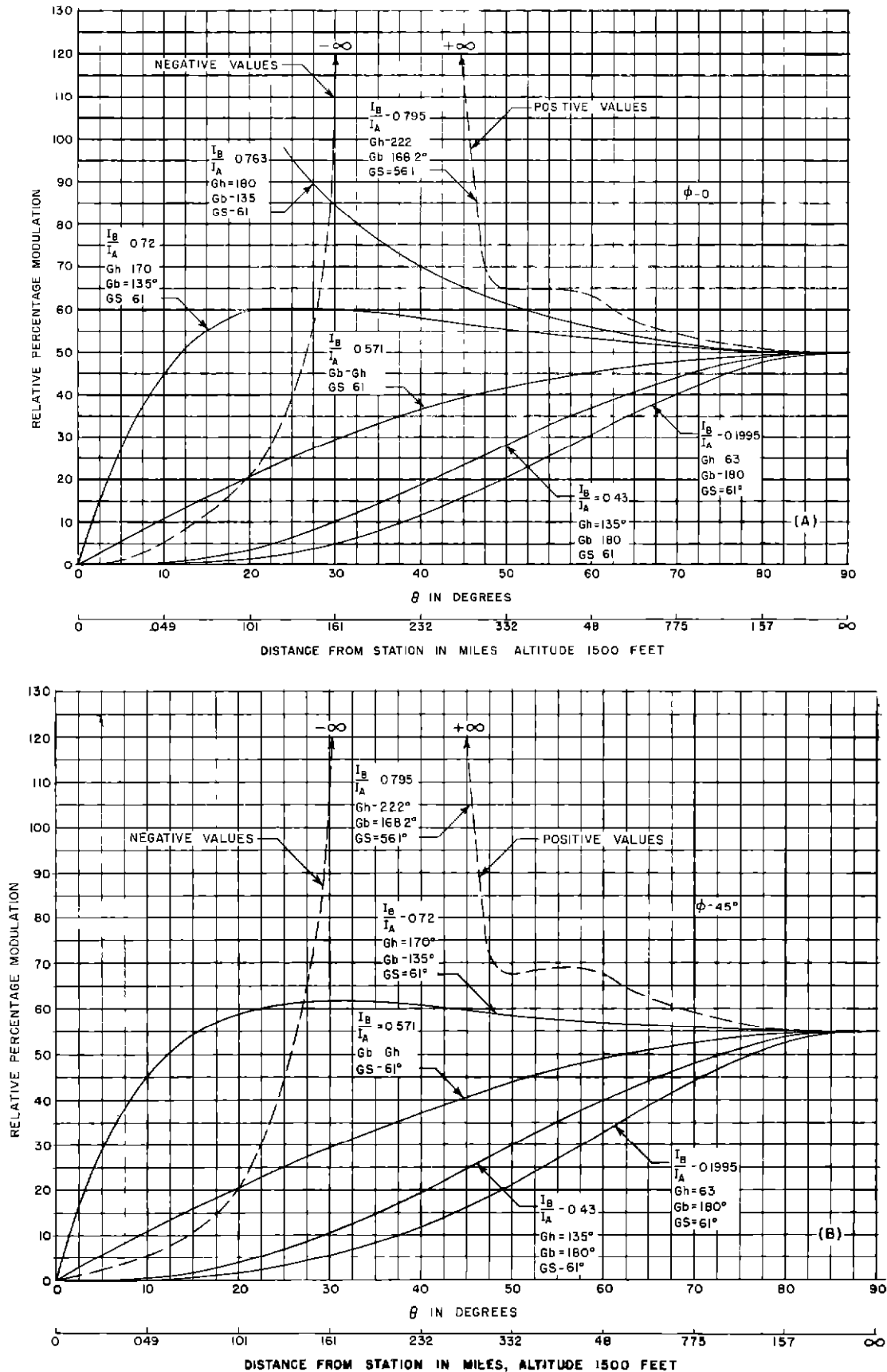


Fig 6 Variable Phase Signal Modulation Percentage Variation Versus Vertical and Bearing Angles

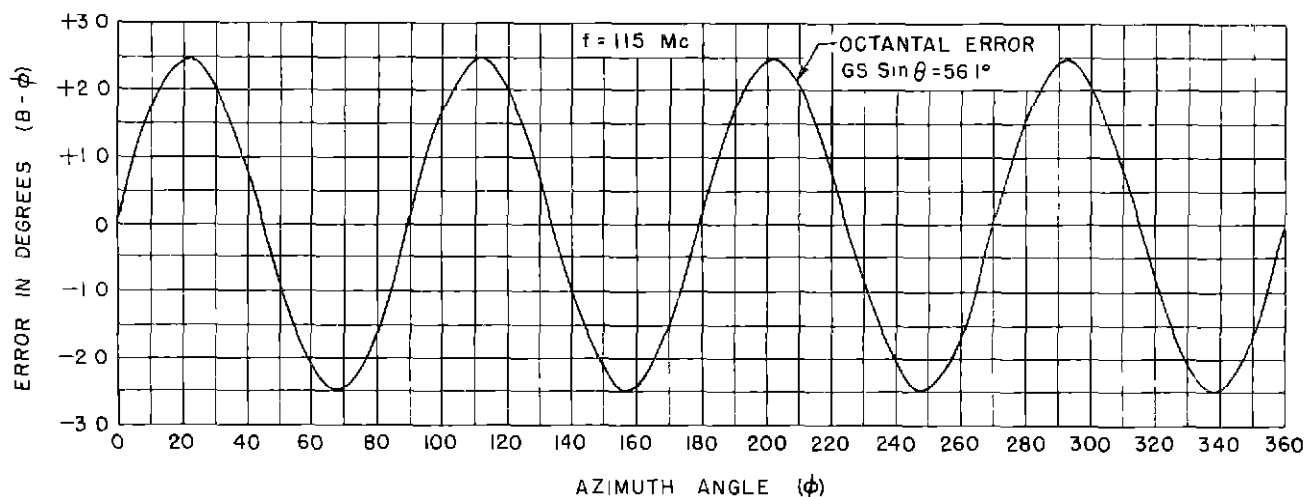


Fig 7 Theoretical Error Variations Versus Azimuth Angle

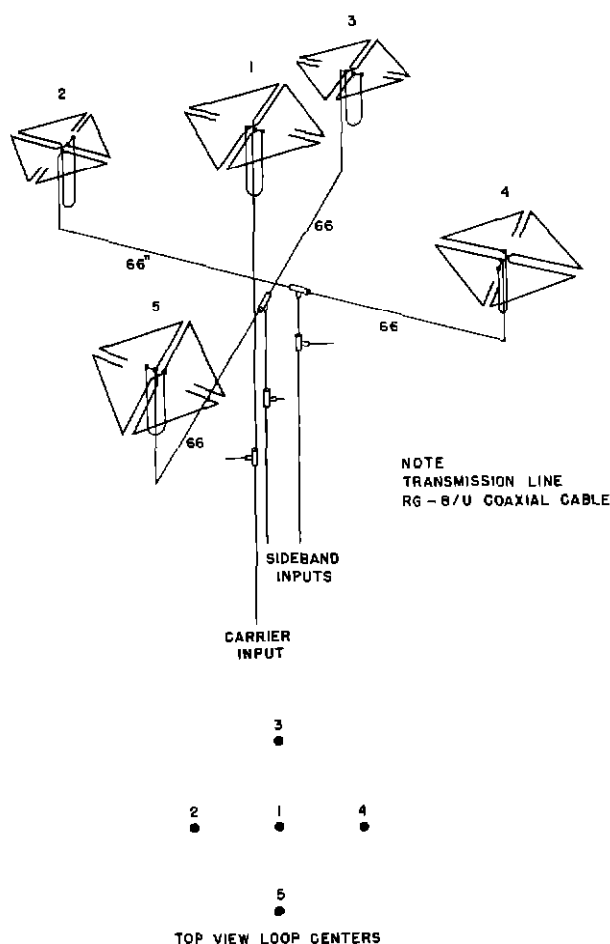


Fig 8 Five-Loop Omnidirectional Antenna and Transmission Line Arrangement

action between loops when grouped together under normal operating conditions. The loop array was mounted at the center of a circular platform elevated about eight feet above ground. Provisions were made to rotate the platform through an angle of 360° . A horizontal dipole connected to a diode was used as a field detector. The field detector was calibrated by locating the instrument about 100 feet from a loop antenna and comparing the diode current with the loop antenna current measured with a closely coupled rf milliammeter. Field intensity measurements were made over the frequency range of 112 to 118 Mc.

The horizontal plane pattern of the center loop antenna was obtained by feeding rf power to the loop and plotting the relative field strength indicated by the field detector for each 10° position of the loop, through 360° . The pattern so obtained is very nearly circular in shape. The maximum field pattern change in terms of maximum field varied from 7.4 per cent at 112 Mc to 1.2 per cent at 116 Mc.

It is desirable to adjust the length of the lines connecting the loops of each sideband pair, refer to Fig 8, for minimum parasitic current which is introduced by the center antenna current. Since a virtual short circuit exists at the T joining the two loops of a pair with respect to parasitic currents, the impedance connected to the T by the goniometer and associated lines will have little effect on the parasitic currents. The length

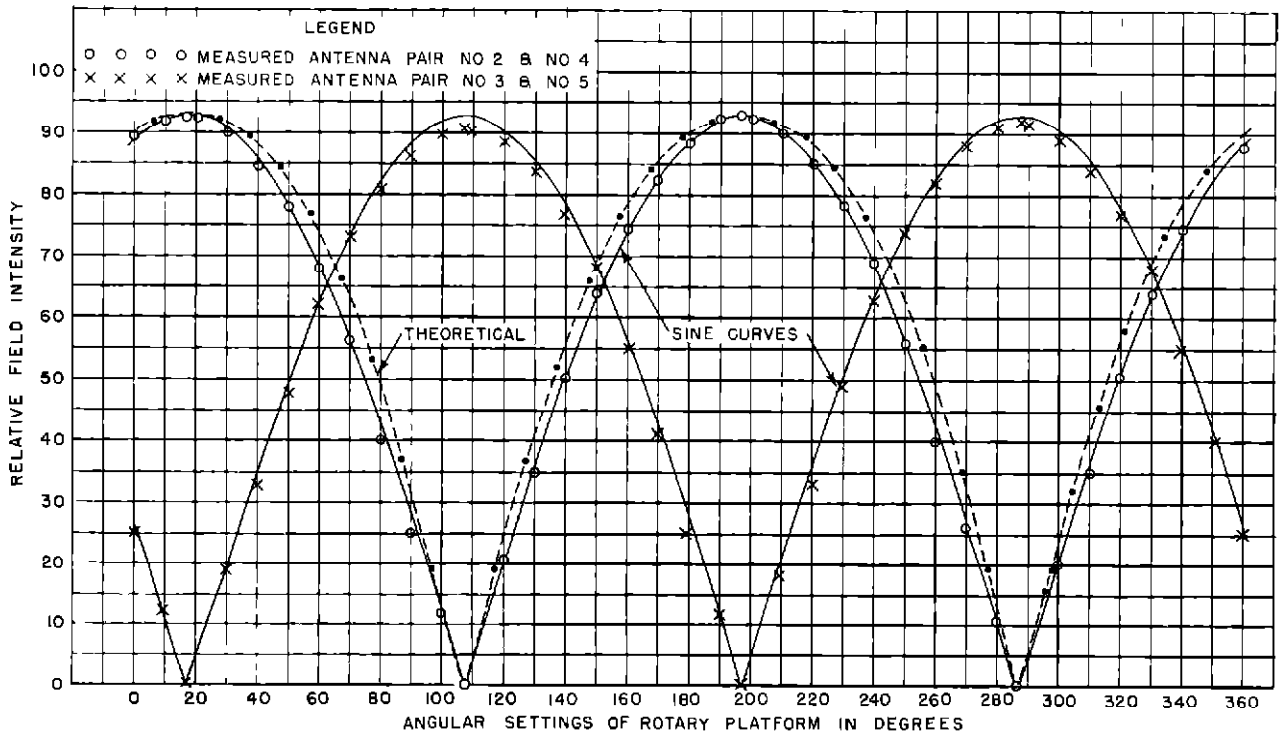


Fig 9 Sideband Loops Horizontal Plane Field Patterns With all Five Loops in Place

of 66 in of Fig 8 was arrived at by trying various lengths until the parasitic currents in the sideband loops reached a minimum. The minimum parasitic current condition was determined at 115.1 Mc, however, the 66 in length was checked throughout the band of omnirange frequencies and found to vary from three per cent of center loop current appearing in each sideband loop at 112.1 Mc to 5.3 per cent at 117.9 Mc.

Since the line lengths joining pairs of loops have been determined, the correct operation of the sideband pairs of loops may be determined prior to any impedance matching. If the current ratio is unity and the phase angle 180° for currents of each pair of radiators, the required conditions for producing the desired field pattern will be met. Conversely, if the field patterns are figure-eight in shape with deep nulls located 180° apart, and if the maxima are displaced 90° from the nulls with amplitudes of equal values, the currents have the correct phase angle and amplitude.

Each sideband pair was energized in turn and relative field strengths measured as the array was rotated through 360° . The re-

sultant data were plotted and are shown in Fig 9. It may be seen from the data that the phase angle between the currents in each pair of sideband loops is 180° and the current ratio is unity. In order to locate the exact position of the nulls for each sideband pair, a sensitive dc microammeter was used to indicate the diode current in the field detector. The loops were excited with approximately 200 w of rf power. The field detector was suitably located to indicate a sharp rise in rectified current when the antennas were rotated to either side of the exact null position. The accuracy of readings was better than 1° .

The center and sideband antennas were matched to their respective transmission lines with the aid of a slotted line and probe. Prior to matching the lines, the probe was adjusted for minimum loading effect on a test line. This was accomplished by terminating the test line in a standard resistive dummy load having a resistance equal to the characteristic impedance of the test line, in this case 52 ohms. The slotted line was simply a section of RG 8/U cable with suitable slots spaced 1 in apart for insertion of the probe. With a vacuum tube voltmeter connected at

one point on the slotted line, the probe was connected to a point along the line about one-half wave from the voltmeter toward the load end. The probe was then adjusted until the voltmeter reading was not affected by the presence of the probe across the line. The standing wave ratio obtained with the standard dummy load termination was approximately 1.02. The center antenna was then checked and produced a standing wave ratio of 6.0 at 115 Mc. Matching was accomplished with a length of 52 ohm line and an open-circuited stub, resulting in a final standing wave ratio of 1.06. The sideband antenna pairs were matched to present identical loads to their respective feed lines. It is important that the loads presented to the sideband feed lines be made as closely alike as possible, otherwise the figure-of-eight amplitudes will not be equal and will produce a quadrantal bearing error.

The antenna array was originally housed in a shelter eight feet square and approximately ten feet high. Wood and masonite materials were used throughout in its construction. The over-all error in the system was found to be approximately 6.5° . This error is typical of a number of flight calibration errors obtained with the receiving equipment in a DC-3 type aircraft, and includes all errors contributed by the ground

station and receiving equipment. When the receiving equipment was removed from the aircraft and set up about one mile from the omnirange, a ground calibration, obtained by rotating the antenna array through 360° , produced an over-all error of 3° .

After a series of tests failed to uncover the discrepancy between flight and ground calibration errors, attention was directed to the antenna shelter as a possible source of error. The shelter was mounted on a circular track to enable its rotation through any desired angle. With the receiving equipment set up approximately one mile distant from the station, the antenna shelter was rotated through 360° . On-course variations were recorded for each 20° of rotation, with the results shown in Fig 10. Figs 11 and 12 show flight calibration errors obtained for different orientations of the antenna shelter with respect to the antenna array. These curves show that the shelter contributed some error to the system. The shelter was then removed and a flight calibration conducted, resulting in an over-all error of 3.5° . A ground calibration taken under similar conditions produced an error of 3.0° .

From the results of all the tests, it was concluded that a change in the configuration of the house was desirable to reduce the error to a minimum. Accordingly, a cylindrical

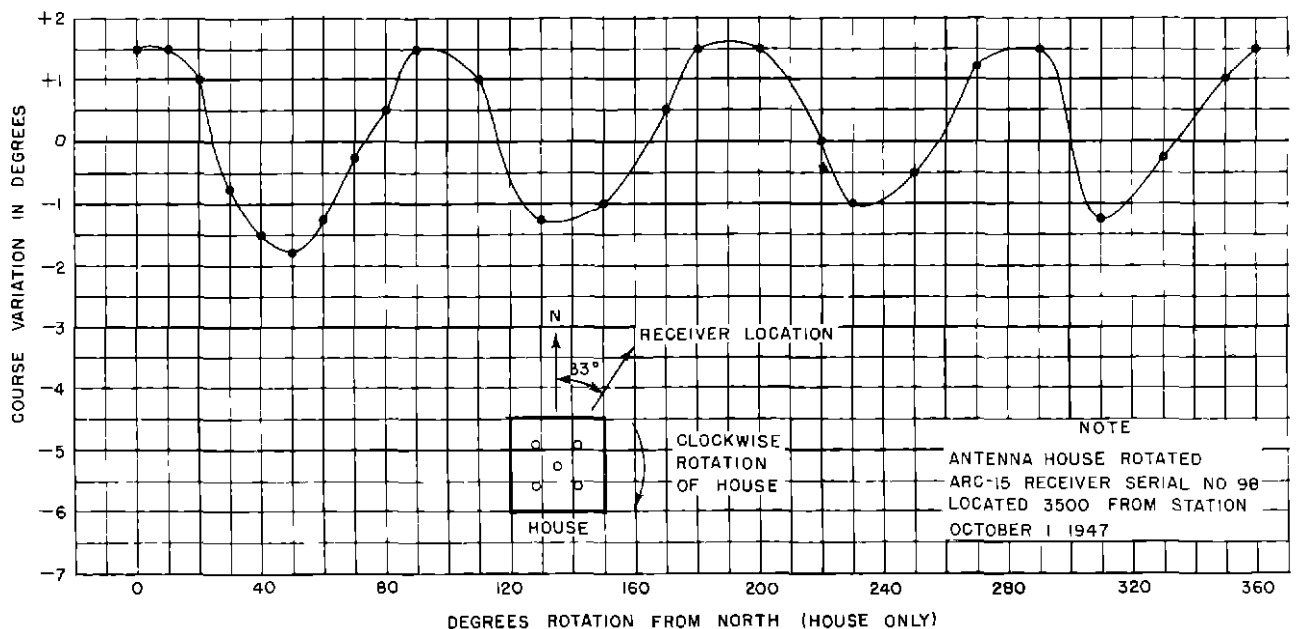


Fig 10 Course Variation Versus Rotation of Shelter

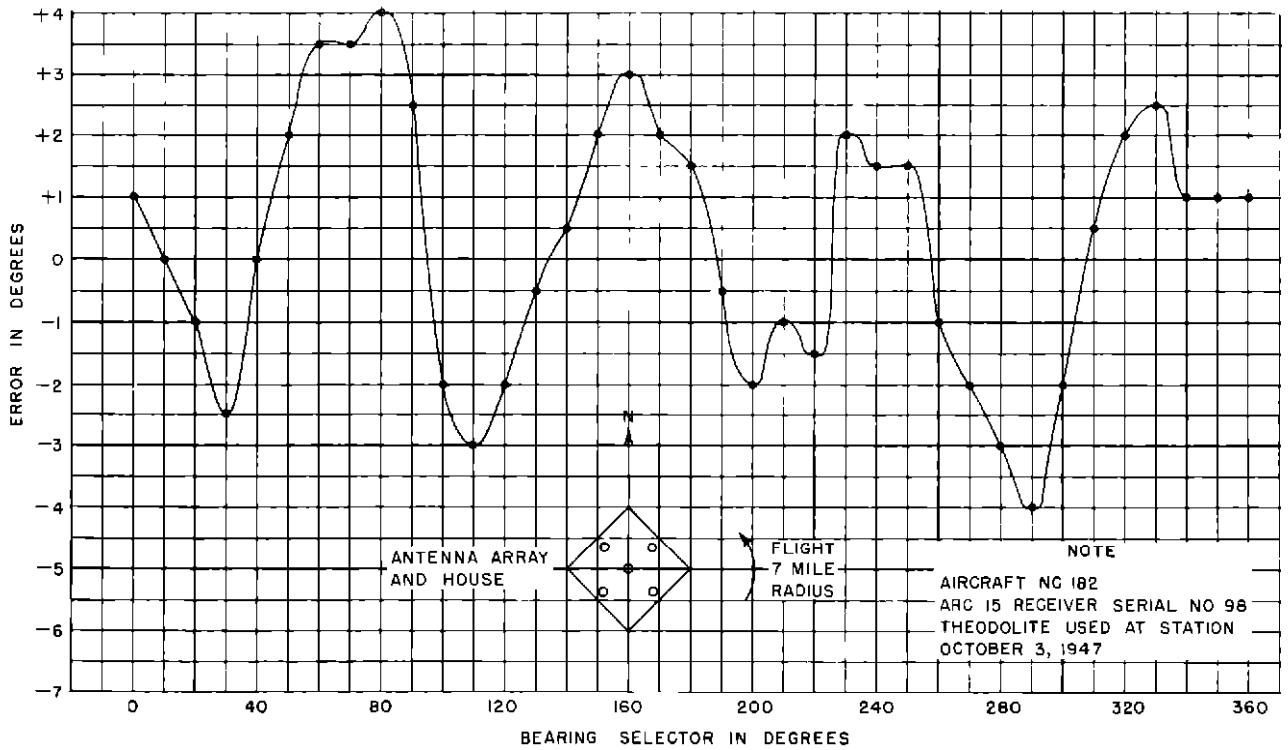


Fig 11 Flight Calibration Error for Shelter Sides Facing 45 Degrees from Cardinal Directions

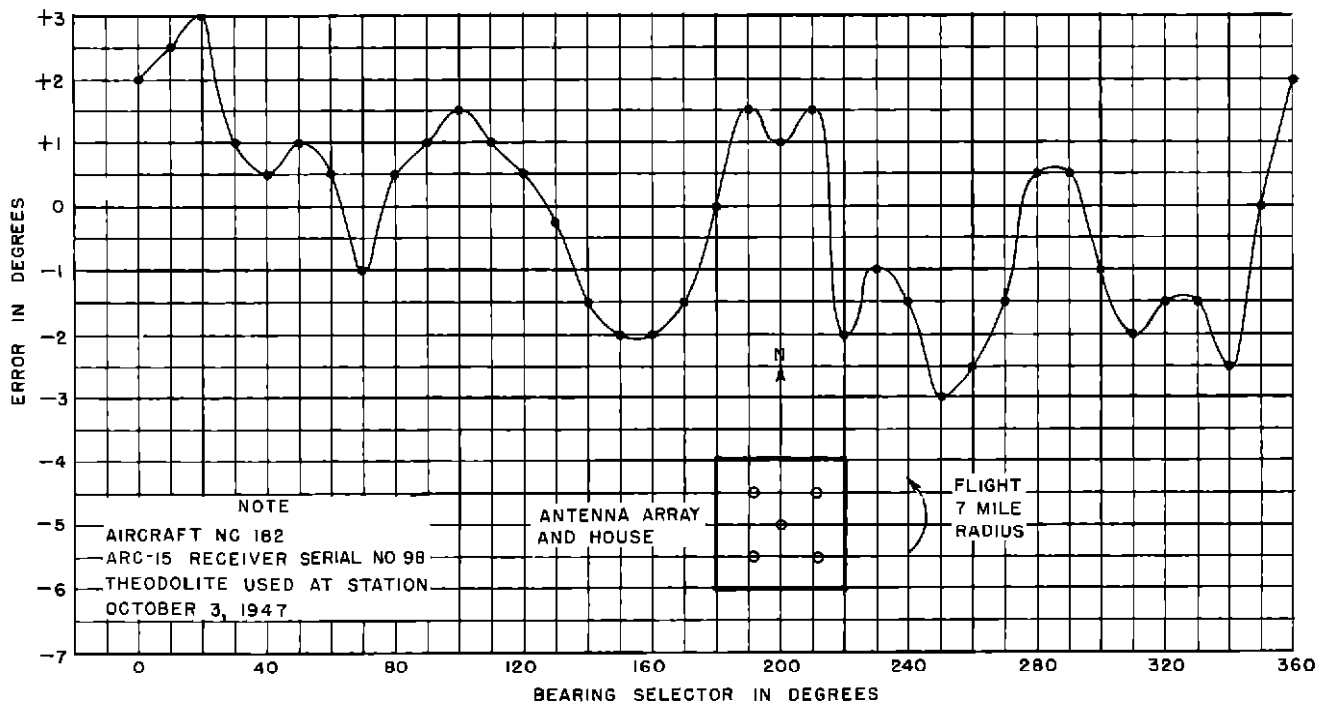


Fig 12 Flight Calibration Error for Shelter Sides Facing Cardinal Directions

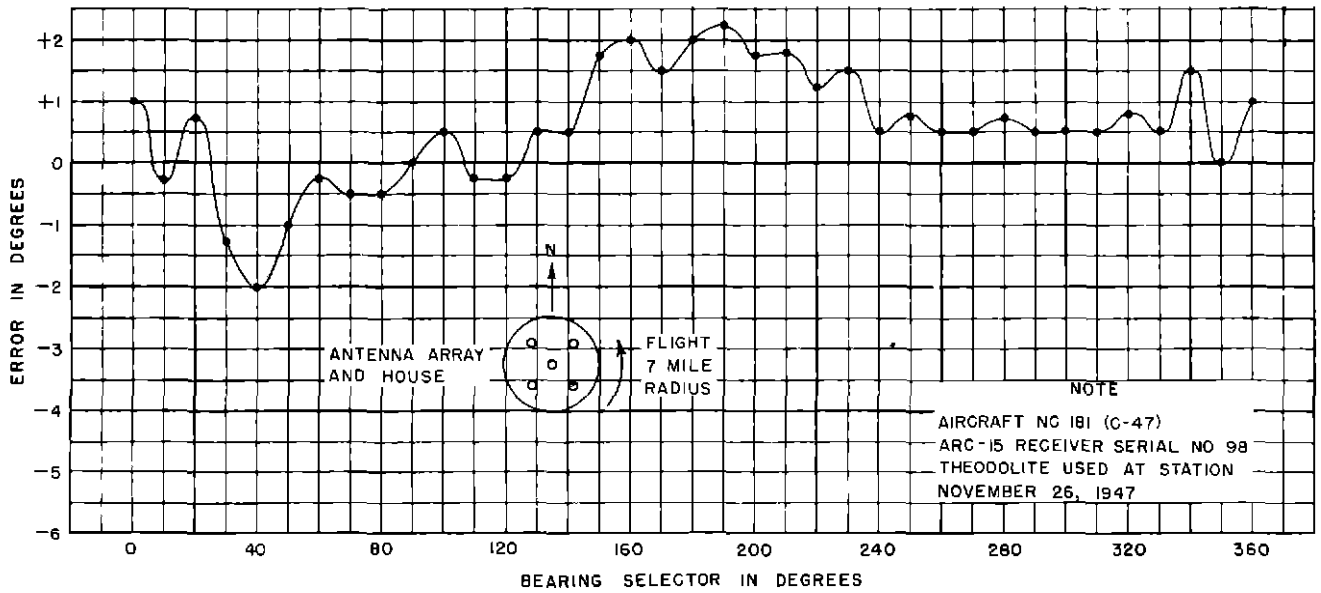


Fig 13 Flight Calibration Error With Cylindrical Shelter Installed

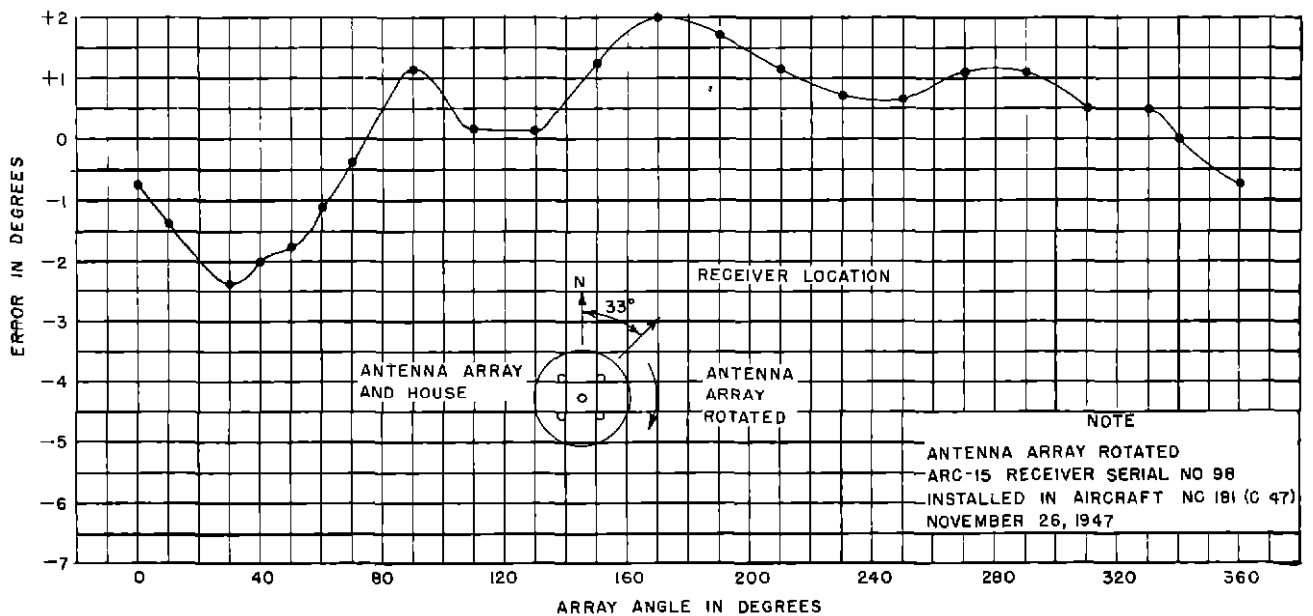


Fig 14 Ground Calibration Error With Cylindrical Shelter Installed

wooden shelter eight feet in diameter and ten feet high was installed. Figs 13 and 14 show the errors measured for flight and ground calibrations with the cylindrical shelter installed. The calibration curves show complete agreement between ground and flight tests with the antennas in a shelter.

Fig 6 shows the expected variation of modulation percentage of the variable phase

signal with vertical angle. Flight tests were conducted to verify the theory and to determine the characteristics of the course while passing over the station. Fig 15 shows reproductions of recordings of the course deviation indicator deflection and the reference and variable phase signals when flying over the omnirange. The level of the variable phase signal is essentially a measure of the

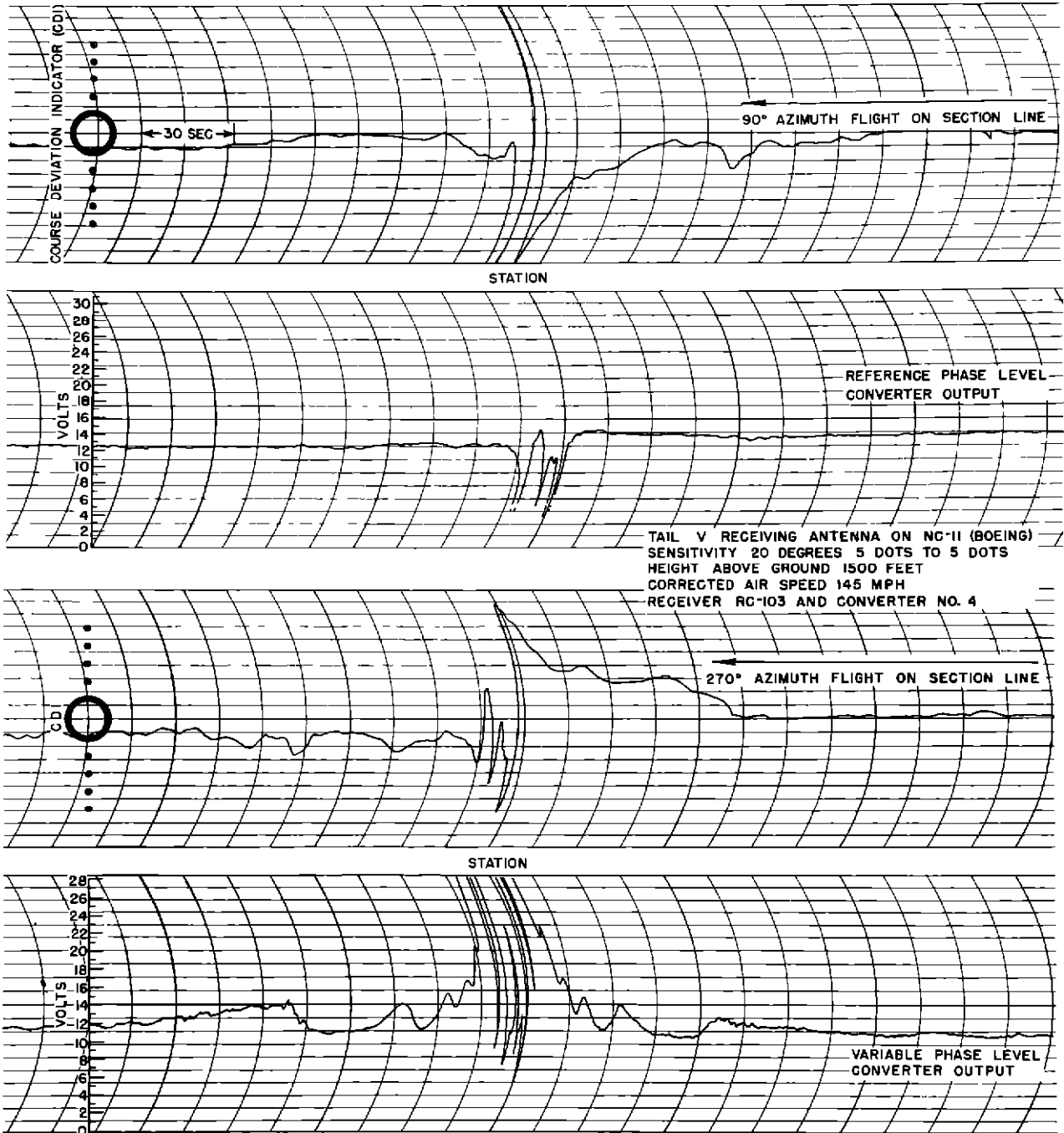


Fig 15 Flight Test Recordings of Variable and Reference Phase Signal Levels and Course Line Deviation Indicator Deflection for Five-Loop Top Center Array

modulation percentage as long as the receiver is in automatic volume control. The modulation percentage increases near the station as predicted by theory, when $G_h = 240^\circ$ and $G_b = 180^\circ$, as shown in Fig 6. It is interesting to note that there are three nulls in the

recording of the reference phase signal. Since the reference phase signal is radiated from the center antenna exclusively, equation (3) accounts for the three nulls since $G_h = 240^\circ$. The middle null is caused by the null of the center loop while the other two nulls are

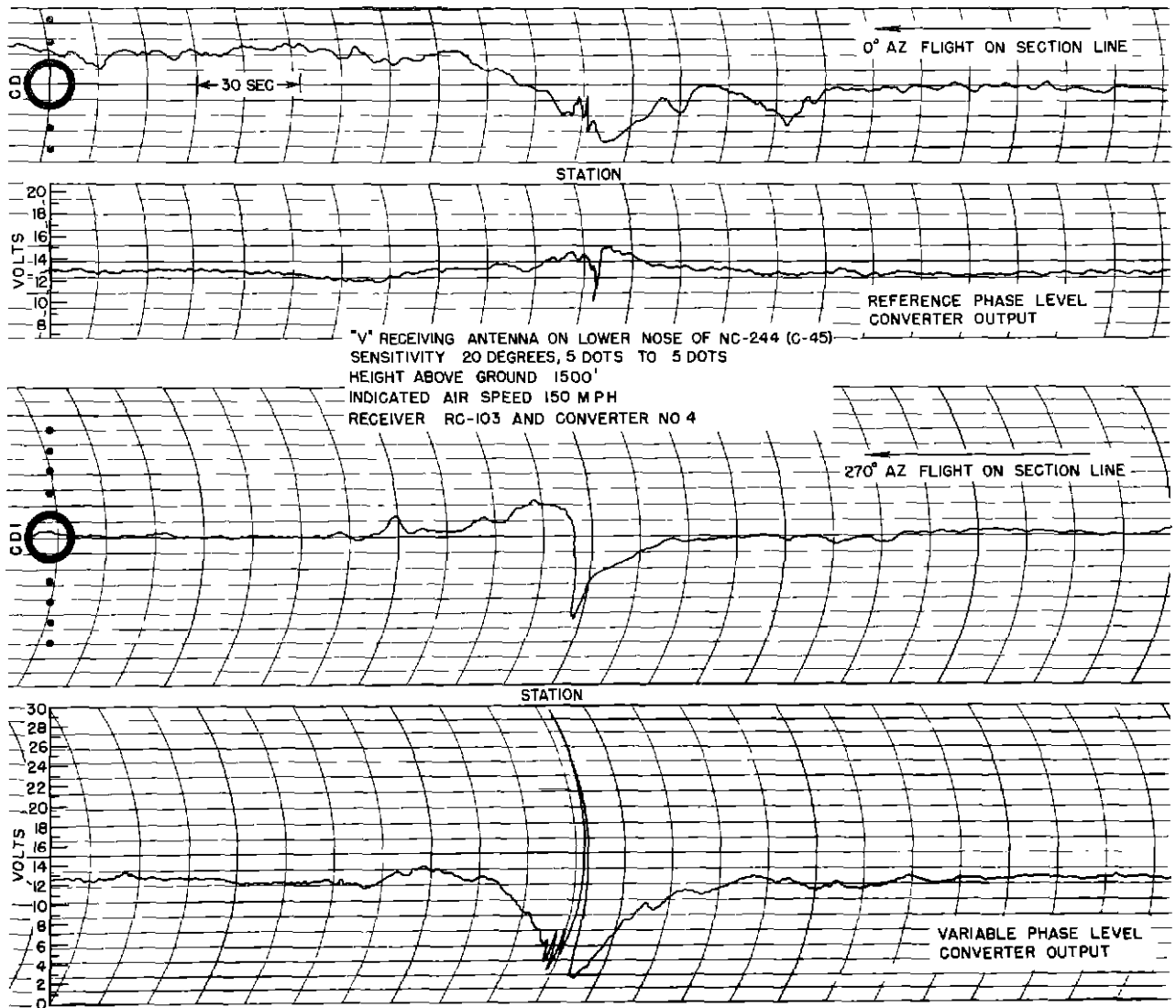


Fig 16 Flight Test Recordings of Variable and Reference Phase Signal Levels and Course Line Deviation Indicator Deflection for Five-Loop Lower Center Array

caused by reflections from the counterpoise. Flight tests were conducted with the center loop of the array lowered to a position below the sideband loops. The dimensions for this mode were $G_h = 120^\circ$ and $G_b = 180^\circ$. Fig 16 shows the deflection of the course line deviation indicator and the reference and variable phase signal levels, as obtained during a flight over the station. The single null would be expected by considering equation (3), where $G_h = 120^\circ$, and the decrease in variable phase signal modulation near the station was predicted by the theory as indicated in Fig 6.

Figs 17 and 18 show the vertical plane field strength pattern of the present omnirange antenna array mounted on 15 and 30 foot high counterpoises, respectively. The measurements were made while flying away from the station and include the pattern of a horizontal V receiving antenna located on top of the vertical stabilizer of a DC-3 airplane. It will be seen that the lobes, at small values of θ , are essentially independent of counterpoise height, because the energy is reflected from the counterpoise instead of the ground. On the other hand, the lobes at large values of θ are dependent upon counterpoise height.

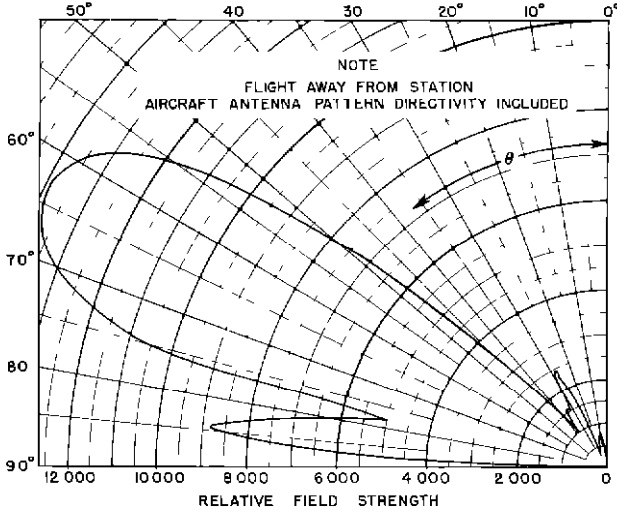


Fig 17 Measured Vertical Plane Field Pattern of Antenna Array Mounted on Counterpoise 15 Feet High

since little energy is reflected from the counterpoise at these angles, and the earth reflects a considerable signal

Goniometer and Subcarrier Generator

The goniometer consists of two mechanical sideband generators on a common drive shaft, rotating at 1,800 rpm. One sideband generator is oriented 90° with respect to the other so that the electrical outputs of the two generators are in phase quadrature at the modulation frequency as shown in Fig 19(A). The important capacities of one of the sideband generators are shown schematically in Fig 19(B). The goniometer plates are shaped in such a way as to make

$$C_1 = K_2 (1 - \cos \rho t) \quad (10)$$

$$C_2 = K_2 (1 + \cos \rho t) \quad (11)$$

for the No 1 sideband generator, and

$$C_3 = K_2 (1 + \sin \rho t) \quad (12)$$

$$C_4 = K_2 (1 - \sin \rho t) \quad (13)$$

for the No 2 sideband generator

where

K_2 = a constant, depending upon the maximum capacity attained between plates

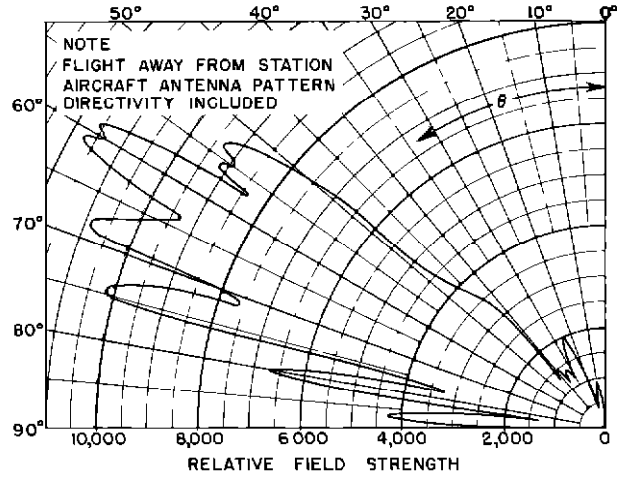


Fig 18 Measured Vertical Plane Field Pattern of Antenna Array Mounted on Counterpoise 30 Feet High

ρt = the number of degrees of rotation of the rotor

Fig 20(A) is a schematic diagram of sideband generator No 1. A voltage E of frequency $\frac{\omega}{2\pi}$, is applied to the circuit. It is required that the expression for the load current I_1 be found. This may readily be done by applying Thevenin's theorem and finding the open circuit voltage e'

$$e' = E \left(\frac{C_1 - C_2}{C_1 + C_2} \right) \quad (14)$$

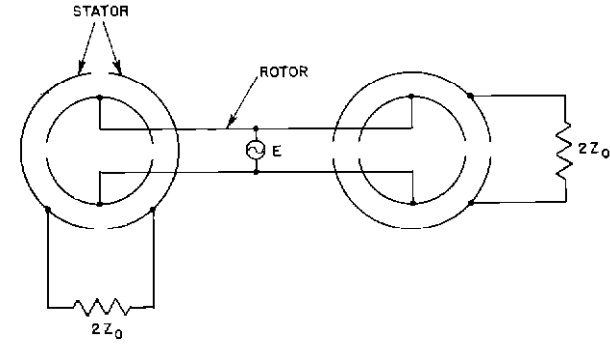
The generator E is then replaced with a short circuit and the circuit appears as shown in Fig 20(B)

$$I_1 = \frac{e'}{2Z_o + \frac{-2/\omega^2 C_1 C_2}{-j(\frac{1}{\omega C_1} + \frac{1}{\omega C_2})}} \quad (15)$$

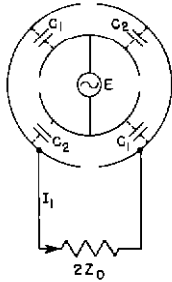
$$= \frac{E}{2} \frac{\omega C_1 - \omega C_2}{Z_o (\omega C_2 + \omega C_1) - j} \quad (16)$$

Substituting the values of C_1 and C_2 from equations (10) and (11) in equation (16) gives

$$I_1 = \frac{E \omega K_2 \cos \rho t}{j - 2\omega Z_o K_2} \quad (17)$$



(A) ARRANGEMENT OF STATOR AND ROTOR PLATES



(B) ONE SIDE BAND GENERATOR SHOWING CAPACITIES

Fig 19 Electrical Components and Connections of Goniometer

Equation (17) may be shown to contain only the upper and lower sidebands of an amplitude modulated wave, by substituting the instantaneous value of E into equation (17)

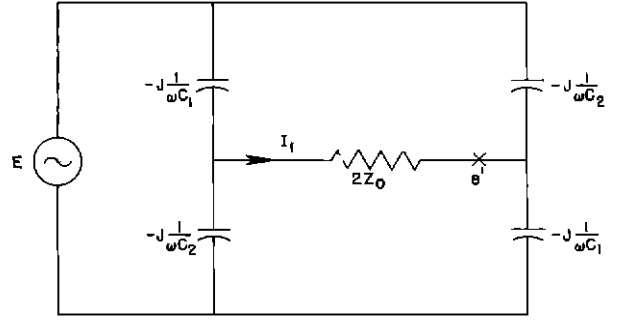
$$I_1 = E_m \sin \omega t \frac{\omega K_2 \cos \rho t}{j - 2\omega Z_0 K_2} \quad (18)$$

$$= \frac{E_m}{2} \left(\frac{\omega K_2}{j - 2\omega Z_0 K_2} \right) [\sin (\omega t + \rho t) + \sin (\omega t - \rho t)] \quad (19)$$

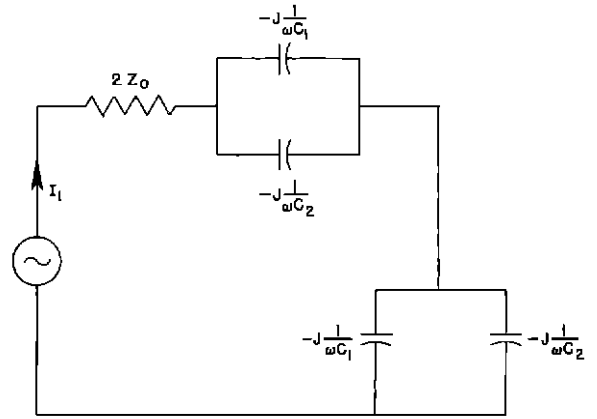
Equation (19) clearly indicates that the current in load $2Z_0$ is made up of two frequencies, one $\frac{\rho}{2\pi}$ higher, and the other $\frac{\rho}{2\pi}$ lower, than the carrier frequency $\frac{\omega}{2\pi}$

An analysis of the No 2 sideband generator gives the following expression for the load current

$$I_2 = E \left(\frac{\omega K_2 \sin \rho t}{j - 2\omega Z_0 K_2} \right) \quad (20)$$



(A)



(B)

Fig 20 Schematic Diagrams of Sideband Generator

This equation takes a form similar to equation (19) when $E_m \sin \omega t$ is substituted for E as follows

$$I_2 = \frac{E_m}{2} \left(\frac{\omega K_2}{j - 2\omega Z_0 K_2} \right) [\cos (\omega t - \rho t) - \cos (\omega t + \rho t)] \quad (21)$$

Equation (21) shows that the No 2 output consists of sidebands only and is similar to (19) but 90° out of phase at the modulation frequency

Fig 21 shows a view of the goniometer. Two rotors, each having four plates, are mounted one at each end of a longitudinally split rotor shaft to form one section of the sine wave modulating capacitors. The rotor is driven at a speed of 1,800 rpm by means

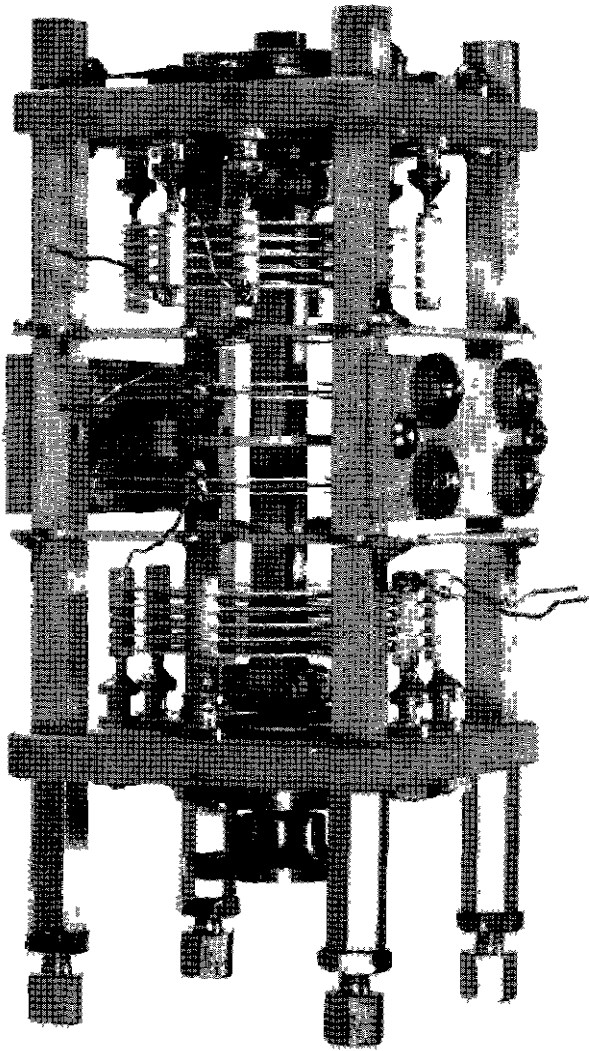


Fig 21 View of Goniometer With Shield Plates Removed

of a synchronous motor. The stators consist of five plates each, angularly displaced by 90° . The goniometer receives unmodulated rf power from the modulation eliminator and delivers two rf outputs having amplitudes proportional to the sine and cosine of the rotational angle of the goniometer. Transmission line balance sections are required to permit operation of the balanced goniometer from concentric coaxial cable. The medium for coupling rf carrier from the modulation eliminator to the sine wave modulating capacitors consists of a pair of rotor plates, located near the center of the rotor shaft and in close relation to a set of stators consisting of two plates each. Faraday plates prevent

capacitive coupling between the modulating stators and the coupling stators. A 360° dial with a vernier indicator permits determination of the rotor position. The dial is adjusted to indicate zero when the rf power from one of the two output circuits is a minimum.

A schematic diagram of the goniometer circuits is presented in Fig 22. The input impedance to the goniometer is 40 to 60 ohms resistive, and -10 to $+10$ ohms reactive, over the frequency range of 112-118 Mc. The input is resonant at 115 Mc. The rated rf power input is approximately 100 w.

If the goniometer is terminated and energized in the same way as it is in normal operation, but instead of rotating at 1,800 rpm, it is turned by hand, data for a set of curves may be obtained similar to those of Fig 23 where, curve 1 is the voltage from one output, and curve 2 is from the other output. There is a phase reversal after passing through a minimum, which is not indicated on the figure. This may be checked by measuring the resultant field of the carrier pattern, plus the pattern produced by one goniometer output. It has been found in practice that sufficient accuracy can be obtained if the null locations are 90° apart, $\pm 2^\circ$, and the maxima are equal to within ± 5 per cent. The wave form should be a true sine wave with not more than five per cent harmonic distortion.

A dynamic test of the goniometer, to determine quickly its operational performance, consists of terminating one output of the goniometer at a time, in a 52 ohm dummy load, and reading the 30 cps phase produced by the other goniometer output at the station monitor. The difference between the two phase readings should be $90^\circ \pm 1^\circ$.

The 9.96 kc subcarrier, which is frequency modulated at 30 cps is produced by an electromechanical subcarrier generator in the form of a tone wheel. The subcarrier generator and goniometer are driven on a common shaft. Teeth, machined into the periphery of the wheel, vary the magnetic field during rotation, producing a voltage in a pick-up coil.

The subcarrier generator was designed from data obtained from the following analysis, the FM wave desired at the output of the subcarrier generator may be expressed by

$$e = E_{m1} \sin (2\pi f_0 t + m \sin 2\pi f_1 t) \quad (22)$$

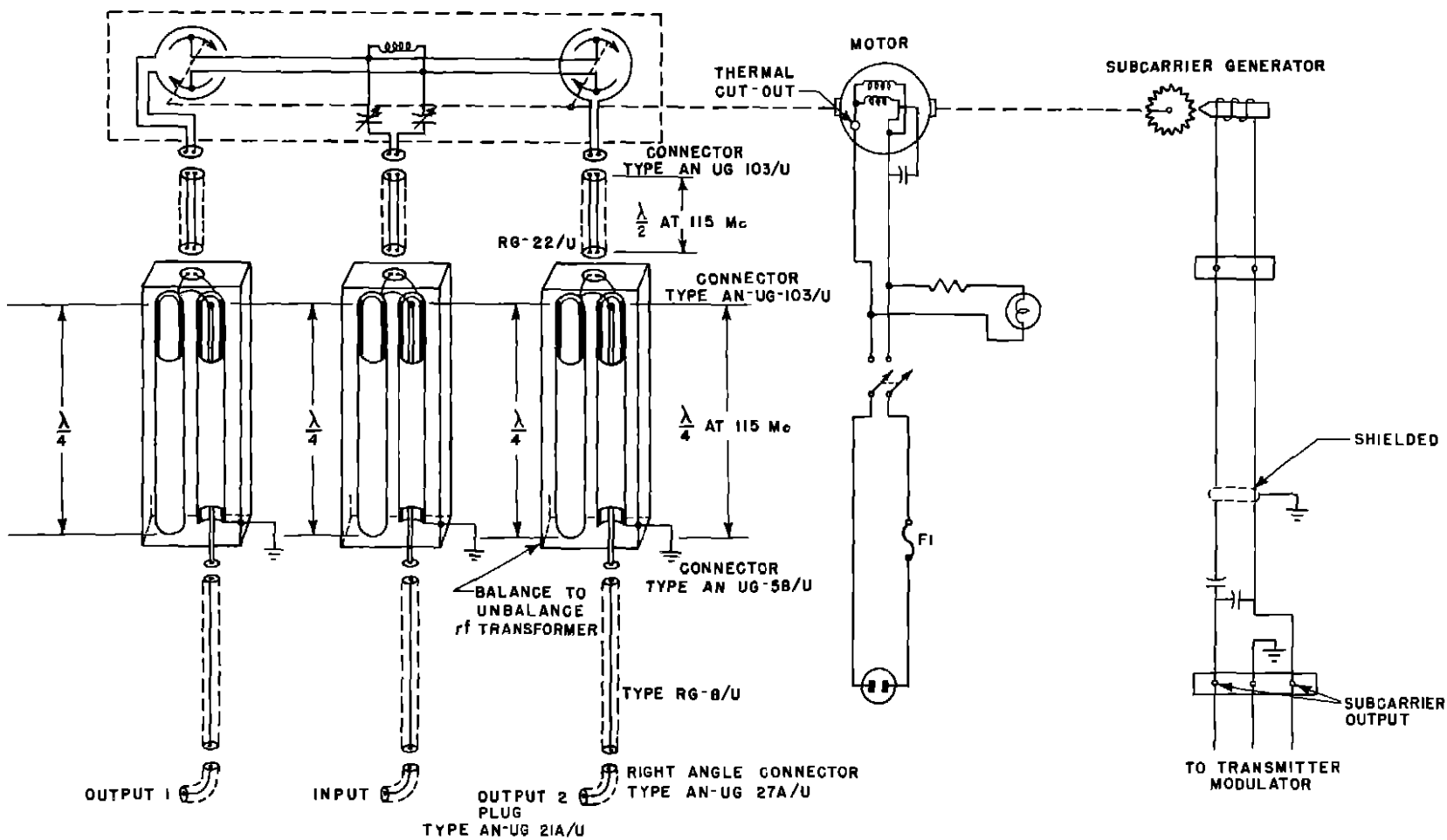


Fig 22 Schematic Diagram of Goniometer Assembly Type CA-1231

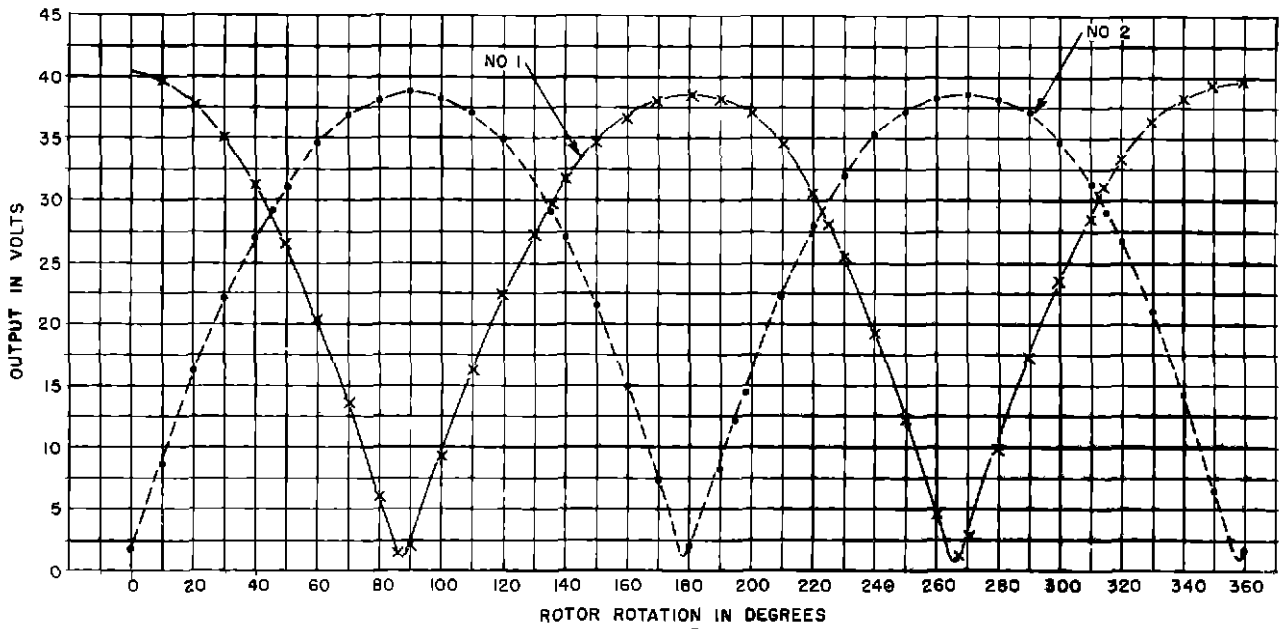


Fig 23 Goniometer Sine Characteristics

where

E_{m1} = a constant

f_o = carrier frequency

f_1 = modulation frequency

m = modulation index

The voltage appearing across a winding of N turns depends on the time rate of change of flux and other factors which are assumed constant

$$e = K_3 N \frac{d\phi}{dt} \quad (23)$$

where

K_3 = a constant depending upon core material, units, etc

From equations (22) and (23)

$$e = K_3 N \frac{d\phi}{dt} = E_{m1} \sin(2\pi f_o t + m \sin 2\pi f_1 t) \quad (24)$$

Equation (24) shows that if the flux ϕ , varies with time in a definite manner, the desired voltage wave will be produced. It can be seen from the diagram in Fig 24 that, when the

pickup is opposite a tooth, the voltage e will be zero, since the time rate of change of flux is zero. The flux distribution is unchanged when a tooth is directly opposite the pickup. The flux will vary as the tooth passes the pickup and a new cycle starts, when the next tooth is opposite the pickup.

Hence, from equation (24)

$$2\pi f_o t + m \sin 2\pi f_1 t = 2\pi n \quad (25)$$

where

n denotes the tooth number starting with 1

If the wheel is designed so that one revolution produces one complete cycle at the frequency f_1 , the time for one revolution equals $\frac{1}{f_1}$

Then

$$2\pi f_o \frac{1}{f_1} + m \sin \left(2\pi f_1 \frac{1}{f_1} \right) = 2\pi n_1 \quad (26)$$

hence

$$n_1 = \frac{f_o}{f_1} = \text{the total number of teeth} \quad (27)$$

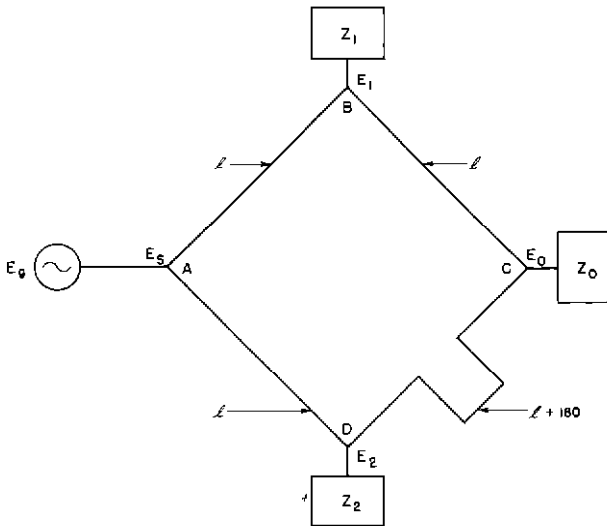


Fig 25 Block Diagram of Modulation Eliminator

other three terminals of the bridge are connected to impedances Z_0 , Z_1 , and Z_2 , which are normally pure resistances. Z_0 represents the load impedance presented by the capacity goniometer. The characteristic impedance of each of the transmission lines of the bridge also is Z_0 . When $Z_2 = Z_1$, the bridge is balanced. A voltage E_s , at point A sets up traveling waves in the branches ABC and ADC, which arrive at point C equal in magnitude and opposite in phase. Thus, the voltage E_0 at point C is zero. When $Z_2 \neq Z_1$, the output voltage E_0 is not zero and power is delivered to the load.

The oscillograms reproduced in Figs 26(A) and 26(B) show the required performance of the modulation eliminator. All instantaneous voltages that exceed the modulation trough value are reduced to the trough value. This is accomplished by making both Z_1 and Z_2 resistive loads. The value of Z_2 is a function of input voltage, equal to $\frac{\Delta e_A}{\Delta i_A}$, for all values of e_3 equal to or less than the trough value, see Fig 27. When the instantaneous voltage e_3 exceeds the trough value, it is convenient to consider e_3 as the sum of two voltages, e_1 and e_2 . The part e_1 sees Z_2 as $\frac{\Delta e_A}{\Delta i_A}$ while Z_2 appears to e_2 as $\frac{\Delta e_B}{\Delta i_B}$. Since $\frac{\Delta e_A}{\Delta i_A} \neq Z_1$, while $\frac{\Delta e_B}{\Delta i_B} = Z_1$, for reasons stated, e_2 will produce no output, whereas,

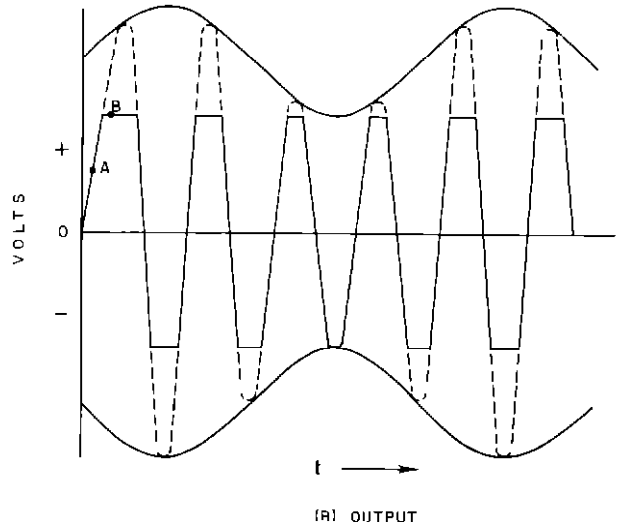
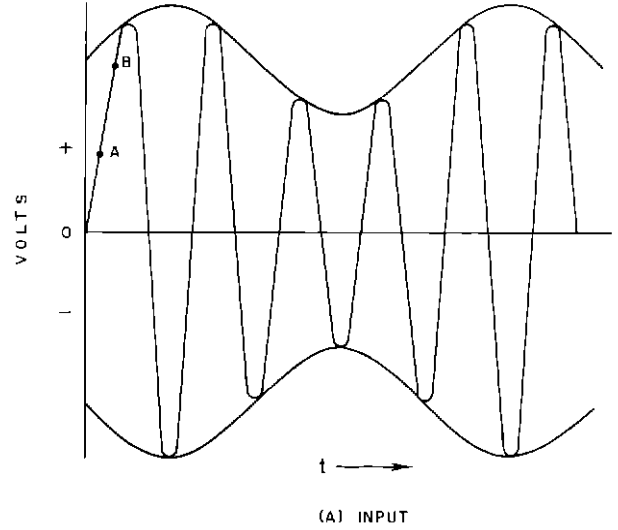


Fig 26 Voltage Wave Forms of Modulation Eliminator

e_1 and values of e_3 less than e_1 will produce an output. Point A, Fig 26(A), corresponds to point A, Fig 26(B), and $Z_2 \neq Z_1$, therefore $E_0 \neq 0$. A short time later at point B, Fig 26(A), $Z_2 = Z_1$ for the increment exceeding the trough value, so that the instantaneous voltage output is that marked by point B, Fig 26(B). Only that portion of the applied voltage, which exceeds the trough value, is cancelled at the output of the modulation eliminator.

While a complete analysis of the modulation eliminator would be very complex,

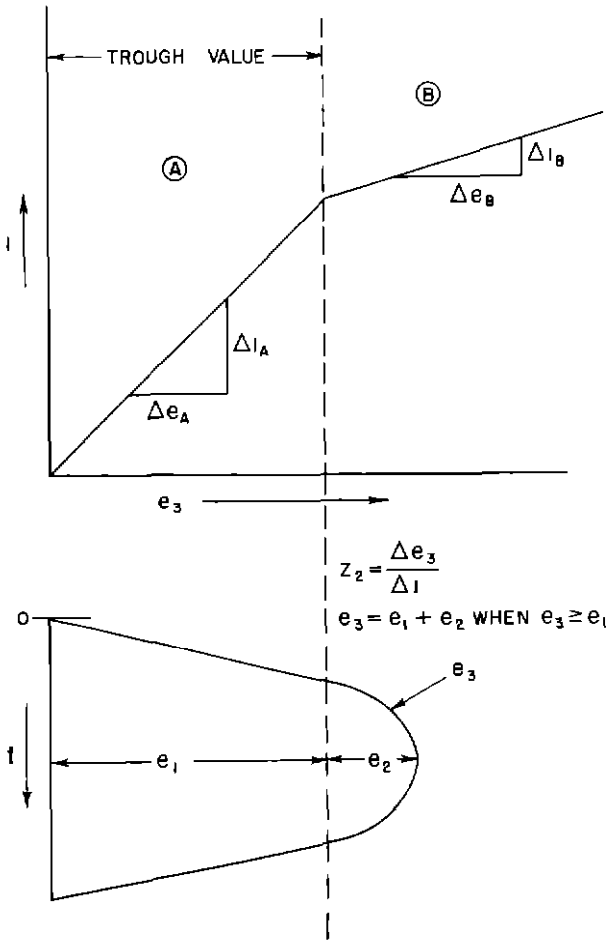


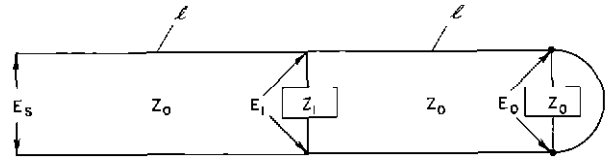
Fig 27 Graphical Representation of Z_2 as a Function of the Instantaneous Input Voltage

since it involves treatment of instantaneous voltages, some understanding of its operation can be had by a steady state analysis. This is given in the following analysis, where $Z_2 = Z_1$ for the first part, and $Z_2 \neq Z_1$ for the second part.

When $Z_2 = Z_1$, there is a virtual short circuit at C, Fig 25, since $E_0 = 0$. Fig 28(A) illustrates one-half of the bridge under this condition. It can be shown that

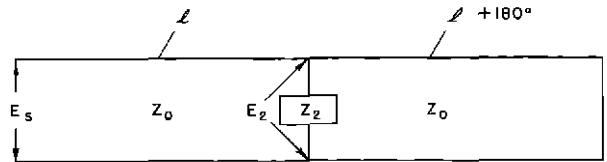
$$E_1 = \frac{E_s}{2 \cos \ell + j \frac{Z_0}{Z_1} \sin \ell} \quad (30)$$

Referring to Fig 28(B), the equivalent circuit of the other half of the bridge,

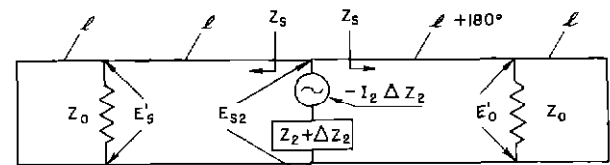


(A) UPPER HALF OF BRIDGE SHOWN IN FIG 25

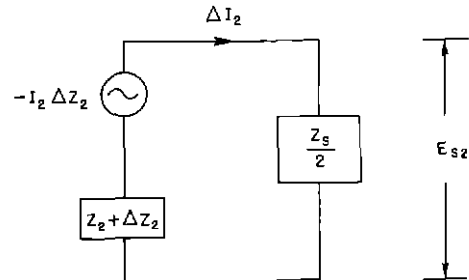
$$\left. \begin{matrix} Z_1 = Z_2 \\ E_0 = 0 \end{matrix} \right\} \text{VIRTUAL SHORT AT } Z_0$$



(B) LOWER HALF OF BRIDGE SHOWN IN FIG 25



(C) SCHEMATIC DIAGRAM OF BRIDGE WHEN VARIABLE AND DUMMY LOAD IS NOT EQUAL



(D) CIRCUIT DIAGRAM OF (C) SIMPLIFIED

Fig 28 Circuits Used in Analyzing Operation of Bridges

$$E_2 = \frac{E_s}{2 \cos \ell + j \frac{Z_0}{Z_2} \sin \ell} \quad (31)$$

also

$$I_2 = \frac{E_s}{Z_2} \frac{1}{2 \cos \ell + j \frac{Z_0}{Z_2} \sin \ell} \quad (32)$$

Let the variable load Z_2 be changed to $Z_2 + \Delta Z_2$. This change is equivalent to inserting

a generator in series with $Z_2 + \Delta Z_2$ in accordance with the Compensation Theorem ¹³ Figs 28(C) and 28(D) represent the bridge circuit arrangement for determining the change in current due to a change in Z_2

$$Z_s = Z_o \frac{-\tan \ell + j2}{2 \cot 2\ell + j} \quad (33)$$

$$\Delta I_2 = \frac{-I_2 \Delta Z_2}{Z_2 + \Delta Z_2 + \frac{Z_s}{2}} \quad (34)$$

$$E_{s2} = \frac{-I_2 \Delta Z_2 Z_s}{2(Z_2 + \Delta Z_2) + Z_s} \quad (35)$$

By using the lossless transmission line equation for voltage, and equation (35), the following expression for E'_O is obtained

$$E'_O = -\frac{1}{2 \cos \ell + j \sin \ell} \frac{-I_2 \Delta Z_2 Z_s}{2(Z_2 + \Delta Z_2) + Z_s} \quad (36)$$

Equation (36) may be rewritten using equation (32) with the result

¹³T. E. Shea, "Transmission Networks and Wave Filters," D. Van Nostrand Co., Inc. New York, p. 56

$$E'_O = \frac{1}{2 \cos \ell + j \sin \ell} \frac{4Z_2 Z_s}{2(Z_2 + \Delta Z_2) + Z_s} \frac{E_s}{Z_2} \frac{1}{2 \cos \ell + j \frac{Z_o}{Z_2} \sin \ell} \quad (37)$$

and finally

$$E'_2 = (I_2 + \Delta I_2)(Z_2 + \Delta Z_2) = \frac{E_s}{Z_2} \frac{1}{2 \cos \ell + j \frac{Z_o}{Z_2} \sin \ell} \left(1 - \frac{\Delta Z_2}{Z_2 + \Delta Z_2 + \frac{Z_s}{2}}\right) (Z_2 + \Delta Z_2) \quad (38)$$

where the primes denote that Z_2 is replaced by $Z_2 + \Delta Z_2$

The efficiency of the bridge is defined as

$$\text{Efficiency} = \left[\frac{|E'_O|^2}{Z_o} + \frac{|E_1|^2}{Z_1} + \frac{|E_2|^2}{Z_2 + \Delta Z_2} \right]^{-1} \frac{|E'_O|^2}{Z_o} \quad (39)$$

where

Z_o , Z_1 , and $Z_2 + \Delta Z_2$ are real. Table I is a

TABLE I

Conditions	$Z_o = 52 + j0$ ohms	$E_1 = E'_1$	(The power output is held constant at 15 watts)
	$E_o = 0$	$ E'_O = 28$ V	

A tabulation of pertinent voltages and efficiencies of the modulation eliminator for several values of ℓ , Z_1 and $Z_2 + \Delta Z_2$

ℓ degrees	Z_1 ohms	$Z_2 + \Delta Z_2$ ohms	Volts				Efficiency Percent
			$ E_s $	$ E_1 $	$ E_2 $	$ E'_O $	
45	393 + j0	16 + j0	78	55	55	13.6	44.5
90	393 + j0	16 + j0	6.2	46.9	46.9	19.2	35.6
90	108 + j0	2700 + j0	58.9	122	122	152	9.2
45	108 + j0	2700 + j0	127	87.2	87.2	92.5	17
180	393 + j0	16 + j0	No output				0
22.5	393 + j0	16 + j0	135	73	73	35.4	14.2

tabulation of data obtained on the modulation eliminator using equations (30) through (39)

A rear view of the modulation eliminator unit is shown in Fig 29, and a schematic diagram of the unit is given in Fig 30. Three of the four bridge arms are composed of solid dielectric lines one-eighth wavelength long at 115 Mc. The fourth arm of the bridge is also composed of solid dielectric line and is five-eighths wavelength long. The ML-322 diodes were especially designed for application in the modulation eliminator. The plate-cathode dc resistance is approximately 80 ohms in the forward direction and approaches infinity in the reverse direction. In order to obtain a low value of diode plate-cathode resistance for satisfactory operation of the circuit, the spacing between plate and cathode was held to about 0.010 in. The plate to cathode capacity of the diodes is neutralized by a variable inductor consisting of a short-circuited section of 70 ohm coaxial line.

The modulation eliminator is tested by observing the output of the unit on an oscilloscope with the dc path of the eliminator opened and then closed. When the dc path is open-circuited, the modulation eliminator is inactive so that the oscilloscope will display the modulation at the output of the transmitter. The transmitter should be modulated 30 per cent with 9.96 kc signal for this test. The dc path should then be closed to permit the unit to function, and the envelope observed. The modulation percentage should be three per cent or less.

Typical power measurements of a modulation eliminator are

P_1 = power output of transmitter = 185 w,

P_2 = power into eliminator = 58 w,

P_3 = power output of eliminator = 13.15 w,

P_4 = power into carrier antenna = 127 w,

efficiency of modulation eliminator = $\frac{P_3}{P_2} = 22.6$ per cent,

efficiency of system = $\frac{P_4 + P_3}{P_1} = 75.7$ per cent

These data were obtained with carrier only from the transmitter. The modulation eliminator

current was 56 ma, and since the unit is set to limit to the trough value of the amplitude modulated envelope, the theoretical maximum efficiency of the equipment, measured as above with the 9.96 kc modulation off, is 67 per cent. This assumes that only the power represented by the voltage above the trough value is lost.

Transmitter and Audio Equipment

The omnirange transmitter¹⁴ is designed to deliver an output of 200 w of carrier in the frequency range 108 to 127 Mc, capable of being modulated 100 per cent over the range 60 to 12,000 cps. The input circuit of the audio section provides for simultaneous transmission of three modulations, including voice, a 9.96 kc subcarrier, and a 1,020 cps tone for the purpose of station identification. The voice and subcarrier levels are each set to produce 30 per cent modulation of the carrier while the tone signal is adjusted for 10 per cent modulation.

Monitor

Proper operation of the omnirange requires that the 30 cps signal of the variable phase channel and the 30 cps signal of the reference phase channel be exactly in phase at magnetic north. In order to maintain a check on this relationship under continuous service conditions, some form of monitoring must be employed. In the early stage of development of the omnirange the method used to indicate the relative phase of the two 30 cps voltages was similar in principle to that used in omnirange receivers. Calibration of the equipment was obtained by substituting signals from a frequency modulated 9.96 kc oscillator equipment. Relays in the phase comparison circuit operated an alarm to indicate when the phase relationships of the two 30 cps signals were out of limits.

A more recent system developed by the Hoffman Radio Corporation achieves essen-

¹⁴U. S. Dept. of Commerce, CAA, "Installation Instructions for VHF Omnirange" Federal Airways Manual of Operations IV-B-2-3. Also, refer to Federal Airways Manual of Operations IV-B-1-3 "Description and Theory of VHF Omniranges" for further equipment description.

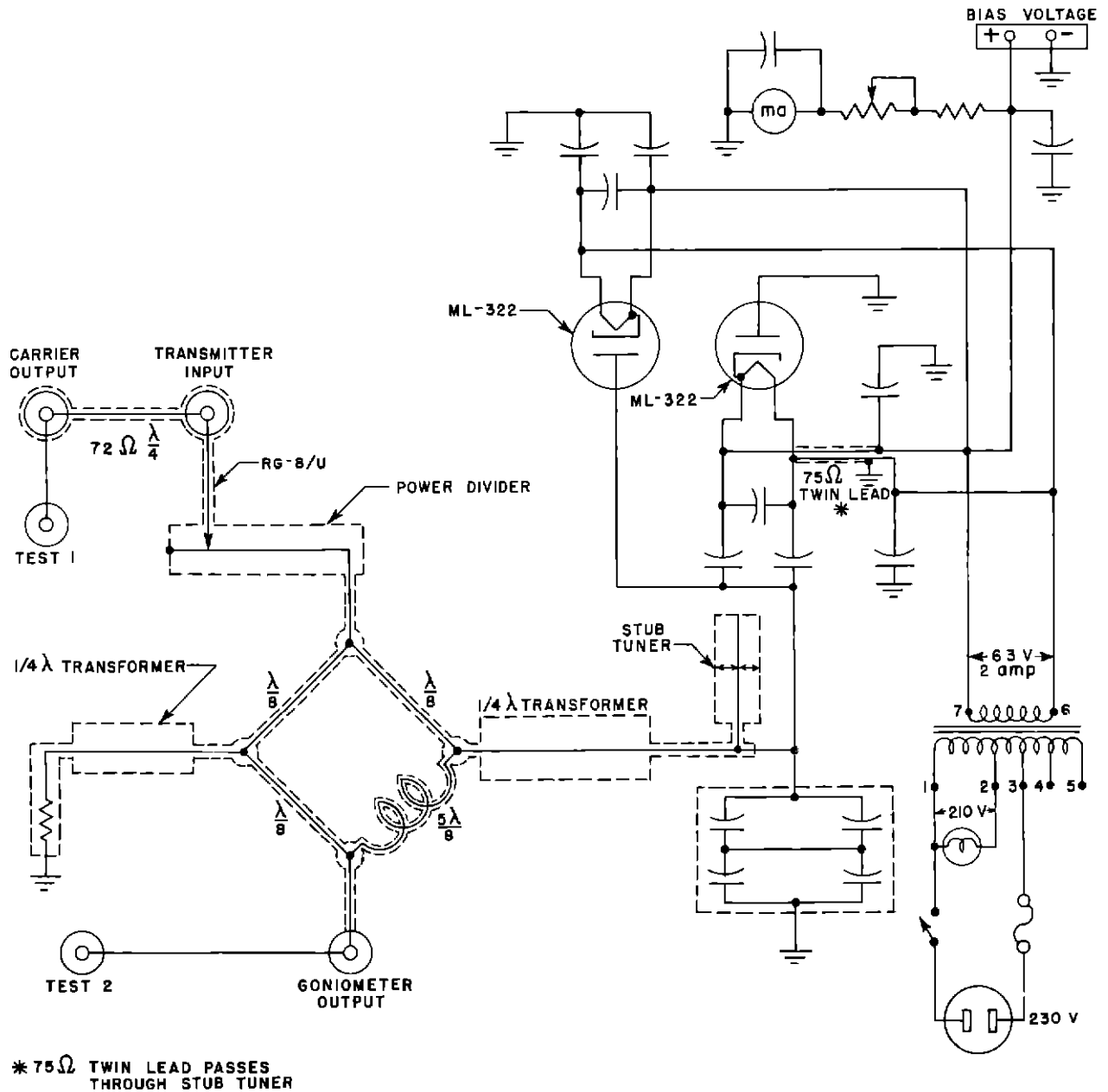


Fig 30 Schematic Diagram of Modulation Eliminator

tially the same results by a different approach to the method of comparing the relative phase of the two signals. In addition to warning of a shift in the relative phase of the signals, alarm circuits are provided to indicate a decrease in amplitude of either the variable phase or reference phase signals. A block diagram of the monitor is shown in Fig 31.

Station Identification

Identification of the omnirange is pro-

vided in two ways. One method utilizes an automatic voice system for the benefit of aircraft pilots who are unfamiliar with the International Morse Code. Station identification is transmitted by voice approximately every 20 sec. The voice is recorded on a sound film which is moved continuously by a motor and suitable arrangement of gears and pulleys to provide repetition of the transmission at any desired interval between 10 and 20 sec. The voice level at the pickup head is amplified

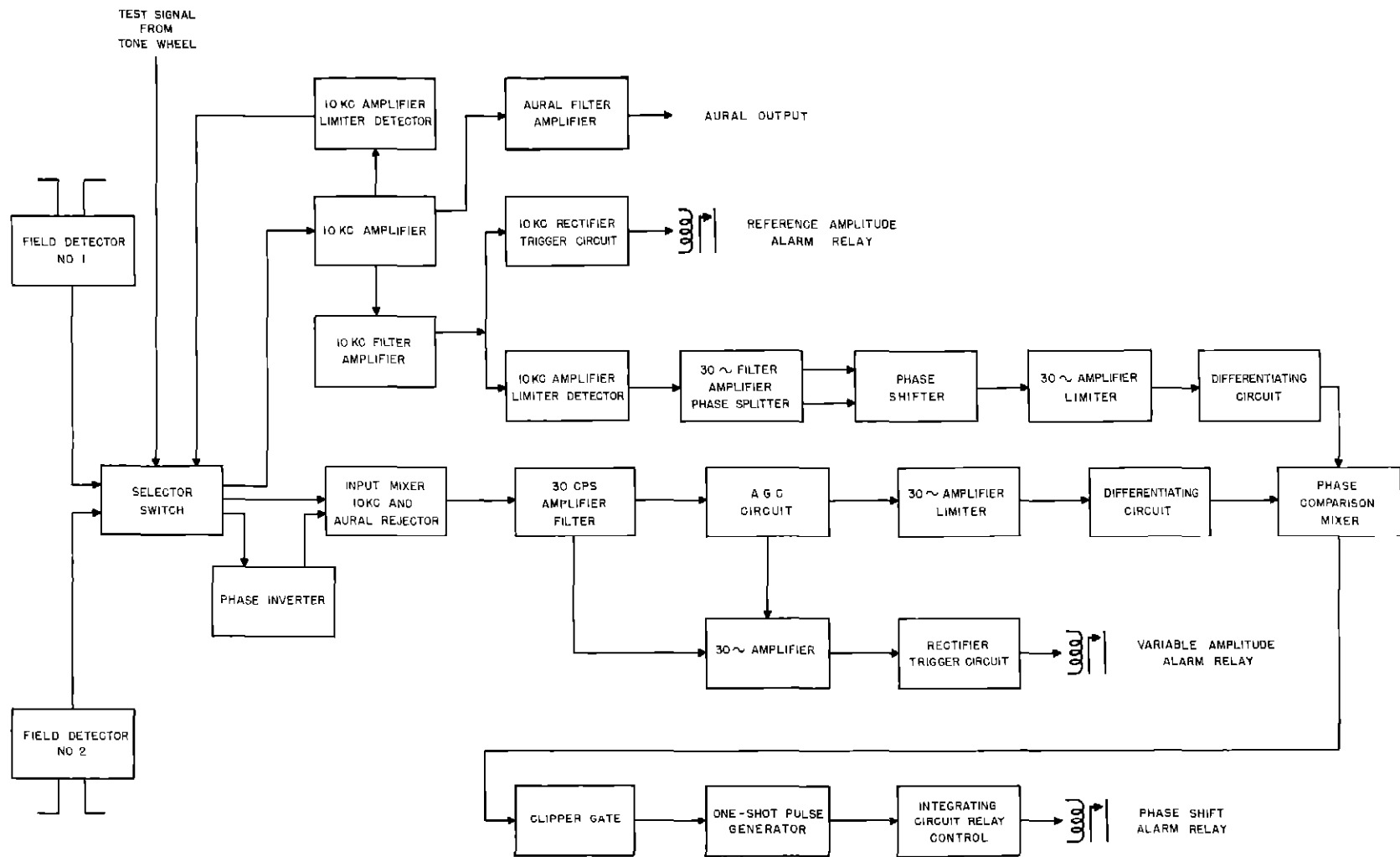


Fig 31 Block Diagram of Monitor

and fed to the driver unit of the carrier modulator. The output from the carrier modulator is adjusted to produce 30 per cent modulation of the rf carrier.

A second method of station identification employs International Morse Code signals. A motor driven keyer, with suitable cam and contact arrangement, transmits a series of dots and dashes in code to produce the identification letters assigned to the station. The af tone used in this connection is 1,020 cps. Modulation of the rf carrier is set at ten per cent. Code identification is transmitted at 15 sec intervals.

AIRBORNE EQUIPMENT

Since 1943, there have been many models of omnirange receiving equipments developed and tested. Although many outstanding improvements have been made in the receiving equipments, the general principles of omnirange operation remain the same. Several types of navigation receivers are now available on the market and others are in process of development. In addition, the development of a low cost, lightweight, private flyer receiver was sponsored by the CAA, and several such receivers are now being marketed.

General Performance Requirements

Some of the important requirements for the receiving equipment may be listed as follows:

- 1 The range, courses and bearing shall be shown in a visual manner.
- 2 It shall be possible for the pilot to select rapidly any range, course to or from the station.
- 3 The course deviation indicator shall, effectively, amplify the course sensitivity in degrees by approximately five times when compared to a 360° indicator of similar size.
- 4 An off-course condition shall produce a direct voltage which can be used with automatic pilot equipment and with a course line computer.¹⁵

¹⁵Francis J. Gross and Hugh A. Kay, "Initial Flight Tests and Theory of an Experimental Parallel Course Computer," CAA Technical Development Report No. 83, September 1948.

5 The receiving equipment shall operate on localizers as well as on two-course and omnirange facilities.

6 The equipment shall be capable of receiving voice communications from localizers, ranges, control towers and communications stations.

7 It shall be possible to provide an automatic indication of the magnetic bearing to the station.

RF, IF, and Detector

In general, the receivers are comprised of either a single, double, or triple superheterodyne rf section and an audio converter section, consisting of filters and measuring circuits which connect to external navigational indicators. Fig. 32 is a block diagram of a typical navigation receiver which operates on the omnirange system and other navigational facilities, such as the two-course range, the 90-150 cps localizer, and the phase localizer. The frequency selection is accomplished by either manually tuning the rf input circuits and simultaneously varying the frequency of a local oscillator, or by step tuning in conjunction with crystal control of the local oscillator. "Crystal saver" circuits are used in step-tuned receivers to decrease the number of crystals required to provide 280 channels at 100 kc intervals over the frequency range of 108.1 to 136 Mc. A delayed action agc circuit is used to provide satisfactory operation of the measuring and indicating circuits. A high level detector having excellent linearity is required to minimize cross modulation of the various modulation components, including the unwanted components produced by propeller modulation.

Fig. 33 shows the results of tests made on two different makes of receivers to determine their sensitivity and agc characteristics. The method used for these tests consisted of applying a simulated omni rf signal through a matching resistor to the input of the receiver and measuring the indicated course-width.

The results of selectivity tests made on these receivers are shown in Fig. 34. The method used for these tests consisted of varying the frequency and output of a signal generator to maintain a constant agc condition in the receiver. The rigid selectivity requirement for airline type receivers is necessary to minimize interference between stations operating at 100 kc separation, when the aircraft is flown at altitudes above 20,000

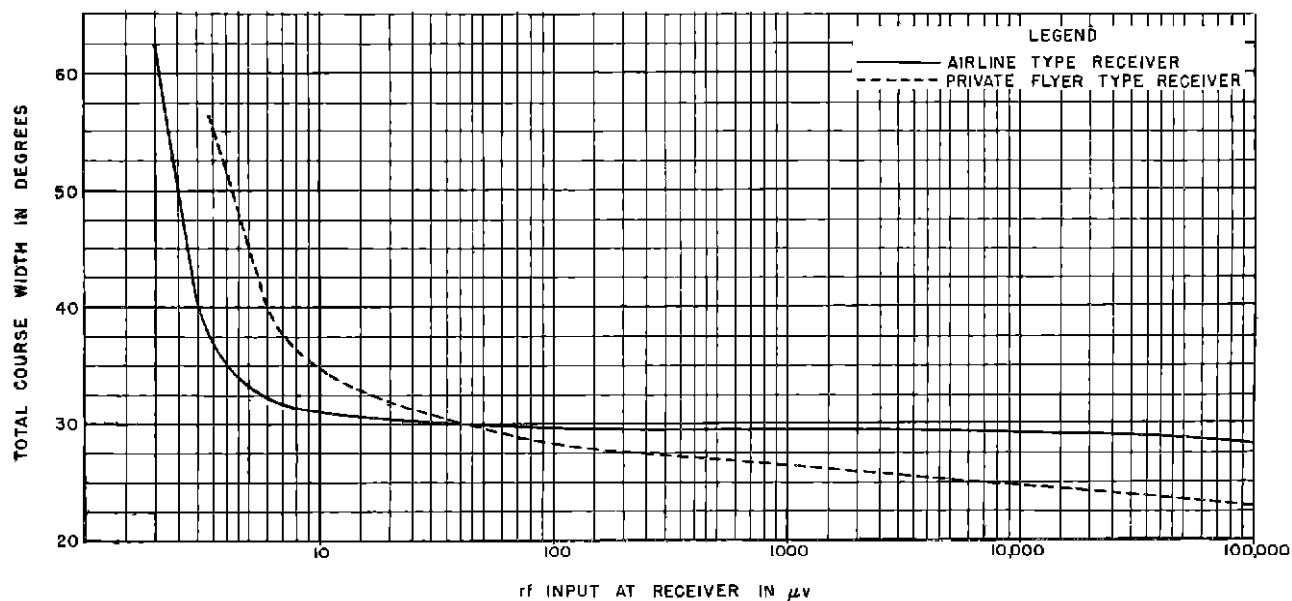


Fig 33 Course-Width Characteristics of Navigation Receivers

feet. It is not expected that private-flyer type aircraft receiving equipment will be used at such high altitudes.

The detector output of the receiver contains a combination of several signals. Suitable filters are necessary to separate these signals. The most important filter is the 30 cps low-pass unit which attenuates the unwanted signal caused by propeller modulation, see Fig 35.

Subcarrier Limiter and Frequency Discriminator

Fig 36 shows several types of limiter and frequency discriminator circuits which have been used in navigation receivers. The limiter is required to remove any amplitude modulation on the subcarrier, which may be caused by the transmitting equipment, propeller modulation or cross modulation in the receiver detector circuit. The discriminator circuit shown in Fig 36(A) is a common type and operates as shown in the vector diagrams 1, 2, and 3. Referring to diagram 1, the voltage E_1 adds to the voltage E_3 to produce a resultant voltage E_4 , which is applied to rectifier V_1 to produce a rectified output voltage across resistor R_1 . In a similar manner, voltage E_2 adds to the voltage E_3 to produce E_5 , which is rectified by V_2 to produce a rectified output voltage across R_2 . The rectified voltages across R_1 and R_2 are opposed

to each other, and, when the subcarrier frequency is 9.96 kc, diagram 1 applies, giving a resultant zero voltage output. In diagram 2 the subcarrier frequency is higher than 9.96 kc, and, the resultant difference between vectors E_4 and E_5 appears across the R_1 R_2 output circuit. Diagram 3 shows the condition when the subcarrier frequency is lower than 9.96 kc. The repetition of these vector conditions at all points throughout the 30 cps modulating cycle will result in the production of a continuous 30 cps voltage across the output of the discriminator. Figs 36(B) and 36(C) show two other limiter and discriminator circuits both of which operate similarly to that shown in Fig 36(A). The curves in Fig 37 show the characteristics of the different types of limiter circuits. The characteristics of the discriminators are given in Fig 38. These were determined by applying a variable frequency signal to the input of the limiter, and measuring the dc output of the discriminators on a high impedance dc instrument.

Phase Shift Methods

The phase angle to be measured by the phase shifter is that between the 30 cps E_{REF} signal, which has the same phase at all directions from the range station, and, the 30 cps E_{VAR} signal, which has a phase which is a function of the magnetic bearing of the aircraft from the station. The E_{VAR} signal is

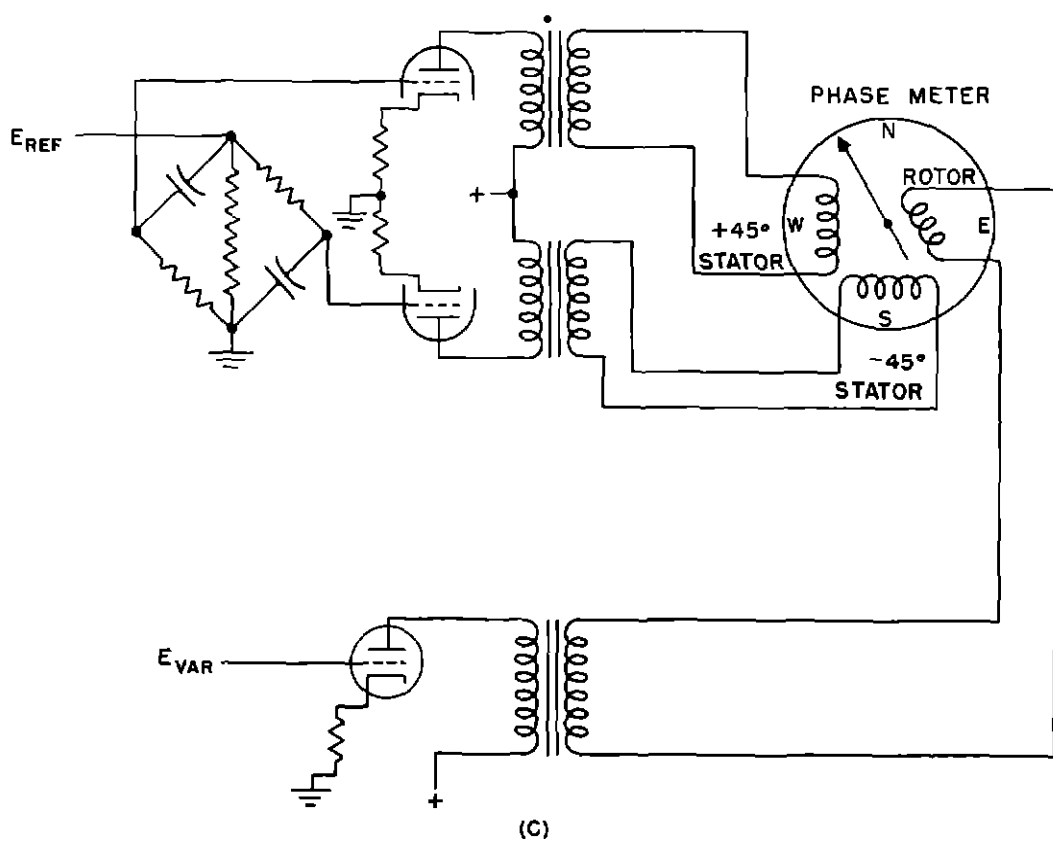
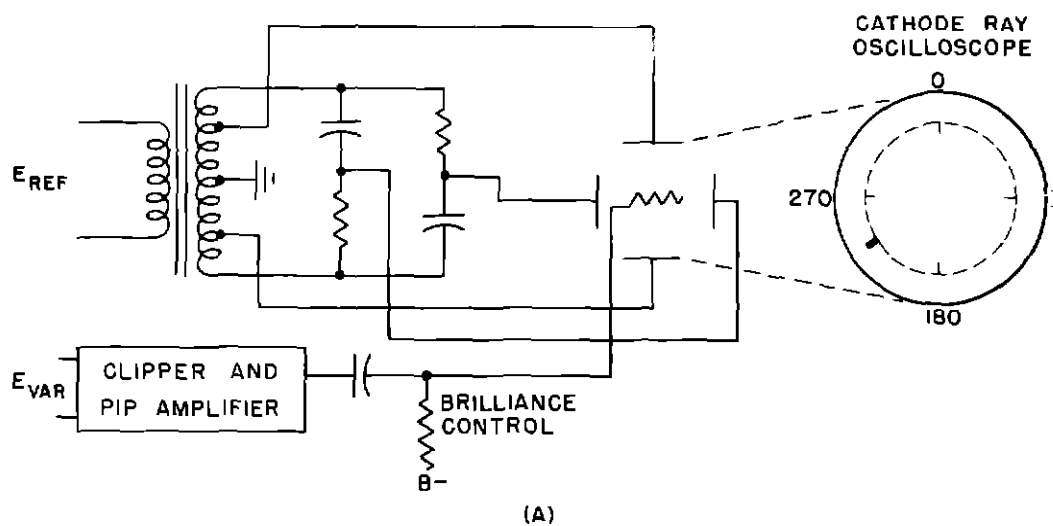
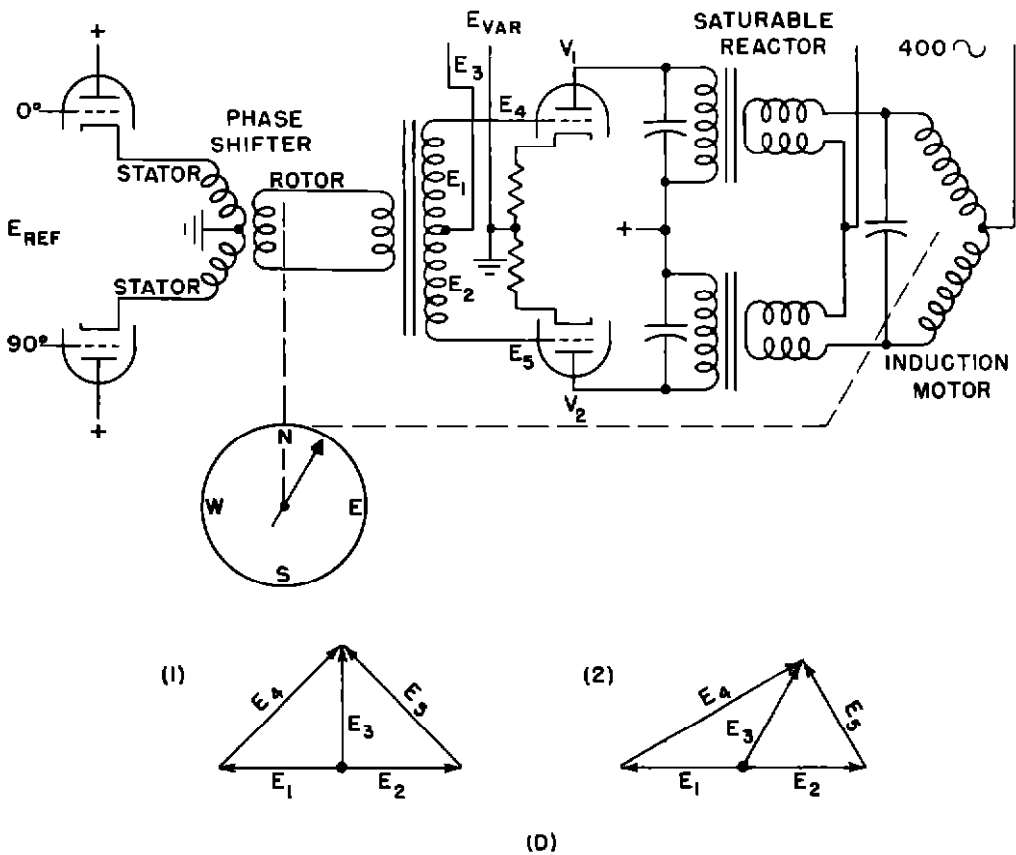
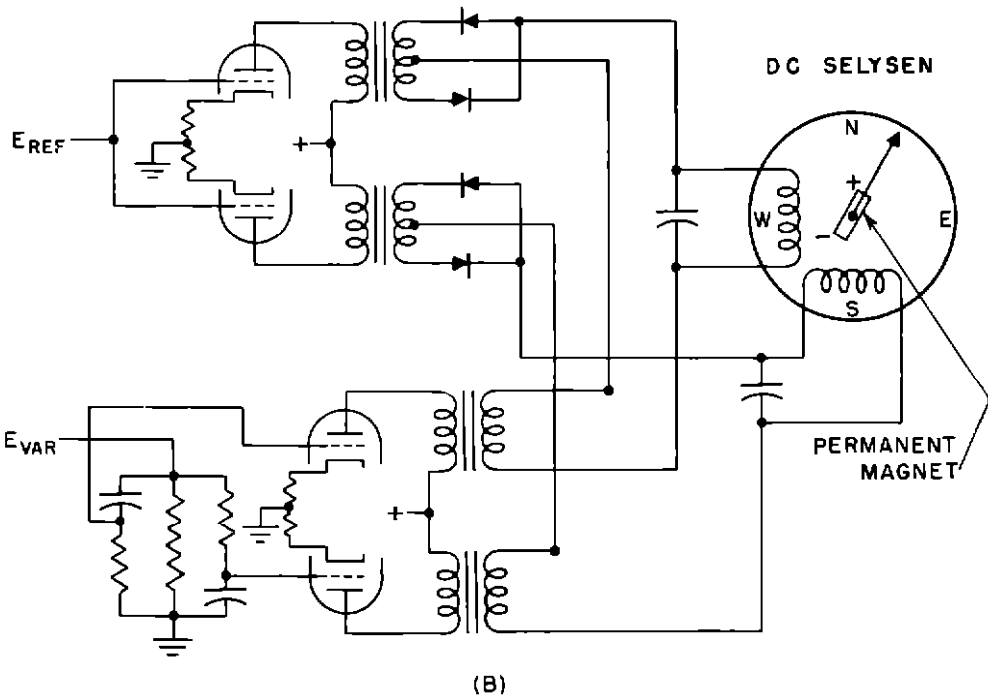


Fig 47 Omnibear



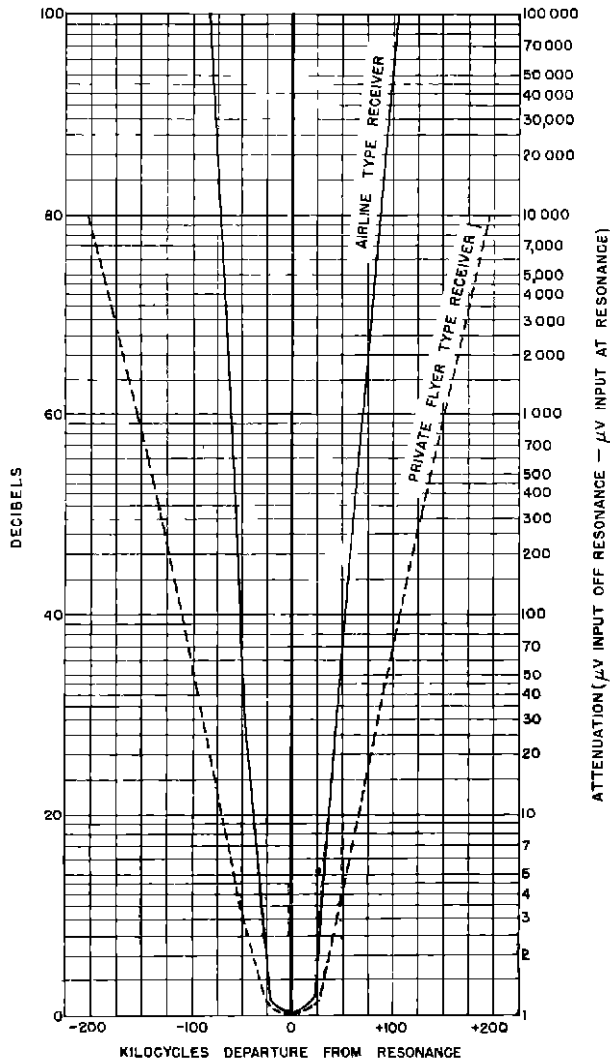


Fig 34 Selectivity Characteristics of Navigation Receivers

in phase with the E_{REF} signal at magnetic north of the station. As the aircraft is flown clockwise around the station, the phase of the E_{VAR} signal lags that of the E_{REF} signal by an amount equal to the magnetic bearing of the aircraft from the station.

As shown in Fig 39, a quadrature circuit arrangement is used to provide the 90° phase difference required for the phase shifter unit. If $R = \frac{1}{\omega C}$ at 30 cps, the phase of E'_1 will be advanced 45° and the phase of E'_2 will be retarded 45° from the phase of E . The stators of the inductive type phase shifter

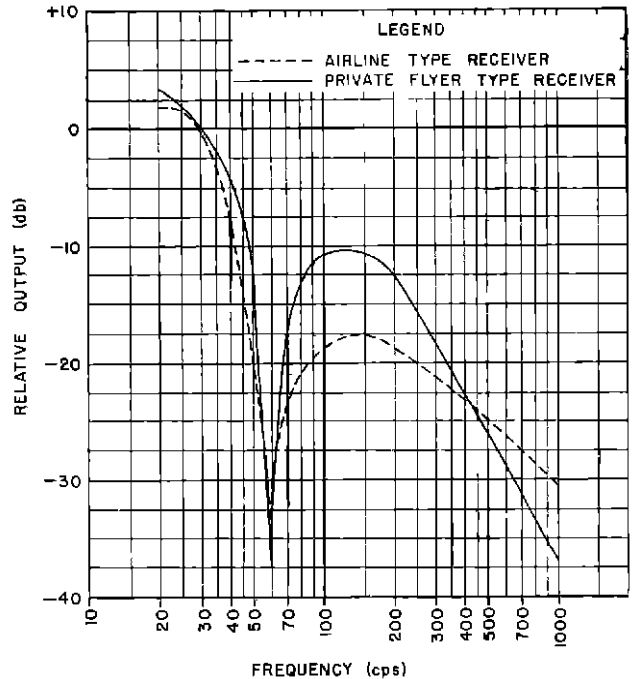


Fig 35 Thirty-cps Low Pass Filter Characteristics

unit will have voltages E_1 and E_2 of equal amplitude, but having a phase difference of 90° . The magnitude of the resultant rotor output is proportional to

$$\sqrt{E_1^2 \sin^2 \theta + E_2^2 \cos^2 \theta} = E_R$$

where

θ = rotor angle in degrees

If $E_1 = E_2$, then E_R is constant for any phase angle.

The phase angle of E_R is ϕ and

$$\phi = \arctan \frac{E_1 \sin \theta}{E_2 \cos \theta}$$

For equal voltages, when $E_1 = E_2$, $\phi = \theta$. The error introduced by unequal voltages E_1 and E_2 will be the difference of ϕ and θ in degrees. The error caused by a five per cent decrease in E_2 is shown in the following tabulation.

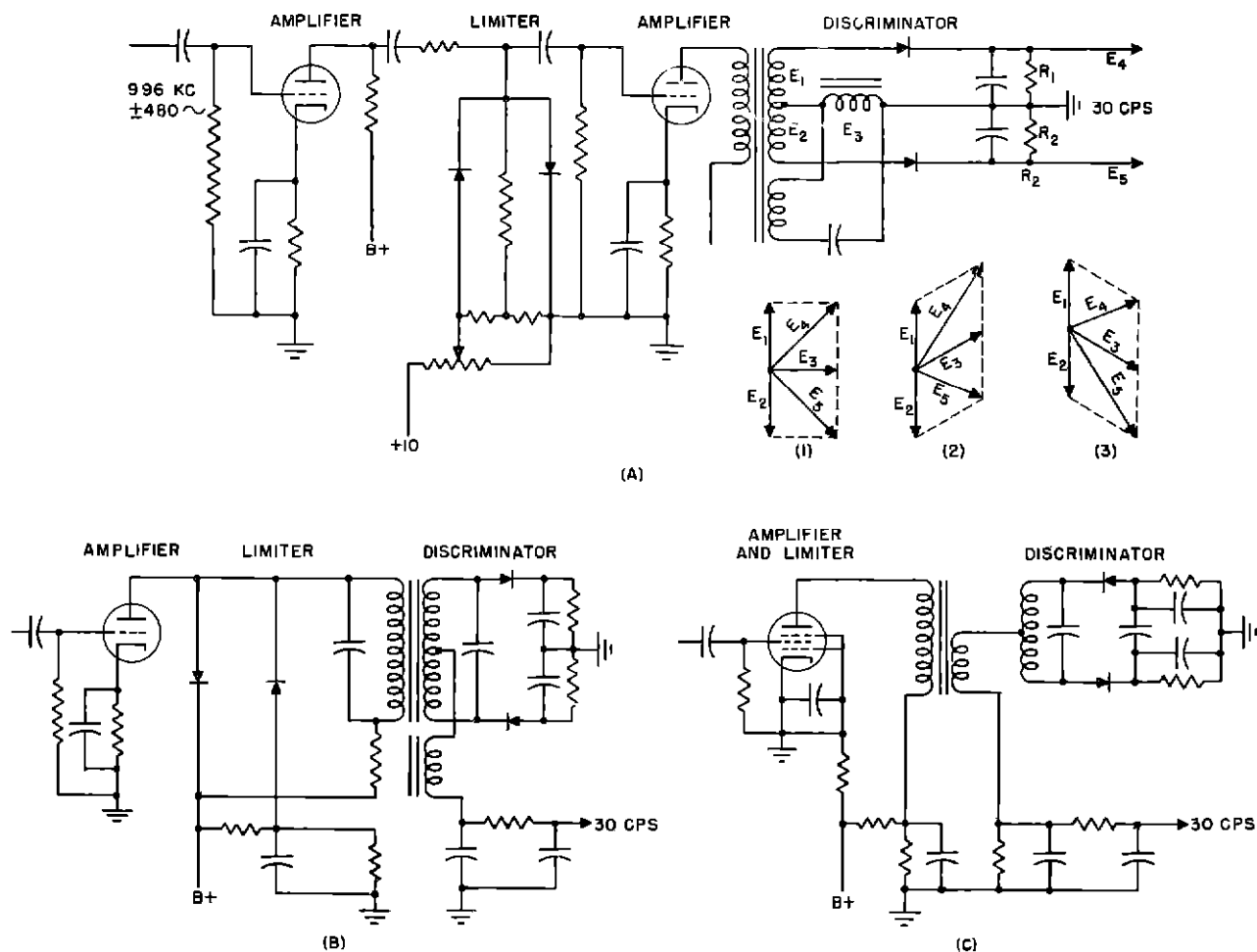


Fig 36 Limiter and Frequency Discriminator Circuits

Rotor Position (degrees)	Rotor Phase (degrees)	Error (degrees)	Rotor Position (degrees)	Rotor Phase (degrees)	Error (degrees)
0	0	0	0	0	0
45	46 4	+ 1 4	45	45 5	+ 0 5
90	90	0	90	91	+ 1 0
135	133 6	- 1 4	135	135 5	+ 0 5
180	180	0	180	180	0
225	226 4	+ 1 4	225	225 5	+ 0 5
270	270	0	270	271	+ 1 0
315	313 6	- 1 4	315	315 5	+ 0 5

The error caused by incorrect phasing of E_1 or E_2 is shown for a 1° increase in the phase angle of E_2 in the following tabulation

Errors also may be caused by variation in power supply frequency at the transmitter. The quadrature relationship of voltages E'_1 and

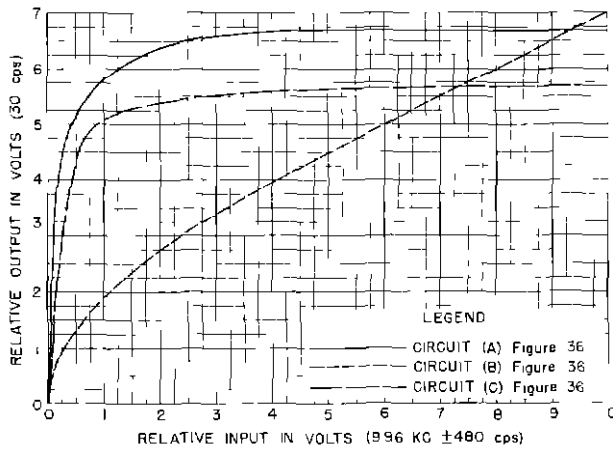


Fig 37 Limiter Characteristics for Circuits Shown in Fig 36

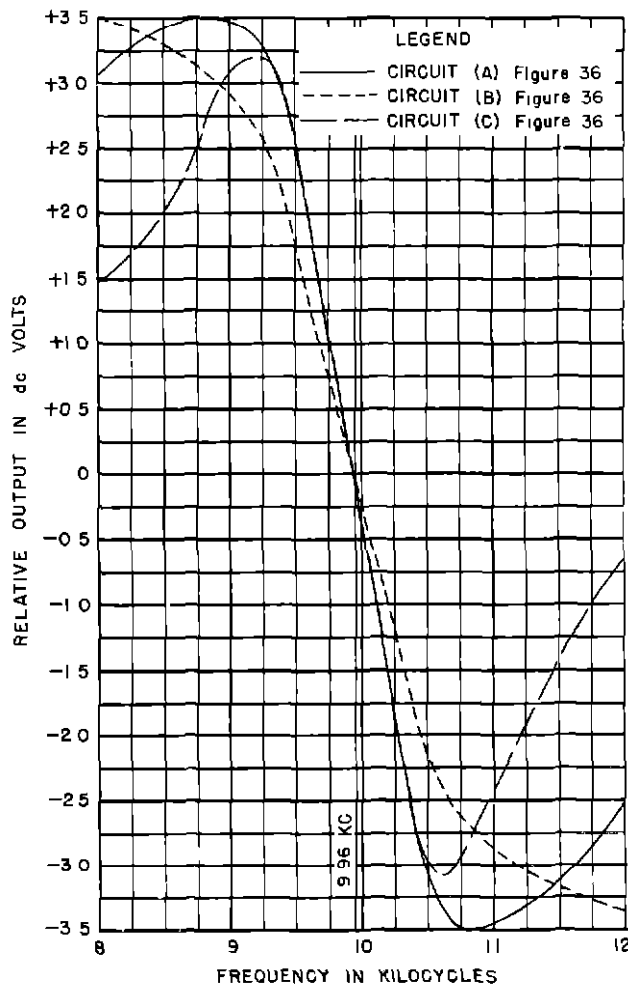


Fig 38 Discriminator Characteristics for Circuits Shown in Fig 36

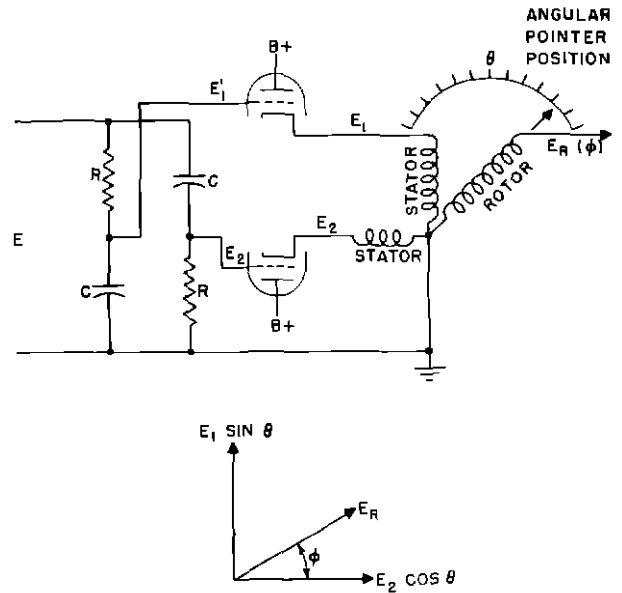


Fig 39 Schematic of Inductive Phase Shifter

E_1' remains unchanged, but their amplitudes will vary with a change in frequency

At 30 cps, $R = X_c$ and $E_1' = E_2' = 0.707 E$

where

$$E_1' = \frac{X_c}{\sqrt{R^2 + X_c^2}} \text{ and } E_2' = \frac{R}{\sqrt{R^2 + X_c^2}}$$

At a frequency of 31.5 cps, the difference in amplitude between E_1' and E_2' is 5.0 percent, which will cause an error of the amount shown in the following tabulation

Rotor Position (degrees)	Rotor Phase (degrees)	Error (degrees)
0	0	0
45	46.4	+1.4
90	90	0
135	133.6	-1.4
180	180	0
225	226.4	+1.4
270	270	0
315	313.6	-1.4

In order that errors produced by the inductive type phase shifters be held to a negligible value, the units are usually con-

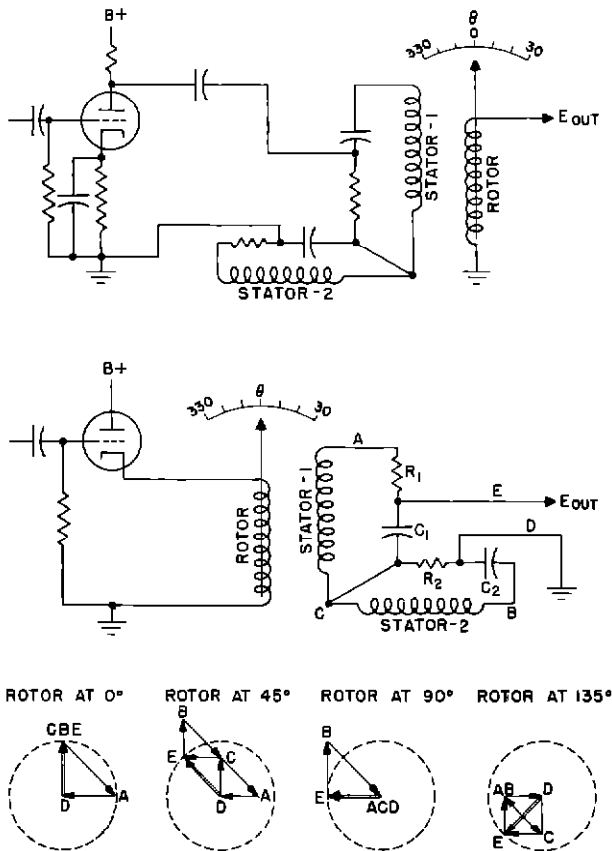


Fig 40 Schematics of Improved Inductive Type Phase Shifters

constructed of high permeability laminated core material similar to Mu-Metal, with a skewed rotor winding connected to a high impedance load. The number of turns on the two stators must be the same, and the two magnetic fields must be in exact quadrature.

Fig 40 shows two arrangements of an improved method for using the inductive type phase shifter unit. In this method a single tube is used to feed the phase shifter, and an RC circuit is connected across each stator. The use of a single tube insures greater reliability. The vector diagrams show the operation of this circuit arrangement.

A resistance type phase shifter as shown schematically in Fig 41(A) also has been used. This phase shifter utilizes a square shaped resistance element which provides a variation of phase equal to the angular pointer position. The amplitude of E_0 varies with the angular position of the potentiometer arm, having four minima of $0.707 E_1$, or $0.707 E_2$ at 90° intervals. The use of a circular shaped re-

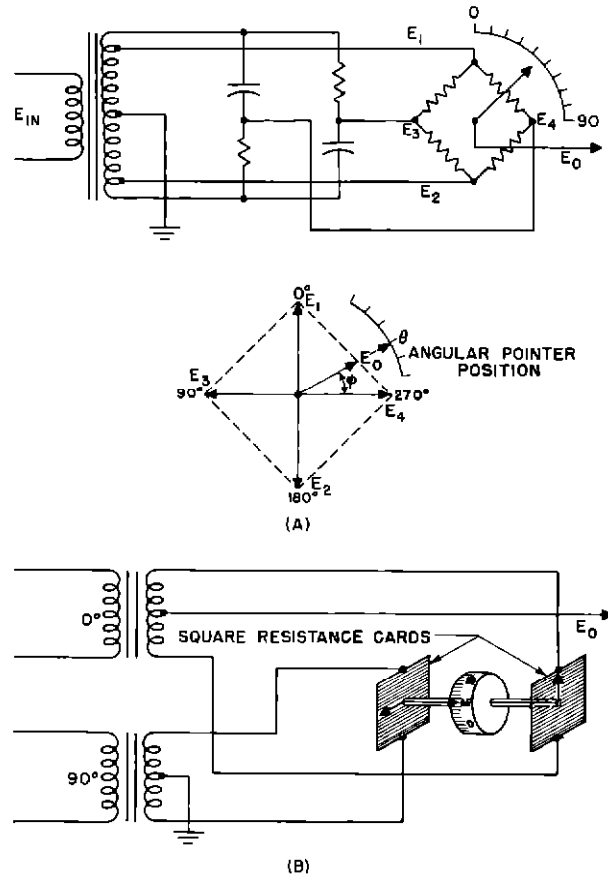


Fig 41 Schematics of Resistance Type Phase Shifters

sistance element requires that the resistance distribution be made to vary sinusoidally through four cycles in order to obtain phase variation which will be directly proportional to the angular position of the pointer in degrees. The resistive type phase shifter shown in Fig 41(B) provides a phase variation proportional to the angular position of the pointer. This is accomplished by the use of two uniformly wound square type resistance cards.

In general, the inductive type phase shifter provides the simplest means of obtaining accurate phase variation, which is directly proportional to the angular position of the rotor and provides constant output for all phase angles. The resistance type phase shifter does not provide constant output, and is difficult to construct to provide accurate phase variation proportional to the angular pointer position. The results of extensive tests made on omnibearing selectors of both the inductive and resistance types show that,

with good quality units and properly adjusted circuits, the measured error can be held to less than 1° . The error in high grade inductive units, including the operating circuit, has been found to be less than $1/2^\circ$.

Phase Comparison Methods

The E_{VAR} signal from the phase shifter unit, commonly known as the omnibearing selector, is mixed with the E_{REF} signal in a phase comparison circuit, in which a zero-center instrument indicates the phase condition. Fig 42 shows one type of phase comparison circuit which has been used in navigation receivers. The circuit operates a dc instrument, which is a desirable feature, since adequate damping is easily obtained and operation into automatic pilot control systems is possible. From an inspection of the circuit diagram, Fig 42(A), it is evident that current through rectifier G_1 causes point C to be positive with respect to point D. Current through rectifier G_2 causes point C to be negative with respect to D. Other polarity conditions may be deduced as follows:

1. If the currents through rectifiers G_1 and G_2 are equal in magnitude, the net charge accumulated by the 1,000 mf capacitor, i.e., the sum of the currents through the indicator, is zero over each alternating current cycle.
2. If the current through rectifier G_1 is greater than that through G_2 , point C has a positive potential with respect to D. Indicator current I_m will flow from point C to D.
3. If the current through rectifier G_2 is greater than that through G_1 , point D has a positive potential with respect to C, and indicator current I_m will flow from point D to C, causing the indicator pointer to deflect in a direction opposite to that in (2).

Vector diagrams b to f, inclusive, indicate phase relationships and indicator currents for various conditions. It has been shown that the resultant direct current through the indicator varies in amplitude and direction, depending on the phase relationship of the applied voltages. Since the instrument indicates average currents, the pointer deflection will be proportional to

where

K is a constant

It follows that the current I changes sign as θ passes through 90° and 270° , respectively. This action is desirable, since it provides "sensing" to the instrument indication, when used in the omnirange system. Sensing is defined here as the relative direction of motion of a course deviation indicator needle, resulting from departure of an aircraft in a definite direction from the desired flight path. The fact that there are two phase angles where the course deviation indicator current is zero, makes it necessary that both phase conditions be resolved and indicated. Two methods of doing this are shown in Fig 43. The methods used have a second phase comparison circuit operating at 90° phase displacement from the first phase comparison circuit, together with an instrument to provide the indication desired. The sensing action of this indication is used in the omnirange system to show whether the numerical reading of the omnibearing selector for an on-course indication of the course deviation indicator, represents the bearing to or from the station. This instrument is commonly referred to as a TO-FROM indicator. In the circuits shown, a small portion of the E_{VAR} and E_{REF} voltages is rectified and fed to the course deviation indicator, to operate the flag alarm movement, which is now included in the latest type indicators.

The results of tests made to determine the output current from the phase comparison circuit, when the phase of E_{VAR} is varied through 360° , are shown in Fig 44. For these tests, the rf input to the receiver was modulated with a simulated omnirange signal. Two types of test equipment were available for these tests, a special laboratory type, built at the Technical Development and Evaluation Center, and a commercial type supplied by the Collins Radio Co.

Flight and laboratory tests conducted to determine the damping required in the course deviation indicator circuit to provide the best performance, showed that damping capacitors in the order of 5,000 mf or greater are satisfactory for omnirange courses, when operating from a source impedance of approximately 1,000 ohms. It was found, however,

$$KI = \left| \frac{\sqrt{E_1^2 + E_2^2 + 2 E_1 E_2 \cos \theta}}{\sqrt{E_1^2 + E_2^2 - 2 E_1 E_2 \cos \theta}} \right| -$$

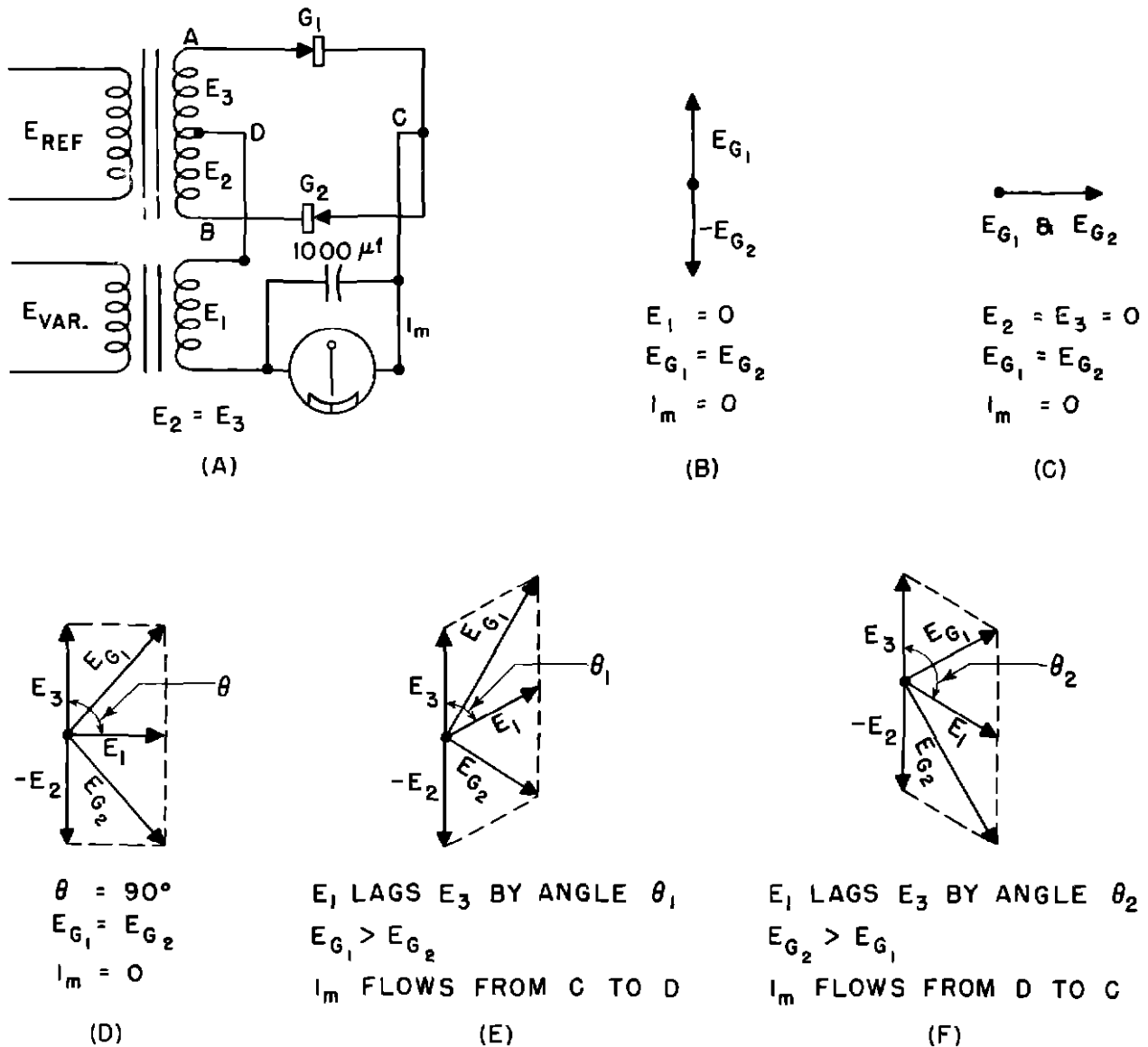


Fig 42 Phase Comparison Circuit and Vector Diagrams

that when flying localizer courses, the resultant lag in the indicated course was objectionable, and that a capacity of 1,250 mf is more desirable. As a result of these tests, it was recommended that a nonpolarized, electrolytic capacitor of 1,250 mf be used on course deviation indicators when the source impedance is approximately 1,000 ohms.

Minimum Omnirange Instrumentation

An example of omnirange instrumentation using the instruments described thus far, is illustrated in Fig 45. In the example shown, the aircraft is south of the station and flying a course to the station and beyond.

The omnibearing selector is set for a course of 350°. When flying this course to the station, the sensing is such that, when the needle of the course deviation indicator deflects from zero center, it is necessary to fly the aircraft in the same direction in which the needle deflects, in order to cause the needle to return to zero center, i.e., if the aircraft is flown to the left of the course, the needle will deflect to the right. To return to the course and have the needle read zero, the aircraft must be flown toward the right.

For the 350° omnibearing course to the station, the magnetic compass in the aircraft reads 350° also, neglecting crab angle and

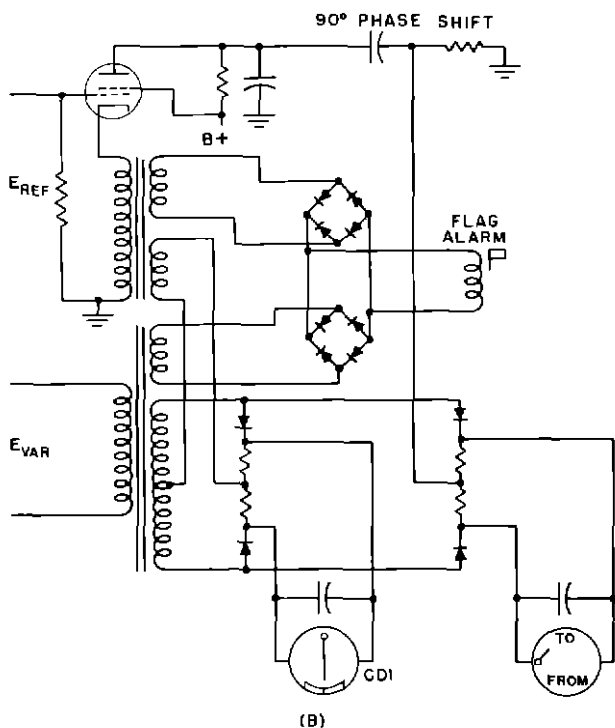
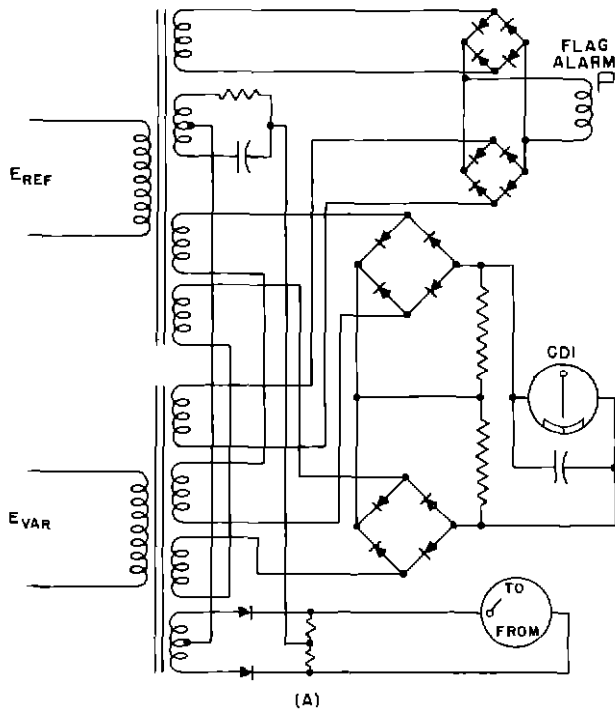


Fig 43 Phase Comparison Circuits With Flag Alarm and TO-FROM Indicators

instrument errors. As the aircraft passes directly over the station, the TO-FROM and course deviation indicators will show several rapid fluctuations. After passing the station, and continuing on the same course, the course deviation indicator will show on-course and have the same sensing as when approaching the station, but the TO-FROM indicator will point to the word FROM indicating that the magnetic bearing of the aircraft from the station is 350° . The magnetic compass will continue to read 350° , since no change of heading has been made.

If, after continuing on this course, the aircraft makes a turn of 180° , to fly the same course back to the station, the course deviation indicator and TO-FROM indicator will not change, except for small variations due to banking, etc. However, the magnetic compass will now read 170° and the sensing will be reversed. Therefore, it is necessary to change the omnibearing selector, to show a course of 170° to the station. This will cause the TO-FROM indicator to point to the word TO, and show the correct sensing of the course deviation indicator. It should be pointed out that, under the correct conditions of flying omnirange courses, the omnibearing selector should read approximately the same as the magnetic compass.

Fig 46 illustrates how the omnirange may be used to provide position and ground speed information to the pilot. The intersection of the two lines corresponding to the bearings observed from any two stations gives the position of the aircraft. A second similar observation made sometime later will provide information that can be used to determine actual ground speed of the aircraft.

The circuits and instrumentation described thus far cover the minimum requirements for omnirange operation. As shown in the block diagram, Fig 32, a switch is provided in the omnirange circuit, which also permits operation of the receiver on the phase comparison localizer facilities.

Omnibearing Indicators

To provide an automatic and continuous indication of the magnetic bearing to the omnirange station requires additional circuits and instrumentation. Four methods which have been used to accomplish this are shown in Fig 47.

The method shown in Fig 47(A) makes

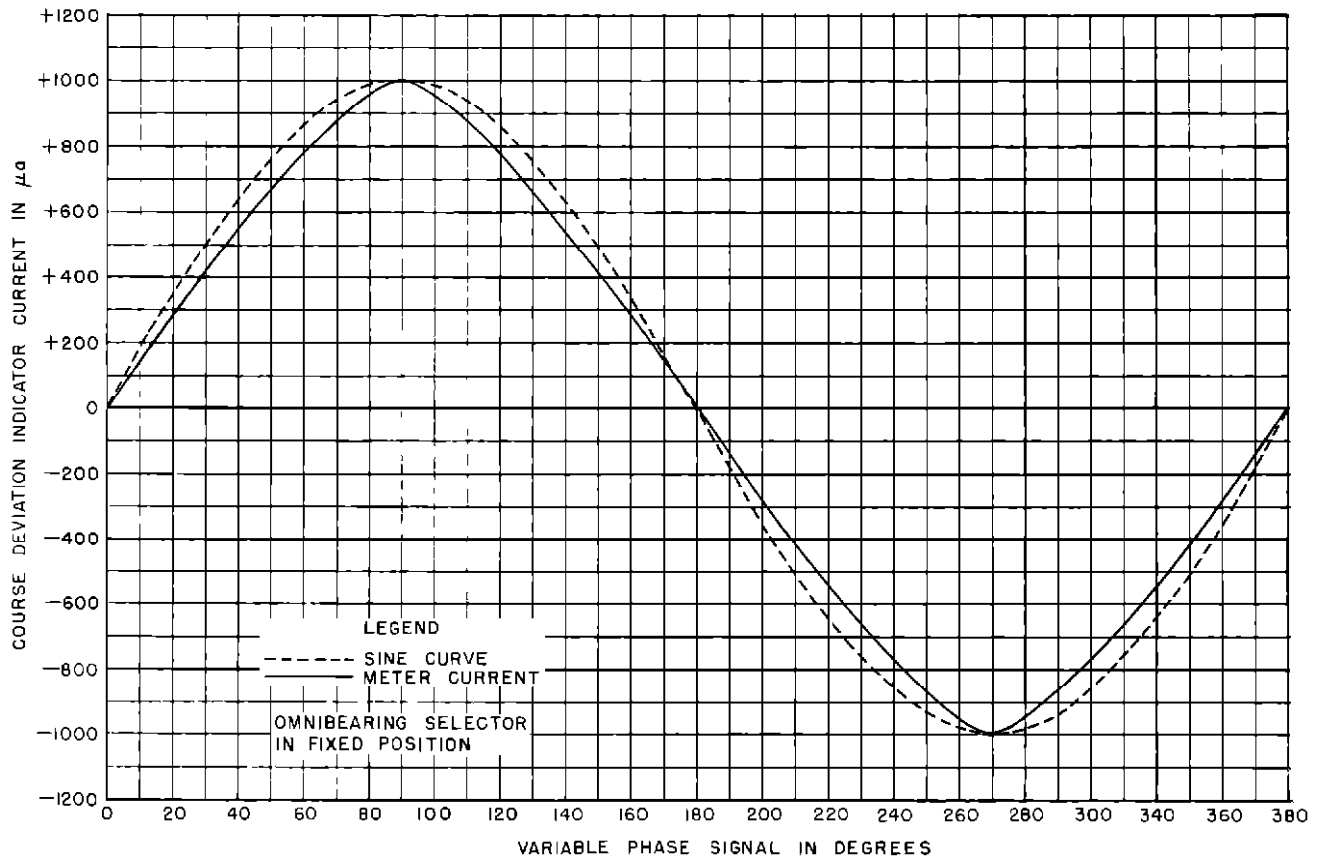


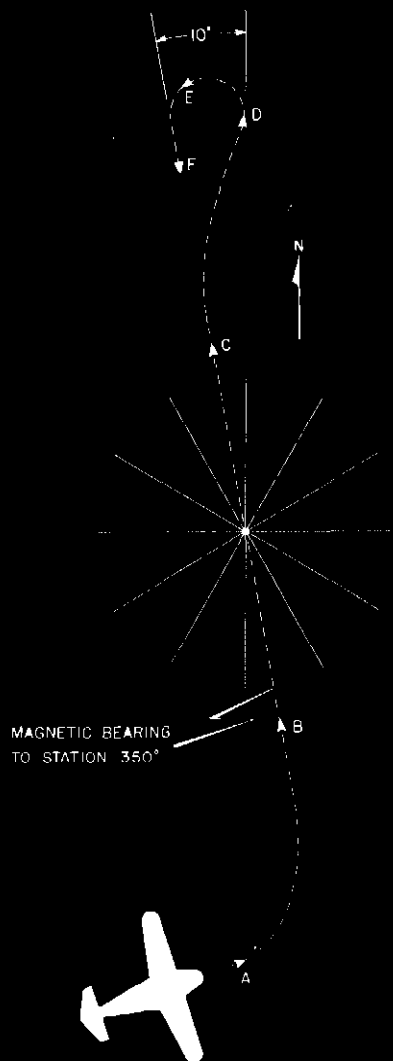
Fig 44 Course Deviation Indicator Current Versus Variable Phase Signal in Degrees

use of a cathode ray tube as the indicator and operates on the principle of controlling the intensity of the electron beam, which is making a circular trace on the screen. A phase splitting circuit is required to provide quadrature 30 cps voltages to the horizontal and vertical deflection plates for producing the circular trace. A triggering circuit produces sharply peaked pulses for the control of the electron beam. The resulting indication is a sharply defined spot on the screen, the angular position of which is determined by the phase relationship of the two voltages E_{REF} and E_{VAR} . This type of indicator operates at a 30 cps rate, and, therefore, cannot be damped for the purpose of removing rapid variations caused by noise, reflecting objects (either stationary or moving), propeller modulation, etc.

The method shown in Fig 47(B) uses a dc selsyn instrument as the indicator. The design of the instrument is similar to that of a magnetic compass, except that a magnetic shield is provided to prevent the earth's magnetic field from actuating the compass

needle, and two magnetic coils are arranged at right angles to each other to produce the magnetic field which actuates the compass needle. The circuit operates on the principle that two phase comparison circuits, having a 90° phase relationship with respect to each other, will produce two direct voltage components which are proportional to the sine and cosine, respectively, of the phase angle between the two 30 cps input voltages. The two direct voltages produce two magnetic fields in the selsyn instrument, and the resultant field causes the compass needle to indicate the phase angle between the two 30 cps input voltages. Satisfactory damping can be obtained by the use of capacitors connected across each field coil. The instrument itself can be damped by a high pole-strength/mass ratio of the cylindrical permanent magnet, and by the damping effect of the copper housing.

A third method which has been used to provide automatic indication of phase angles is shown in Fig 47(C). The instrument shown has two stators at right angles to each other

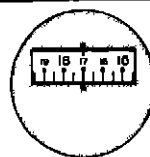
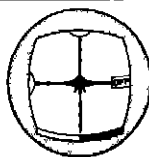


OMNIBEARING SELECTOR

COURSE DEVIATION INDICATOR

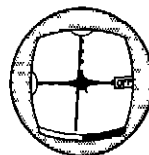
GYRO COMPASS

F



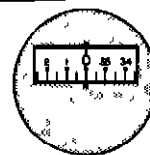
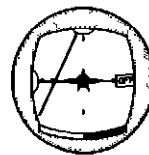
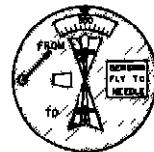
PILOT HAS CHANGED BEARING
SELECTOR TO 170° MAGNETIC
BEARING TO STATION SENSING
NOW CORRECT

E



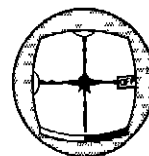
APPROACHING ON COURSE
SENSING INCORRECT

D



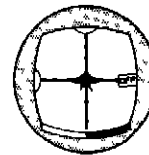
OFF COURSE 10° TO RIGHT

C



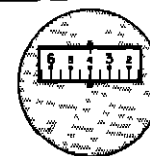
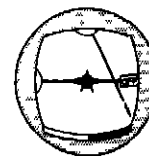
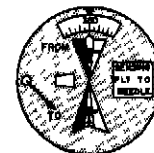
ON COURSE MAGNETIC BEARING
350° FROM STATION

B



AIRCRAFT ON COURSE MAGNETIC
BEARING 350° TO STATION

A



AIRCRAFT APPROACHING SELECTED
COURSE OF 350° (MAGNETIC) TO
STATION CORRECT SENSING

Fig 45 Omnirange Instrumentation

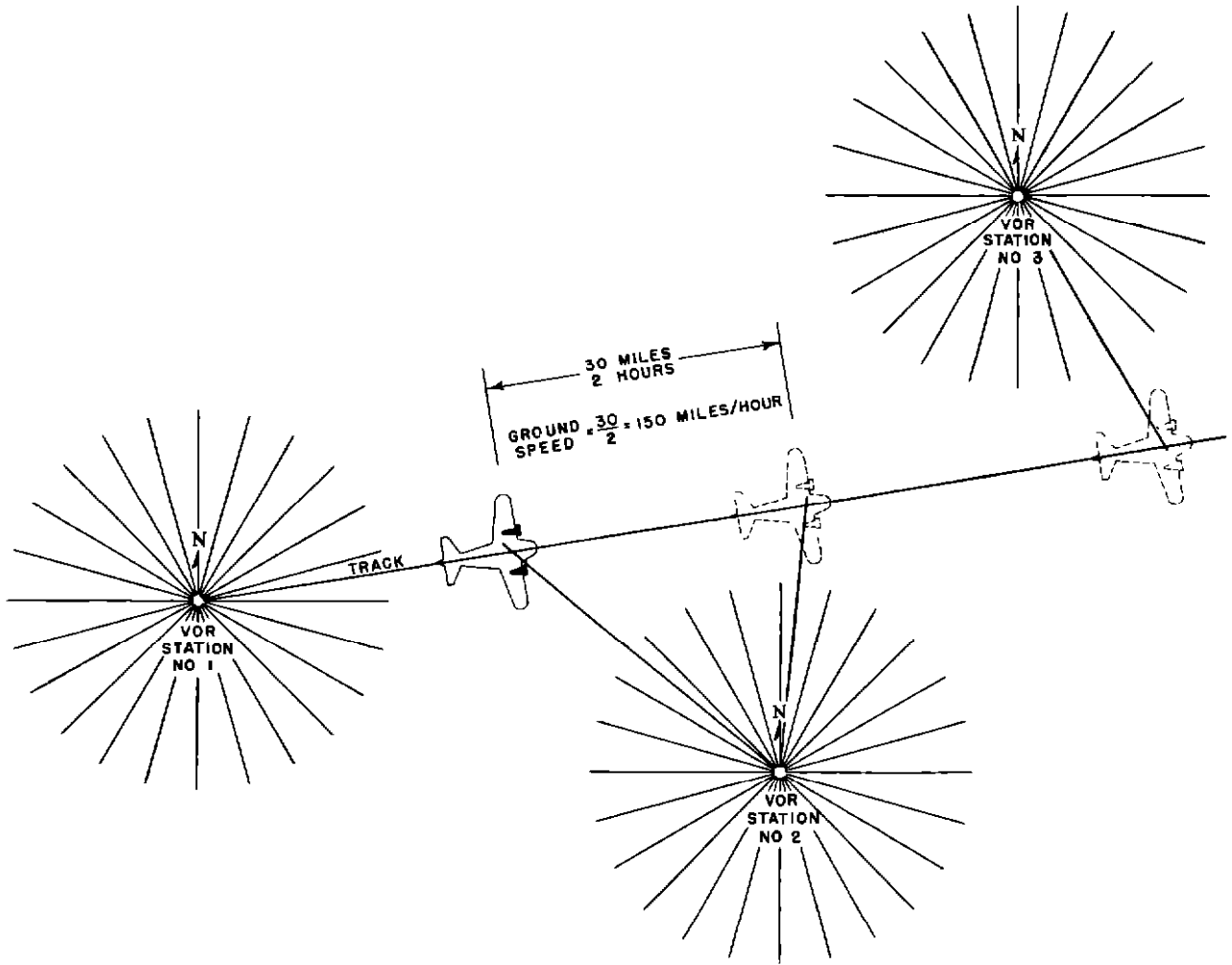


Fig 46 Omnirange Utilization for Determining Position and Ground Speed

and a single rotor winding. The two stators are supplied by the E_{REF} signal in a manner that provides 90° phase difference in the two stator voltages. This produces a 30 cps rotating field. The rotor is supplied by the E_{VAR} signal. This is, in effect, a phase meter similar in principle to the type commonly used in electric power generating stations. The power required to obtain satisfactory operation is excessive, and no easy method of damping is known. The most serious defect of this type of indicator is that, eddy currents generated in the rotor produce large errors when either supply voltage varies in amplitude.

Fig 47(D) shows a fourth method of providing an automatic phase indicator. As shown in the diagram, the E_{REF} signal is

split into quadrature components and fed to the stators of a phase shifter unit. The rotor output is fed into a servo amplifier, where it is combined with the E_{VAR} signal in a phase detector circuit. The phase detector circuit consists of two tubes which are connected to two saturable reactors which, in turn, are connected to a balanced two-phase induction motor. When an unbalance exists, the motor rotates, and, by means of a gear arrangement, turns the rotor of the phase shifter unit to the point where a balanced condition exists. Vector diagram 1, Fig 47(D), shows the condition when the circuit is balanced. The voltages E_1 and E_2 combine with voltage E_3 to provide equal voltages E_4 and E_5 to the grids of tubes V_1 and V_2 . Under this condition, the two saturable reactors have equal currents

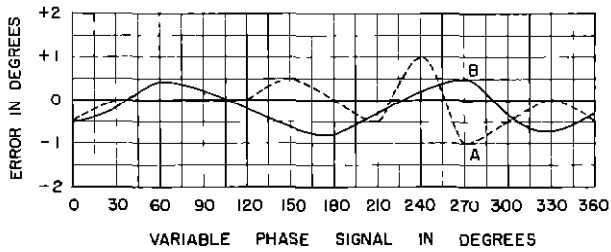


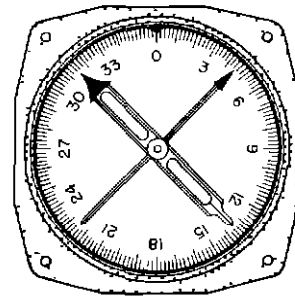
Fig 48 Error Curves of Omnibearing Indicators

flowing through them, and, as a result, the induction motor will not rotate, since its supply circuit is in a balanced condition. Vector diagram 2 shows the condition when the circuit is unbalanced. Voltages E_4 and E_5 are of different amplitude and, as a result, the currents through the saturable reactors are of different amplitudes. This creates an unbalance in the motor circuit, causing it to rotate and turn the rotor of the phase shifter to a position where a balanced condition again exists.

Fig 48 shows the results of tests made to determine the error of two different types of omnibearing indicators when using laboratory test equipment. Curve A shows the error of a dc selsyn instrument when operating in the circuit shown in Fig 47(B), and curve B shows the error of an inductive instrument when operating in the circuit shown in Fig 47(D).

Radio Magnetic Indicator

The navigation indicators described thus far provide omnirange bearing and course information independent of the aircraft heading. An instrument has been developed that is known as the radio magnetic indicator (RMI) which, when used in combination with the omnirange and flux gate or gyrosyn systems, will automatically show both the heading of the aircraft and the magnetic bearing of the aircraft to the station. The instrument is, in effect, an omnibearing indicator, as previously described, together with a servo unit operating from the flux gate or gyrosyn system. The complete omnibearing indicator rotates to a position determined by the heading of the aircraft. The pointer of the instrument will point to the station, and this indication is analogous to that of the 360° indicators used with low frequency automatic radio



RADIO MAGNETIC INDICATOR

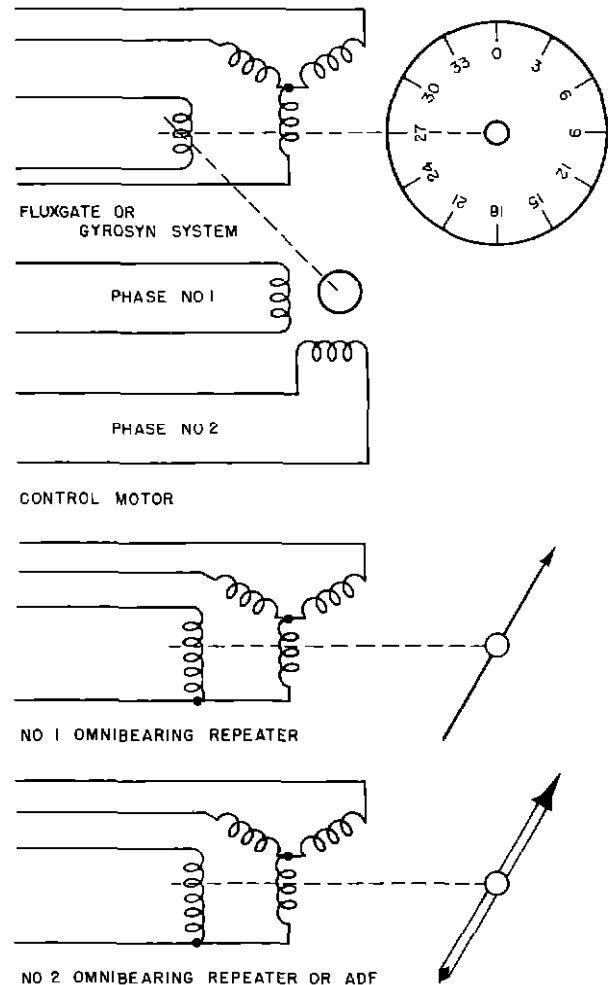


Fig 49 Radio Magnetic Indicator Circuit Diagram

compasses. Fig 49 shows the circuits of this instrument. Fig 50 illustrates the use of omnirange instrumentation, which is similar to that shown in Fig 45, except that the radio magnetic indicator is included.

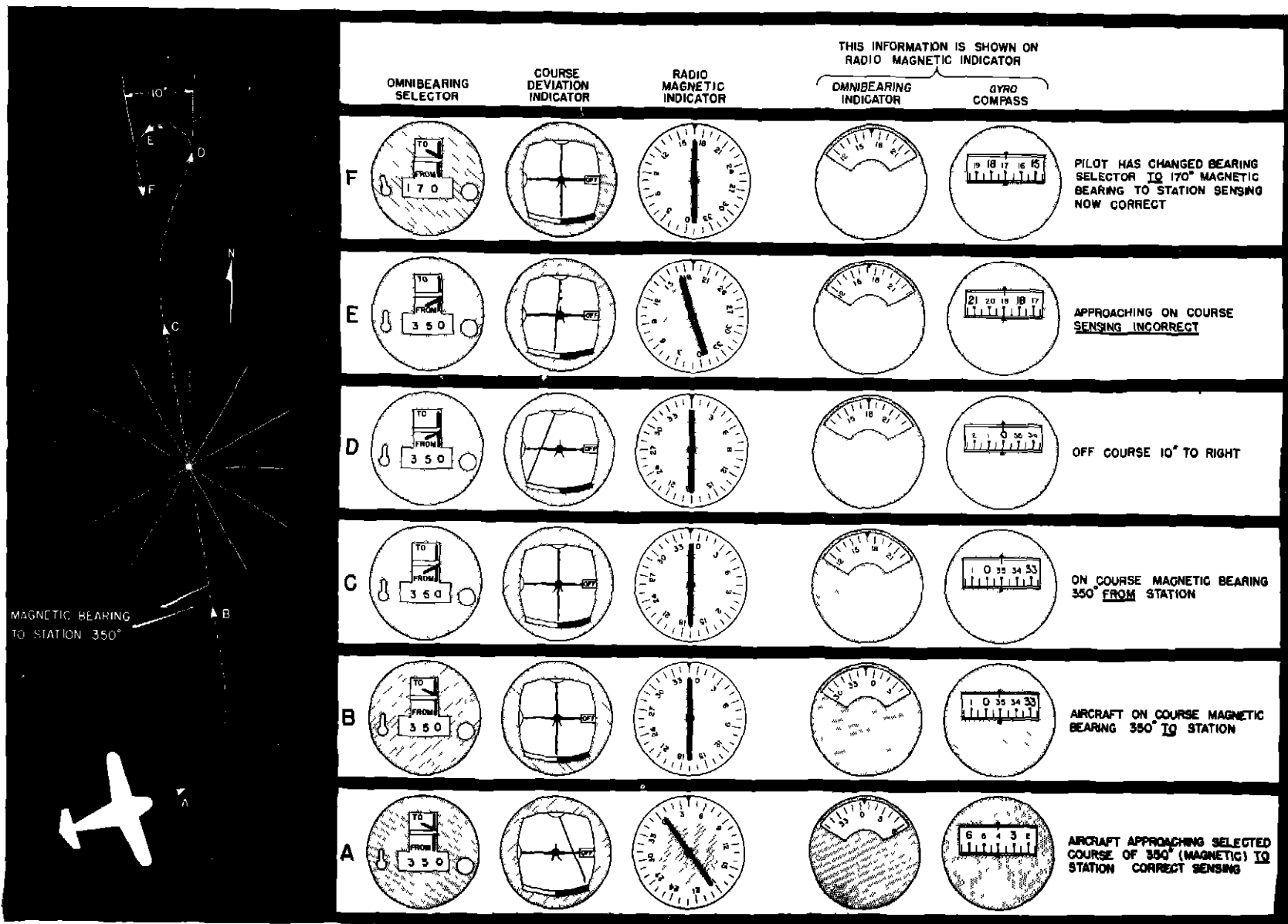


Fig 50 Omnirange Instrumentation Combined With Magnetic Information

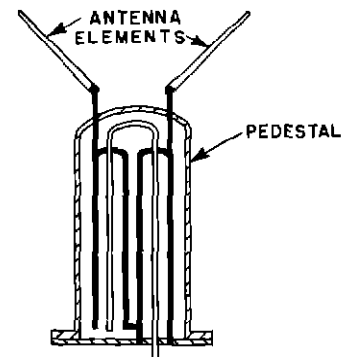
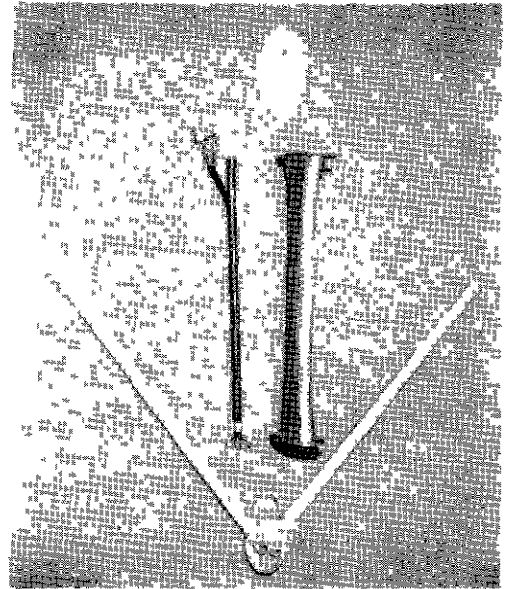
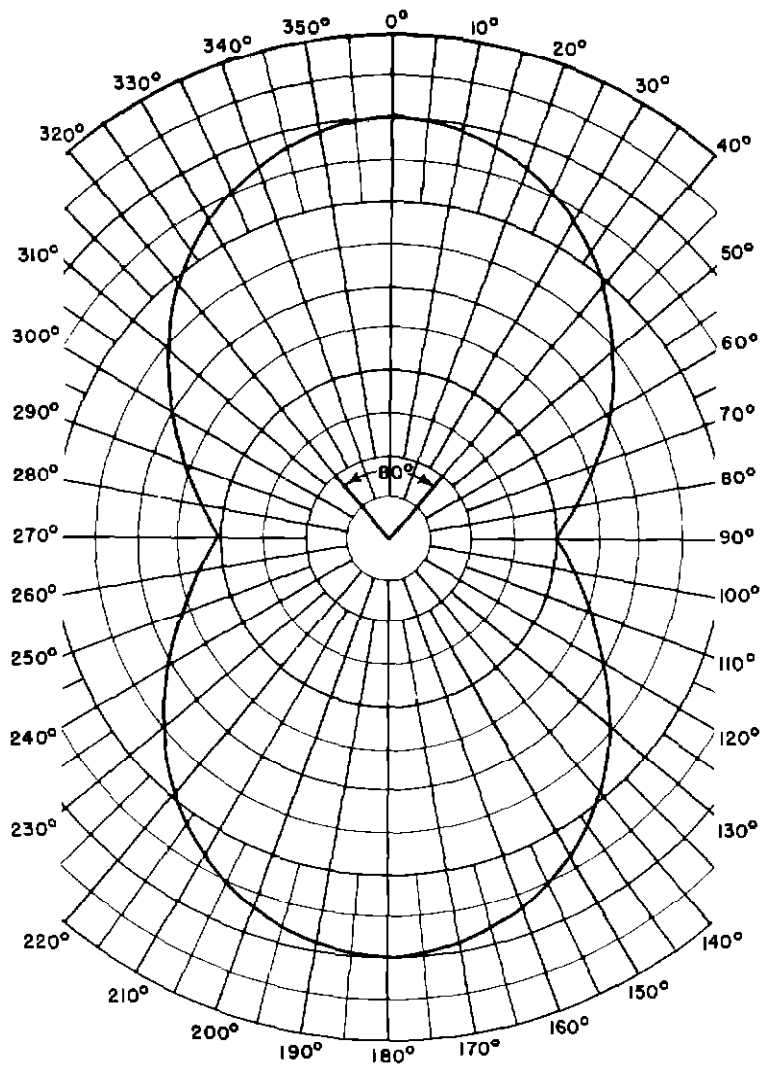


Fig 51 Calculated Field Pattern in Horizontal Plane, Balun Arrangement and Component Parts

Aircraft Antenna

Since the signal radiated from the omnirange station is horizontally polarized, it is necessary that the aircraft antenna be designed to receive horizontally polarized signals. One type of antenna which has been used extensively for reception in the frequency band of 108 to 122 Mc is the V type antenna the parts of which are illustrated in Fig 51. The diagram in this illustration shows the method used to convert from a balanced antenna to a coaxial transmission cable. The impedance matching between the antenna, which has been determined to have a radiation resistance of approximately 33 ohms, and the standard 52 ohm RG 8/U cable, is accom-

plished by using a one-quarter wavelength balun section having 42 ohms impedance. Also shown in this figure is a calculated field pattern for an antenna having one-quarter wavelength elements and an apex angle of 80°.

The aircraft antenna is usually installed either on top of the fuselage behind the pilot's compartment or on the tail structure as shown in Figs 52 and 53. For this reason, it is necessary to make antenna measurements over a ground plane and also in free space. Standing wave ratio measurements of the V type antenna between 108 and 122 Mc for free space conditions showed a minimum of 1.3 and a maximum of 3.0. Similar measurements made over a ground plane showed a standing

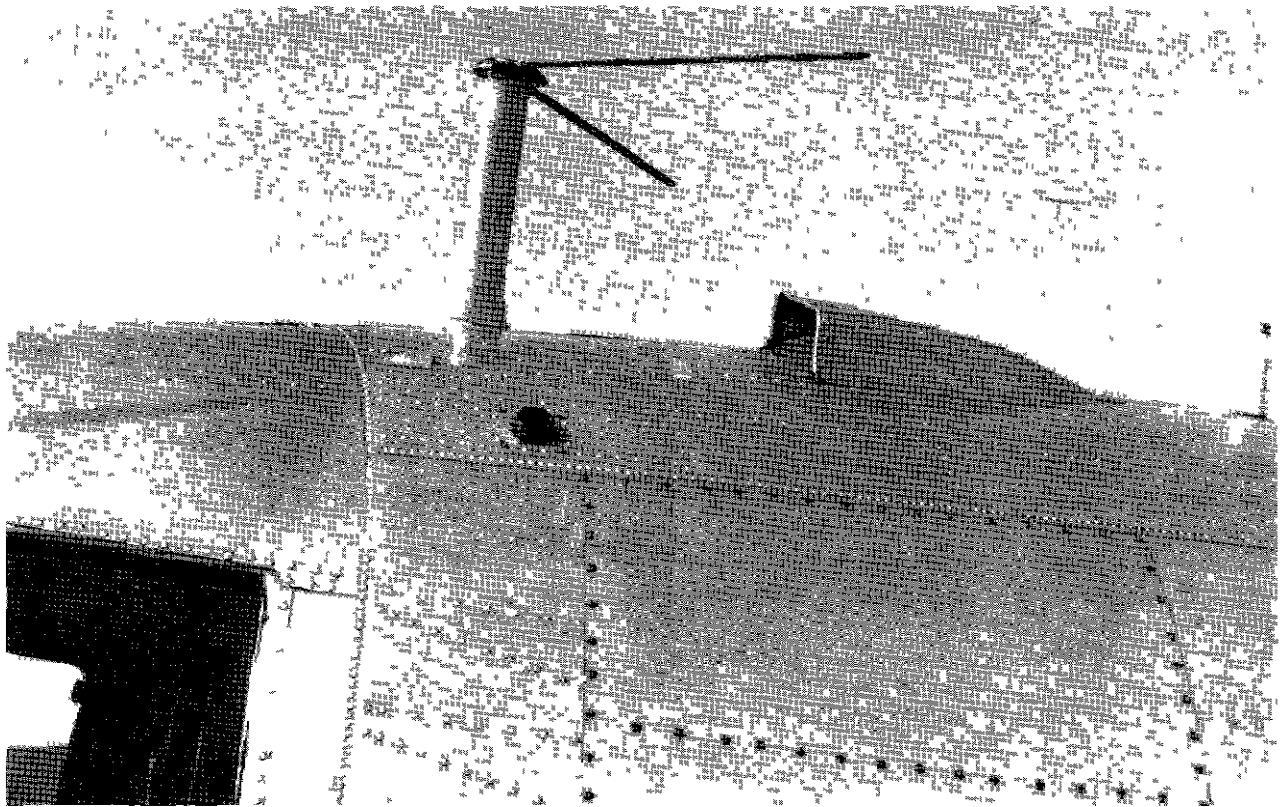


Fig 52 Antenna Mounted on Fuselage

wave ratio minimum of 1.4 and a maximum of 3.0. A slotted transmission line was used to make these measurements. Fig 54 shows the comparison of gain measurements with respect to a standard dipole antenna.

Receivers and Their Characteristics

In the early stage of development of the omnirange system, several experimental airborne receiving equipments were developed and tested. One experimental model developed in 1945 used a localizer receiver, Air Forces Type BC-733-D which was modified for omnirange operation by attaching an omnirange converter unit and changing the frequency range from 108-112 Mc to 113-117 Mc. The receiver was of the superheterodyne type and had six crystal-controlled channels. Many difficult problems were encountered in the development of the omnirange converter unit and navigation controls, however, the performance obtained in laboratory and flight tests was very good. Either of two types of omnibearing selectors could be used, one was an inductive type, and the other was a

resistive type. The automatic omnibearing indicator was a dc selsyn instrument. The modified receiver weighed 30 lb and operated from either a 14 or 28 v dc supply. Because of the bandwidth limitation of these experimental receivers, they were eventually replaced by commercial navigation receivers which became available in 1946.

The first commercial omnirange receiving equipment was developed in 1946 by the Aircraft Radio Corporation. The receiver is an 8-tube superheterodyne having continuously variable tuning over the frequency range of 108 to 135 Mc. Bearing indication is provided by means of suitable navigational indicating instruments. Plate voltage is obtained from a dynamotor power supply. The equipment, exclusive of cables and the like, weighs approximately 30 lb, and units are produced for operation on either a 14 or 28 v dc supply. This equipment is designed to receive omnirange, phase comparison, and tone localizer signals, as well as communications.

Fig 55 shows the Type 51R-1 airline

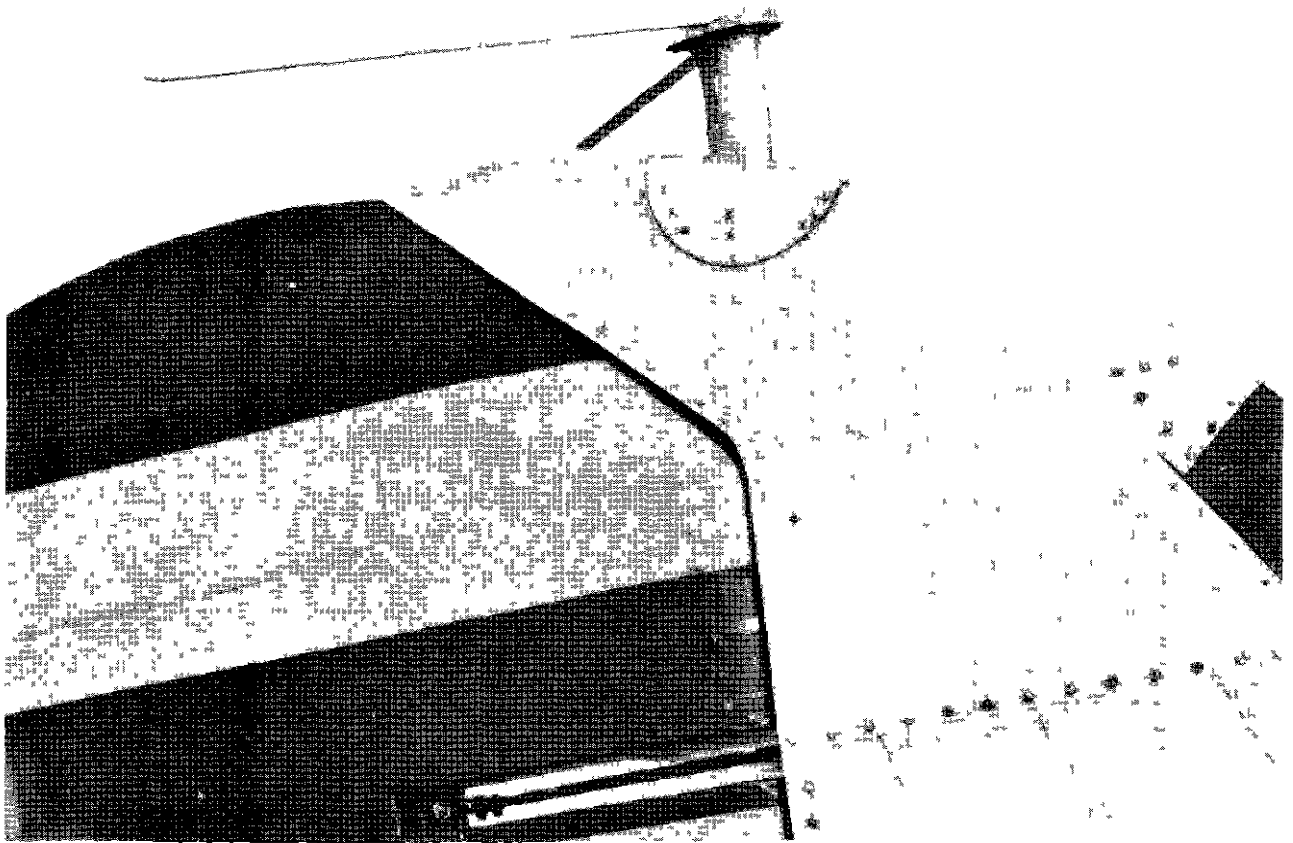


Fig 53 Antenna Mounted on Vertical Stabilizer

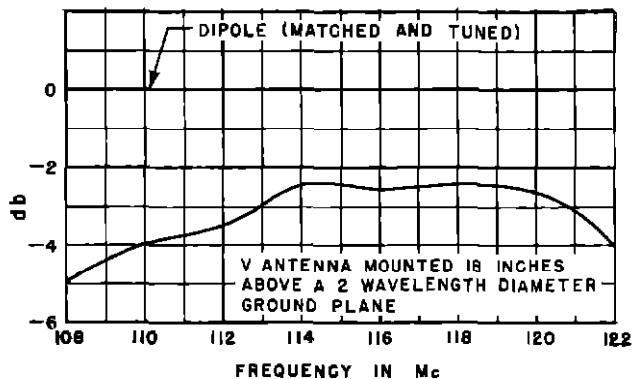


Fig 54 Gain Characteristics of Dipole and V Antennas

to 135 Mc in 100 kc steps by a remotely controlled mechanism called an "autopositioner". Bearing information is provided by a complete set of instruments including, a course deviation indicator with flag alarm, an omnibearing indicator, a radio magnetic indicator, and an omnibearing selector with a TO-FROM meter. Plate voltages are obtained from a dynamotor power supply available for either 14 or 28 v dc operation. In addition, the full instrumentation requires a source of 28 v 400 cps. The total weight of the complete unit is approximately 48 lb, and reception of either tone or phase comparison localizer and omnirange facilities, in addition to communications, is provided.

Late in 1947, a program was undertaken by the CAA to create commercial interest in the development of a low cost, light weight navigation receiver for private flyer use. A

type equipment recently developed by the Collins Radio Co. The receiver is a double superheterodyne which may be tuned from 108

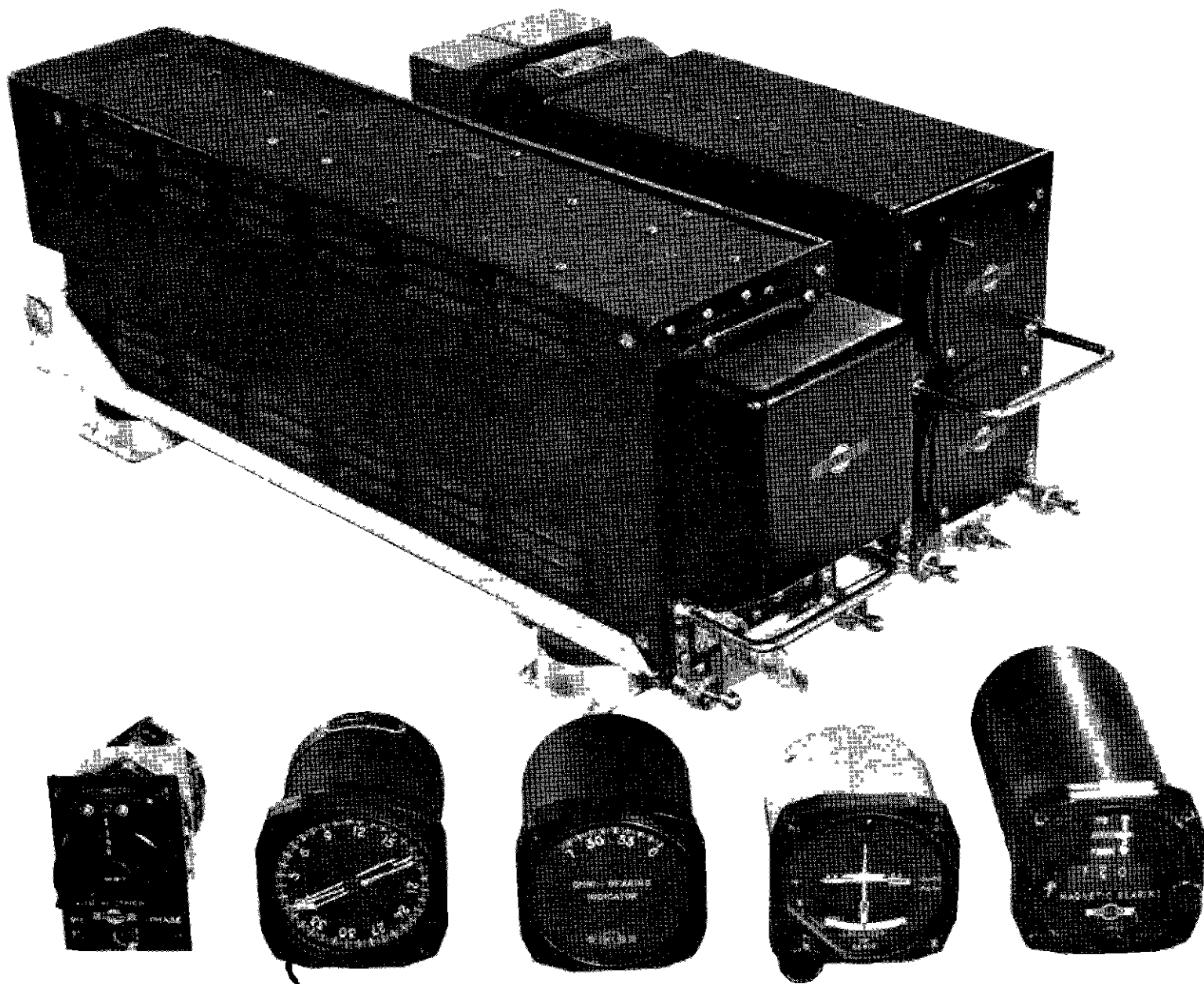


Fig 55 Collins Type 51R-1 Navigation Receiver

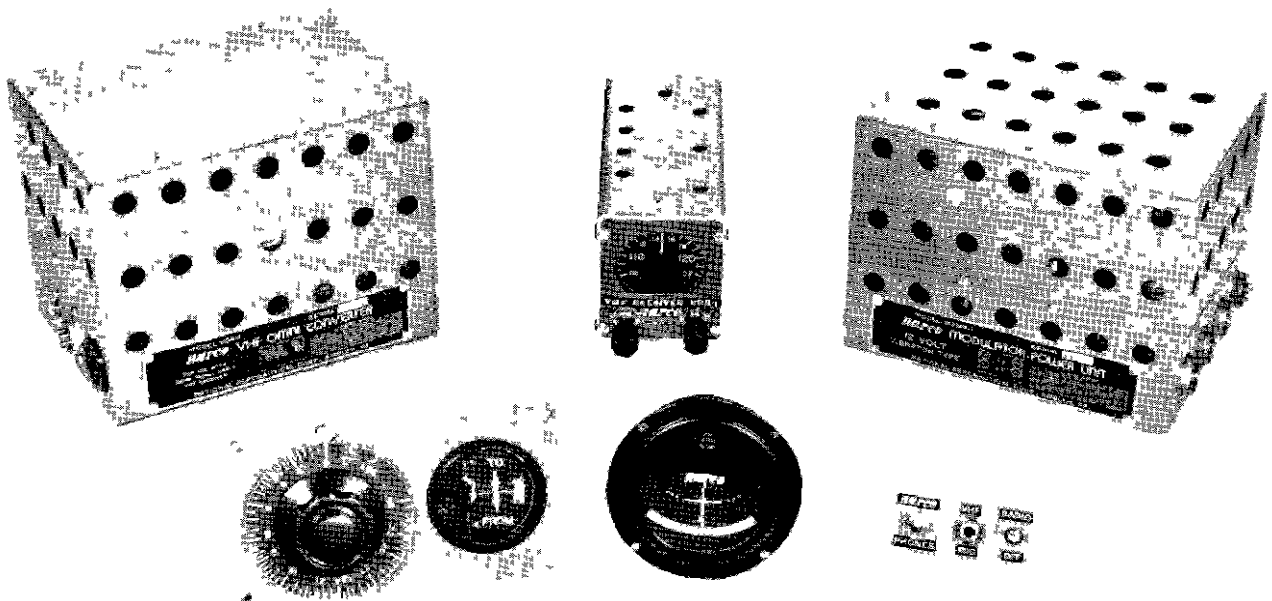


Fig 56 NARCO Model VRA-1 Navigation Receiver

specification was prepared which provides for the minimum of performance considered essential for itinerant flying. To insure that the objective of the program be achieved, bids were obtained on the basis of developing and delivering ten complete receivers and furnishing quotations for additional quantities. As a result, a contract was entered into with the National Aeronautical Corp., the low bidder. Fig 56 shows the Model VRA-1 equipment which was supplied on this contract. The receiver is a 7-tube superheterodyne having continuously variable tuning over the frequency range of 108 to 122 Mc. Bearing information is provided by a tapped-potentiometer type bearing selector, a TO-FROM indicator, and a single needle type course-deviation indicator. Plate voltage may be obtained by either a 12 or 14 v vibrator, or a 24 v dynamotor power supply. The total weight of the unit, exclusive of cables, is 15 lb. and the equipment provides for the reception of omnirange, phase comparison localizer, and communication signals. Provision is made for adding a VHF transmitter unit to this equipment.

OMNIRANGE OPERATIONAL CHARACTERISTICS

Siting of Ground Stations

The VHF omnirange requires reasonably

good sites, and it is important that suitable sites be selected. Surfaces formed by objects such as trees, buildings, wires, hills, etc., re-radiate or attenuate energy from the antenna system, causing course deviation indicator fluctuations.¹⁶ Course errors result if the fluctuations are very slow. A large number of installations offering a variety of siting conditions have been studied to determine siting requirements for satisfactory operation of the omnirange.

To briefly summarize siting requirements, it has been found that the site must be located on flat terrain or on top of a knoll having uniform contours for a distance of 1,500 feet and cleared of all obstacles, such as large buildings, woods, power lines, etc., capable of serious re-radiation, to a distance of 1,000 feet. In addition, all obstacles within 2,000 feet should subtend an angle in the vertical plane of less than 2°, and the power line to the station should be installed underground for a distance of 750 feet.

¹⁶J. M. Lee, R. G. Pamler, and B. M. Lahr, "An Investigation to Determine the Characteristics of Horizontal and Vertical Polarization for Very High-Frequency Two-Course Visual Radio Ranges," CAA Technical Development Report No. 58, July 1947.

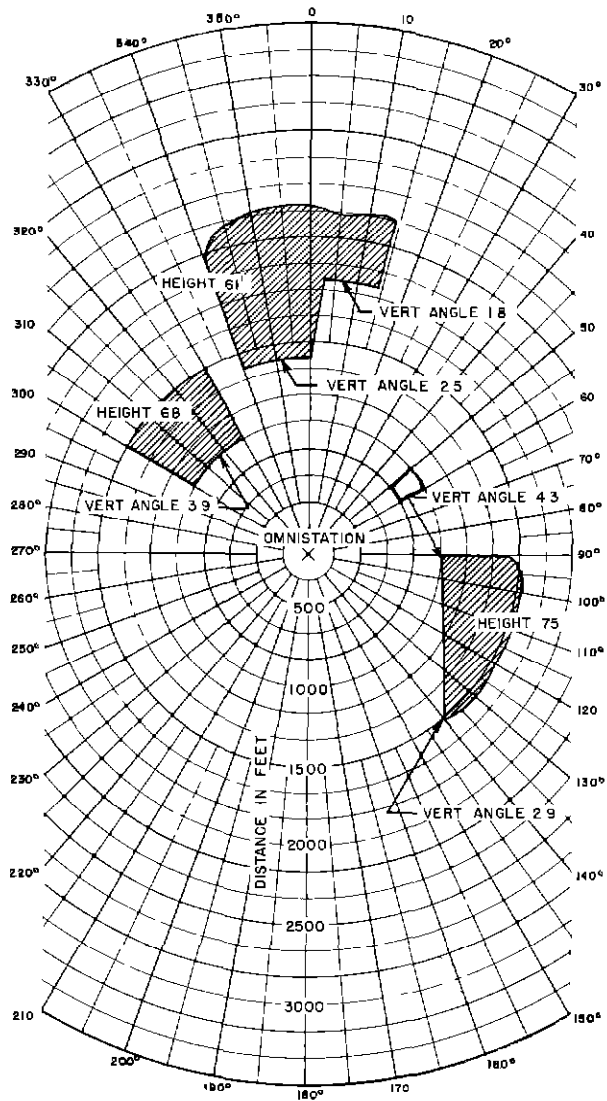


Fig 57 Tree Locations and Heights of the Third Region VOR Site

Examples of conditions found at two sites on level terrain are shown in Figs 57 and 58. In the installation illustrated in Fig 57, flight tests revealed an average scalloping of $\pm 2^\circ$ at a radius of 25 miles, while at the site shown in Fig 58, scalloping was limited to $\pm 1^\circ$.

An installation in a mountainous location indicated that satisfactory results could be obtained if the range is installed on a flat, level-topped hill, at least the height of surrounding terrain. In mountainous terrain it has been found desirable to locate omnirange stations on high ground which is as level as

possible in the vicinity of the station. In all cases it has been found that a counterpoise 15 feet in height or less provides superior courses to a 30-foot type.

Distance Range and Course Deviation Indicator Fluctuations

Flight tests have confirmed the fact that VHF navigational facilities are limited to a usable distance range approximating line-of-sight. Certain rare cases have been reported where the distance range was found to be much greater than line-of-sight for a short time. However, this phenomenon has not been experienced at the Technical Development and Evaluation Center.

Fig 59 shows reproductions of flight recordings of the course deviation indicator deflections, when flying a straight ground track from an omnirange station, and when flying over the station at 10,000-foot altitude. The variation in course-width is indicated by the deflections on the recording, for adjustments of the omnibearing selector, of $\pm 10^\circ$. It will be observed that the course deviation indicator fluctuations are very small in amplitude on this recording. Course fluctuations are caused mainly by poor site conditions at the range stations and, therefore, some stations will show more course fluctuations than others. Although a 20° course-width was used for these tests, flight experience has shown that a 30° course-width is more satisfactory from the pilot's viewpoint. The site conditions at this range station are considered good. The course fluctuations shown on the recording made at 10,000 feet indicate a cone area directly over the station where the bearing information is not accurate. However, these violent fluctuations are such that they provide a positive position indication over the station.

Course Stability

The prototype VHF omnirange which has been operating for more than three years, has been monitored continuously. Faults have occurred at the station, due usually to a tube failure, causing, for example, low power output with very high 9.96 kc modulation, at which time a course measurement by the monitor was not possible because of low signal levels. However, during normal operation the course monitor has indicated a maximum

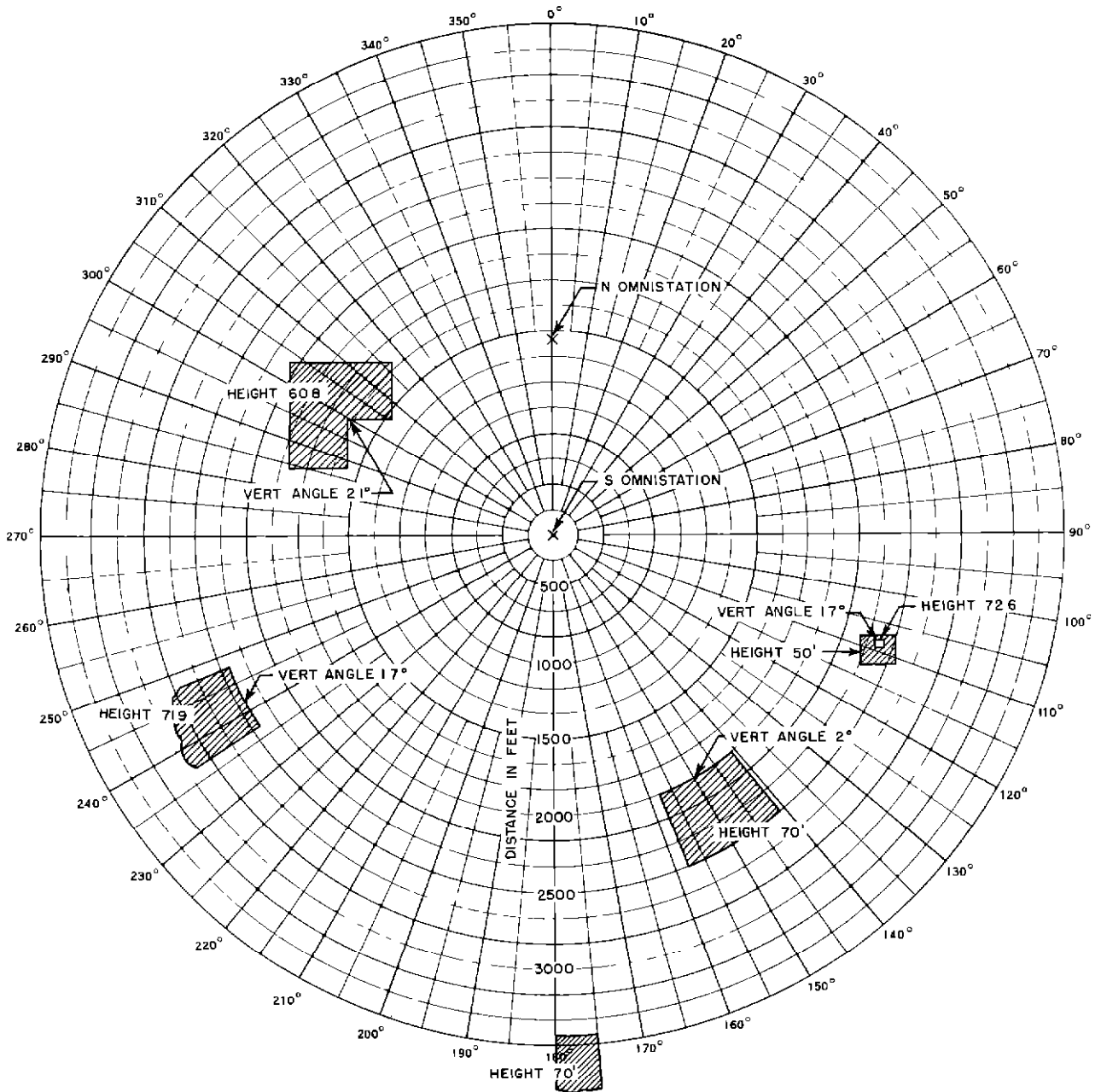
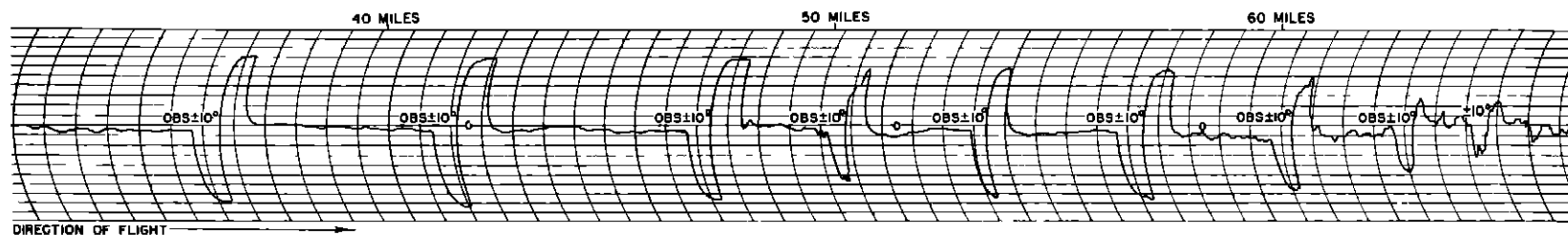
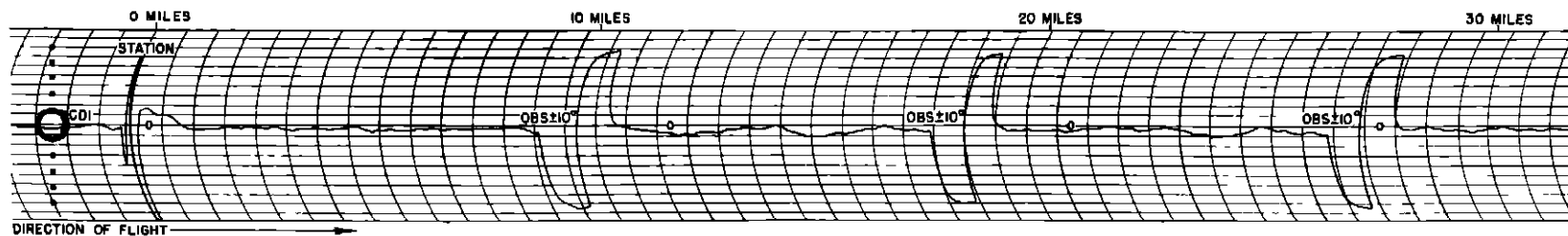


Fig 58 Tree and Building Locations and Heights of the Experimental VOR Site

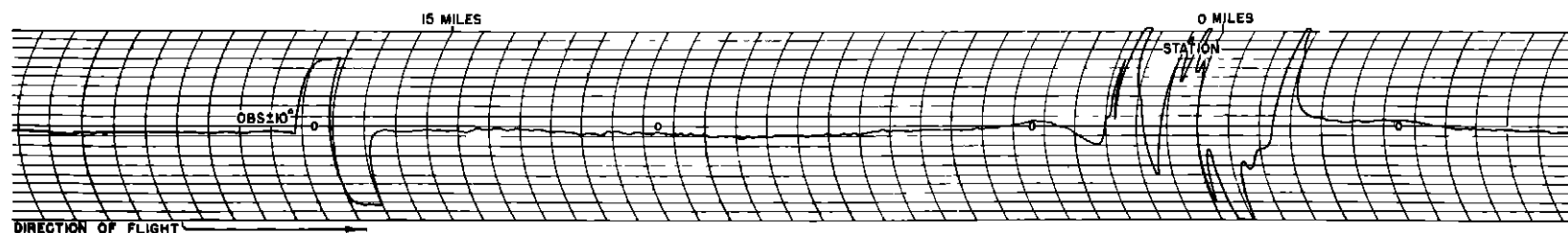
of 1° deviation from the correct reading. Fig 60 shows a set of monitor readings which were taken over a period of 30 days. The monitor antenna is located on a line, magnetic north of the station, where the two figure-of-eight patterns are of equal magnitude, so that any change in relative sizes of the patterns will be observed. Courses in other directions have been checked either by a theodolite flight

calibration of the facility or by turning the antenna array through 360°. Stability comparable to that indicated at the monitor was found.

During the development of the omnirange, the capacity goniometer was fed with unmodulated carrier from the amplifier driving the final rf stage of the transmitter. This arrangement proved unsatisfactory, be-



DISTANCE FLIGHT RECORDING, 1000' ALTITUDE ABOVE GROUND



RADIAL FLIGHT ACROSS VOR 10,000' ALTITUDE ABOVE GROUND

LEGEND

CDI - COURSE DEVIATION INDICATOR
OBS - OMNIBEARING SELECTOR

NOTE

TYPE S1R RECEIVER
TAIL V109 ANTENNA
C47 TYPE AIRCRAFT

Fig 59 Recordings of Course Deviation Indicator at Two Altitudes

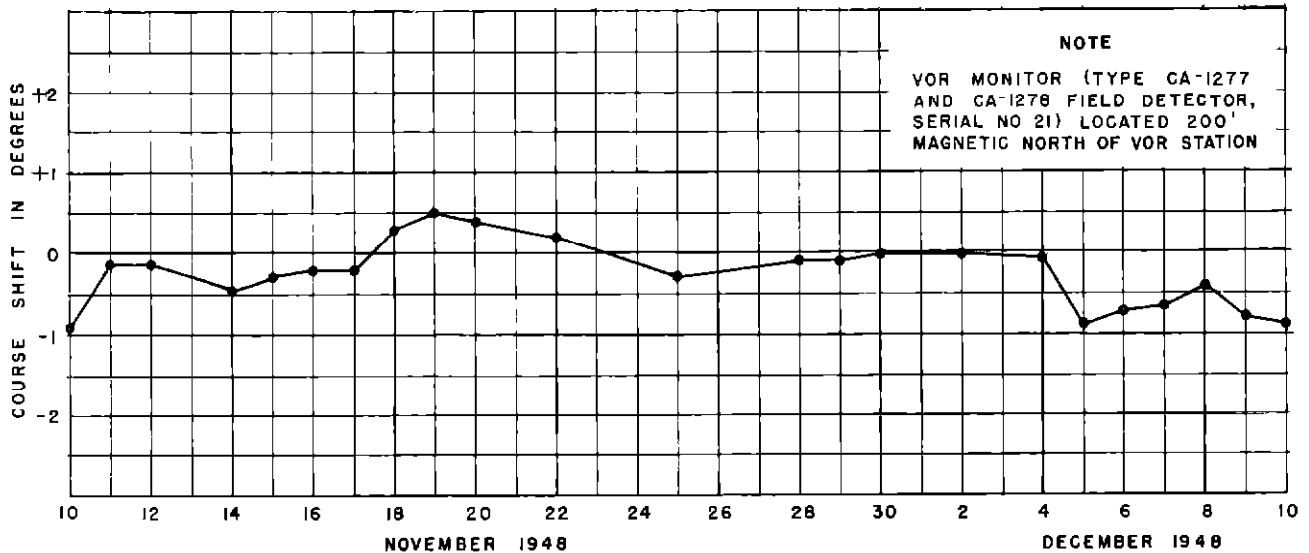


Fig 60 Course Shift as Indicated by the VOR Monitor Versus Time

cause detuning of the power amplifier changed the phase between the energy fed to the goniometer and the center antenna, resulting in a change in courses and in the modulation percentage of the variable phase signal. Figs 61 and 62 show typical examples of the changes in 30 cps modulation percentage and course error caused by detuning. The modulation eliminator was incorporated in the equipment for the express purpose of eliminating the instability caused by detuning effects.

Station Accuracy

Following the completion of the prototype omnirange, a series of tests was conducted to determine the accuracy of the bearing information transmitted from the station. In these tests the antenna array was rotated through 360° , and the phase of the variable phase signal (obtained from a field detector) was compared on a cathode ray oscilloscope with a known amount of phase shift introduced by an accurately calibrated phase measuring device. The calibration which was obtained in this manner is shown in Fig 63.

Eighteen months later, the accuracy of the station was again checked using similar techniques, except for the substitution of a phase standard for the earlier phase measuring device. The results of these tests are shown in Fig 14. To simplify these calibration tests the subcarrier was not transmitted since it had previously been determined that no error was introduced by the

presence of the reference phase signal. The errors of Figs 63 and 14 may be caused by a departure from quadrature relationship in the two outputs of the capacity goniometer, unequal amplitude of the figure-of-eight patterns, incorrect location of the nulls of the figure-of-eight patterns and the like. Reflecting upon the theoretical treatment in an earlier part of this report, Fig 7 illustrated the error curve that was predicted for an omnirange installation, but those shown in Figs 63 and 14 do not adhere to the theoretical pattern. The reasons for the difference are not fully understood at this time, but it is not surprising that a difference exists, since the octantal error curve shown in Fig 7 is based on point source radiators, each producing a circular field pattern of constant phase. The radiators used in practice are far from point source radiators, their patterns are not exactly circular, and the rf phase may vary with azimuth.

Flight Calibration

The flight calibration of an omnirange system is described in a previously published report,¹⁷ and only a brief description of the method used will be given here. Fig 64 shows the method used to calibrate an omnirange

¹⁷T. S. Wonnell, "Flight Calibration of VHF Omnirange System" Technical Development Report No. 69, July 1947.

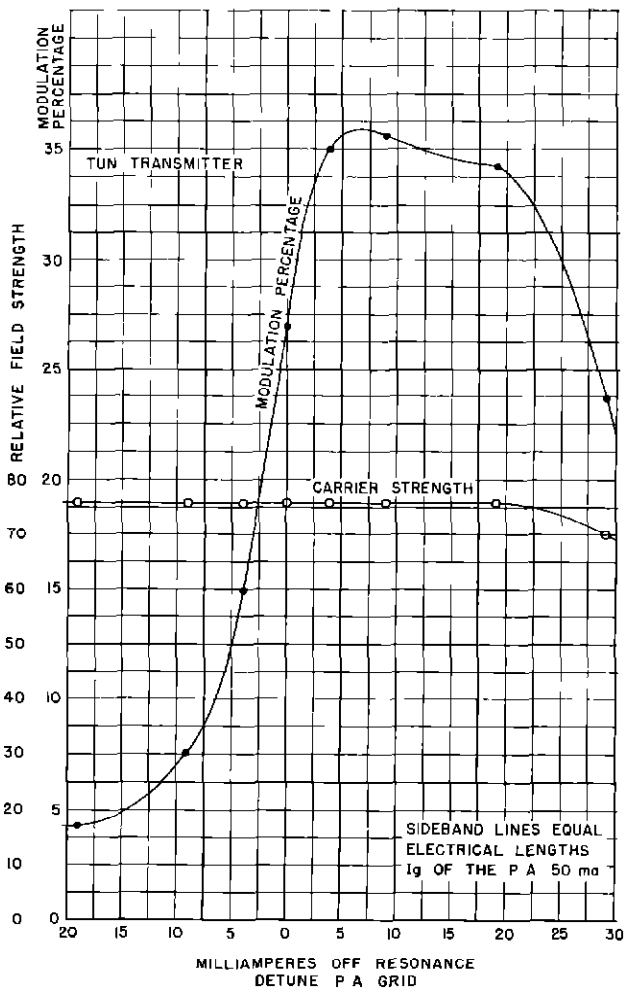


Fig 61 Variable Phase Signal Modulation Percentage and Carrier Strength Versus PA Grid Tuning

station and consists of recording the voltage applied to the course deviation indicator as the aircraft circles the station at a radius of 6 to 15 miles. The omnibearing selector is advanced in 10° steps to keep the course deviation indicator on scale and to provide a recording whereby the indicated magnetic bearing from the range station may be obtained. The indicated bearing is compared with the magnetic bearing, as measured by a theodolite operated on the ground at the range station.

The interpretation of the recording obtained by this method is explained with reference to the sample recording reproduced in Fig 64(C). The exact magnetic bearing, as observed by the theodolite operator, is shown by the leading edge of the marker pen de-

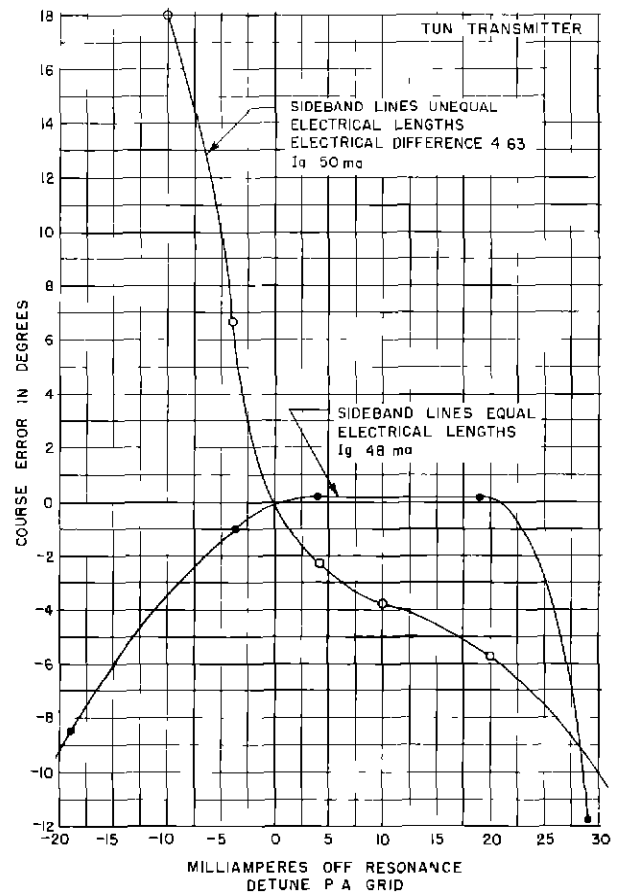


Fig 62 Course Error Versus PA Grid Tuning

flection at the top of the recording. The omnibearing selector settings are shown at the lower part of the recording.

Starting our interpretation of the sample recording from the left, it is seen that with an omnibearing selector setting of 190° at Point B, which is center scale, the indicated bearing of the aircraft is 190° . Point B is extended to Point C which, with respect to the markings made by the theodolite operator, is in error by $+1.8^\circ$. The distance between AD is equal to 5° and by simple proportion the error of Point C is obtained.

Fig 65 is a reproduction of a typical omnirange calibration recording, and Fig 64(D) is the measured over-all error curve of the receiver and transmitting station. The error curve shows that the station must be corrected by 3° to place it at the average error position and the resulting over-all error will be $\pm 1.1/2^\circ$.

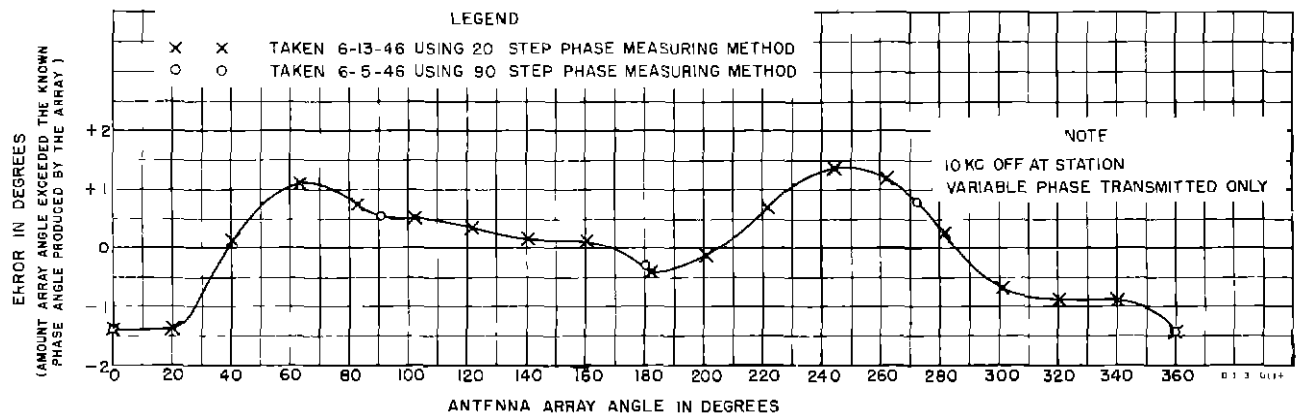


Fig 63 Error Curve of VOR Antenna Array

Polarization Errors

Tests have demonstrated that, while the omnirange antenna array radiates horizontally polarized energy, currents induced on the surface of the pedestals supporting the side-band loops, radiate energy that is vertically polarized. This vertically polarized energy will produce omnibearing indications which are at quadrature with true bearing information, and errors caused by such radiation are termed polarization errors.

If an aircraft equipped with a navigation receiver flies over a fixed ground check point at a number of different headings, the indicated omnibearing may be found to vary with heading. The aircraft has only one correct omnibearing when over the ground check point, and it is independent of heading; consequently, the change in the omnibearing with heading is one form of polarization error and is referred to as push-pull error. The term comes

from early navigational aids work where the course was observed to be pushed ahead of the aircraft, or pulled toward the aircraft when flying across course. The aircraft receives primarily the signal from the horizontally polarized wave; however, as the heading is changed, the ratio of vertically to horizontally polarized pickup varies, producing different omnibearing indications when over a ground check point. Polarization errors in general vary with the type of aircraft and with the location of the receiving antenna on the aircraft. Table II shows how the push-pull error may vary with heading. Many attempts have been made to reduce the polarization error. The most successful of these was the placement of Uskon cloth around the pedestals, as a group, and insulated from the pedestals by wooden strips. This cloth, having an rf resistance of about 377 ohms per square, and extending from the top flange located 39 1/4 in

TABLE II

(Aircraft Located at 0° Azimuth)

Bearing Selector Readings for the Following Headings

Headings (degrees)	0	90	135	180	225	270	315	Maximum Over-all Error
Pedestals exposed	-1.5	0	-3.0	-2.5	+1.0	-3.0	-6.0	7.0
Uskon cloth around pedestals	-1.0	0	-1.5	-1.6	-0.5	-1.0	-1.0	1.6

Push-pull polarization error tests in a DC-3 aircraft with a receiving antenna located just behind the astrodome

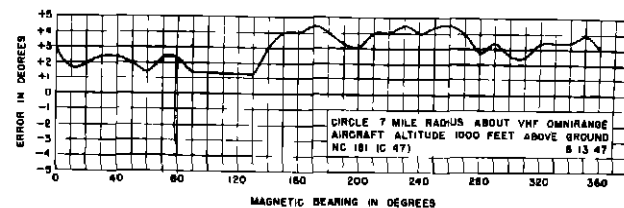
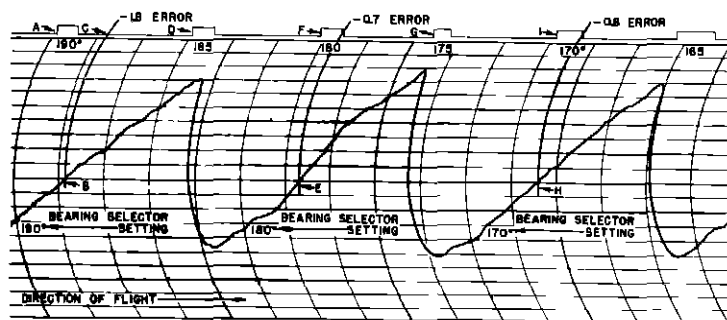
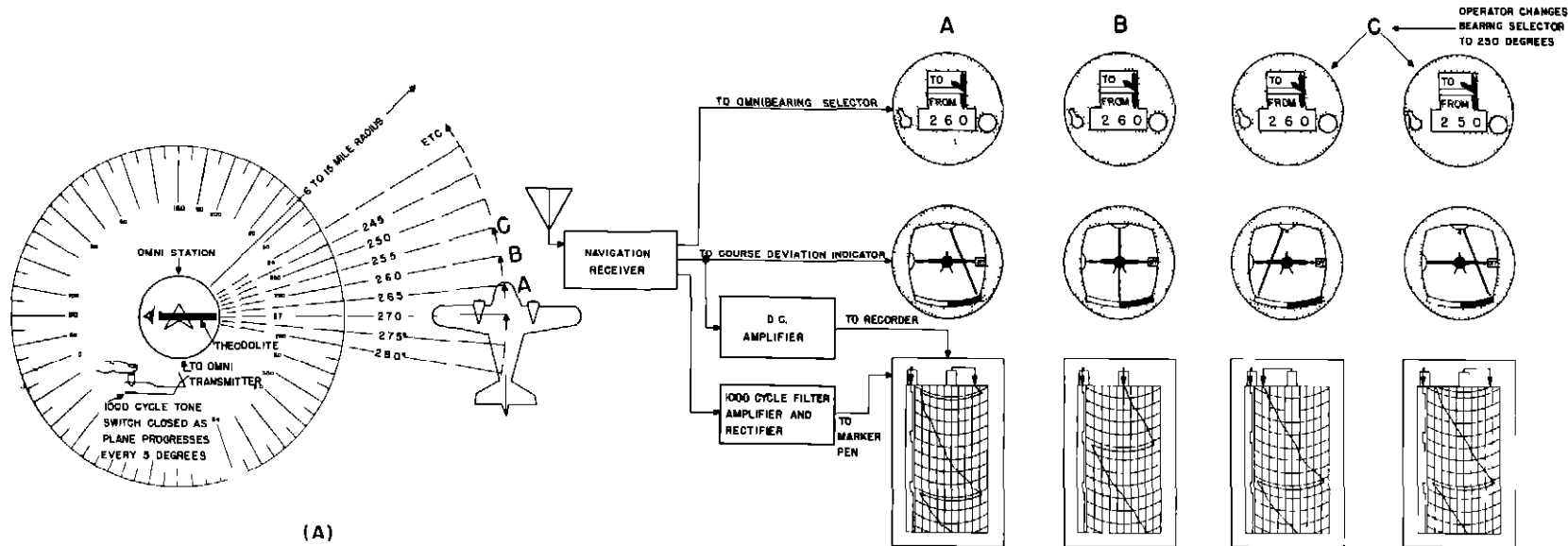


Fig 64 Method Used to Calibrate Omrange Station

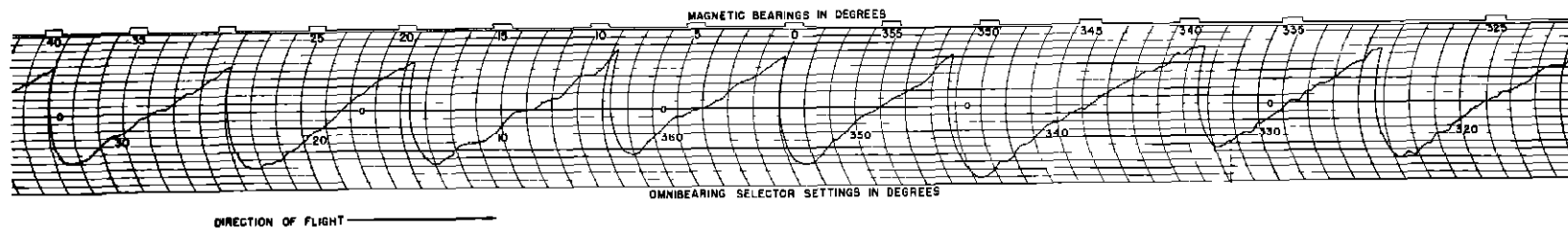
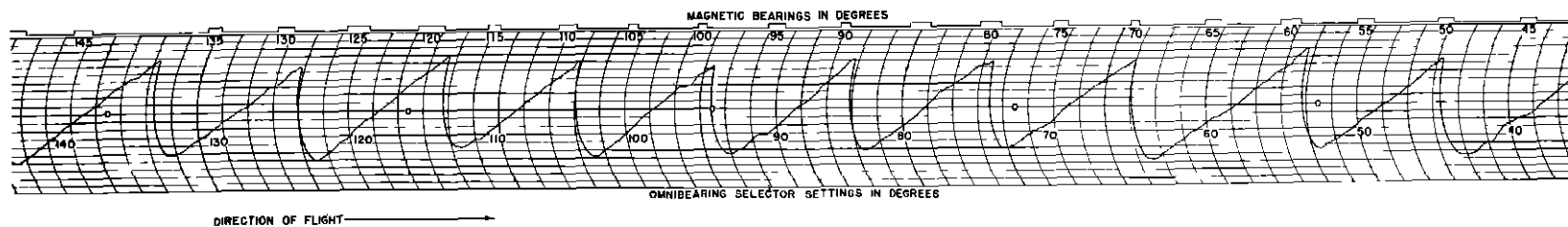
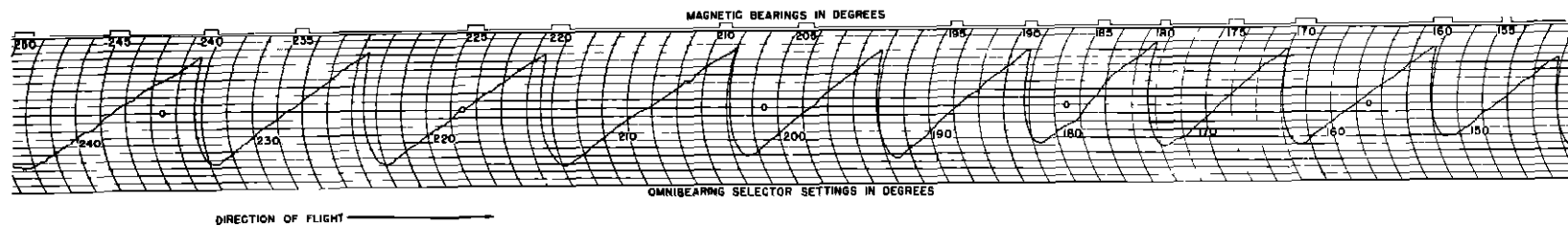
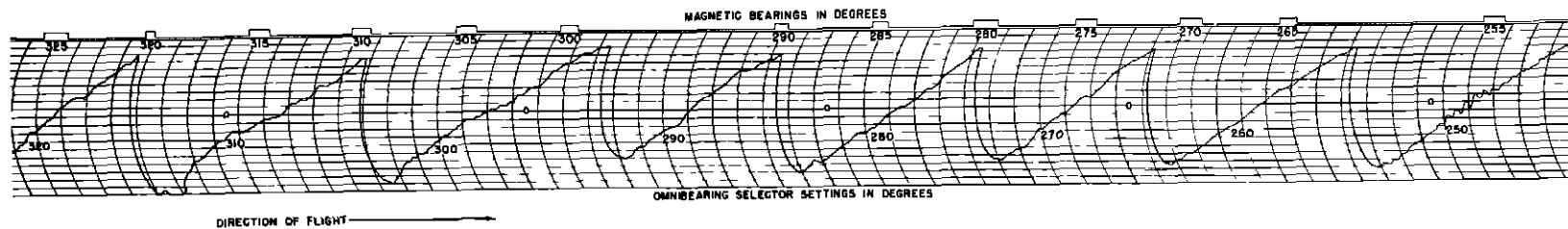


Fig 65 Typical Omnirange Calibration Recording

above the counterpoise to a level $3\frac{1}{4}$ in above the counterpoise. Table II lists the indicated bearings observed when the vertically polarized field was reduced by a factor of approximately four by the use of Uskon cloth.

Another form of polarization error occurs when an aircraft is in a bank or turn. Under these conditions, the indicated omnibearing may change even though its direction from the station is unchanged. This type of polarization error is generally referred to as attitude error. Flight tests made before and after the Uskon cloth was installed showed that the installation of the cloth decreased the attitude errors. Table III lists the maximum errors observed in 360° turns, at a 30° bank, during a flight test in a DC-3 airplane. The tests were conducted at various distances from the station using ARC-15 receiving equipment and the tail V antenna. Table IV shows a comparison of the attitude errors noted when using the tail V antenna and the forward V antenna. These tests also were conducted in a DC-3 airplane using ARC-15 receiving equipment. The Uskon cloth was in place during both tests.

TABLE III

Distance From Station (miles)	Maximum Error	
	With Cloth Installed (degrees)	Without Cloth Installed (degrees)
13.75	± 1.5	± 2.25
23	± 1.75	± 3.4
38	± 2.1	± 3.1

Attitude error at various distances with and without cloth installed

Propeller Modulation

In the early stage of development of the omnirange system, it was observed that aircraft propellers caused modulation of the received signals. The modulation produced by the propellers caused the course deviation indicator to oscillate at an amplitude and rate depending on the amplitude and rate of the propeller modulation. Flight tests were conducted on omnirange systems using 30, 40, and 60 cps for the variable and reference phase signals. It was determined that a frequency of 30 cps would be the most desirable

TABLE IV

Distance From Station (miles)	Maximum Error	
	Tail V Antenna (degrees)	Forward V Antenna (degrees)
13.75	± 1.75	± 2.0
23	± 1.86	± 1.8
38	± 1.75	± 1.25

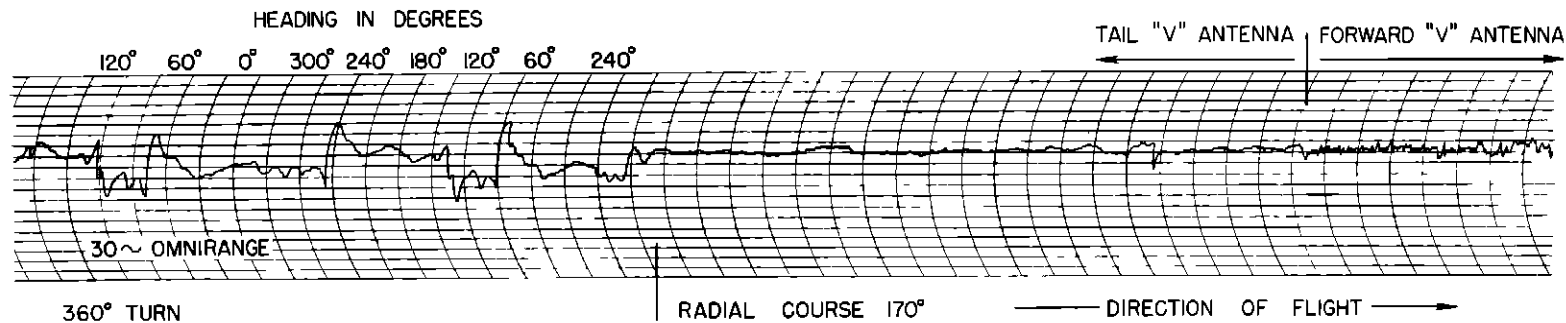
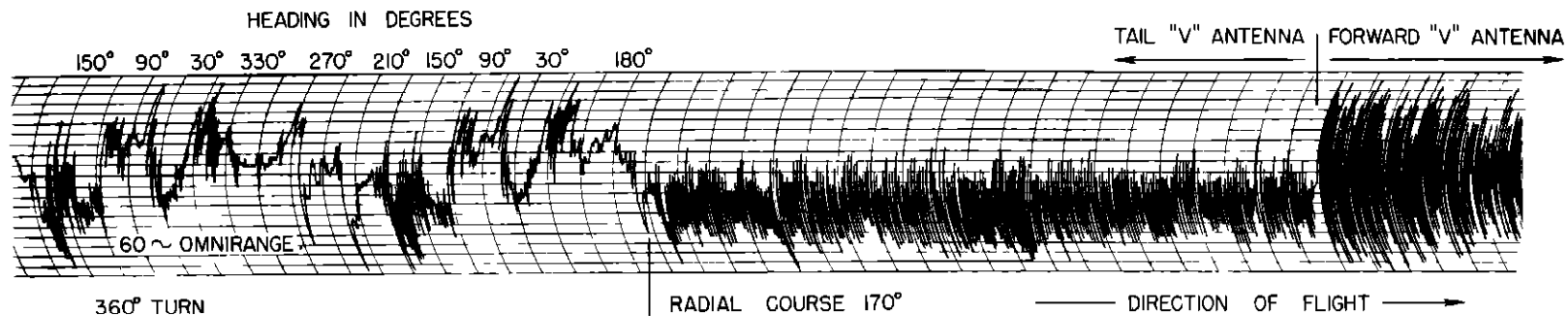
Comparison of attitude errors when using tail V antenna and forward V antenna

since the cruising propeller rpm of all known aircraft produces a propeller modulation frequency higher than 30 cps. Simultaneous flight recordings of omnirange courses using a 30 cps range system and a 60 cps range system are shown in Fig. 66. The engine speed was adjusted to provide a propeller modulation of approximately 60 cps. It will be observed that the 30 cps range is free of variations caused by propeller modulation when using the tail V antenna, and shows only a small variation when using the forward V antenna which is located near the propellers. Recent improvements in navigation receiver design provide further improvement in freedom from propeller modulation effects.

Interference Between Stations

Flight tests have been conducted to determine the interference characteristics existing between omnirange stations operating on the same carrier frequency and on adjacent frequency channels of 100 kc separation. ARC-15 navigation receivers were used for all tests.

To determine the interference area between two omnirange stations operating on the same frequency, the stations at Allentown, Pa., and Raleigh, N. C., separated by 383 miles, were both tuned to 117.5 Mc. The area between the two stations was flown at various altitudes from 12,000 to 20,000 feet and fixes were obtained by means of the MEW radar installation located at the Washington National Airport. The information obtained in the flight tests is shown in Fig. 67. The minimum interference altitude appears to be approximately 14,500 feet since below this level the limiting factor is inadequate signal strength. Above 14,500 feet, the interference area con-



NC-182 (DC-3 / C-47) 2130 RPM BOTH ENGINES
 FLIGHT ALTITUDE 3000 FT - ABSOLUTE
 DISTANCE FROM RANGES - 5 TO 10 MILES

RECEIVER
 30 ~ OMNIRECEIVER NO 7
 LIMITER IN 10 KC REFERENCE CHANNEL
 WEIN BRIDGE IN VARIABLE CHANNEL
 60 ~ OMNIRECEIVER NO 6

ANTENNAS { TAIL "V" COAXIAL TYPE
 { FORWARD "V" DELTA TYPE
 60 ~ OMNITRANSMITTER 125 Mc
 30 ~ OMNITRANSMITTER 114.3 Mc

Fig 66 Comparison of Course Deviation Indicator Fluctuations for 30- and 60-cps Omnitranges

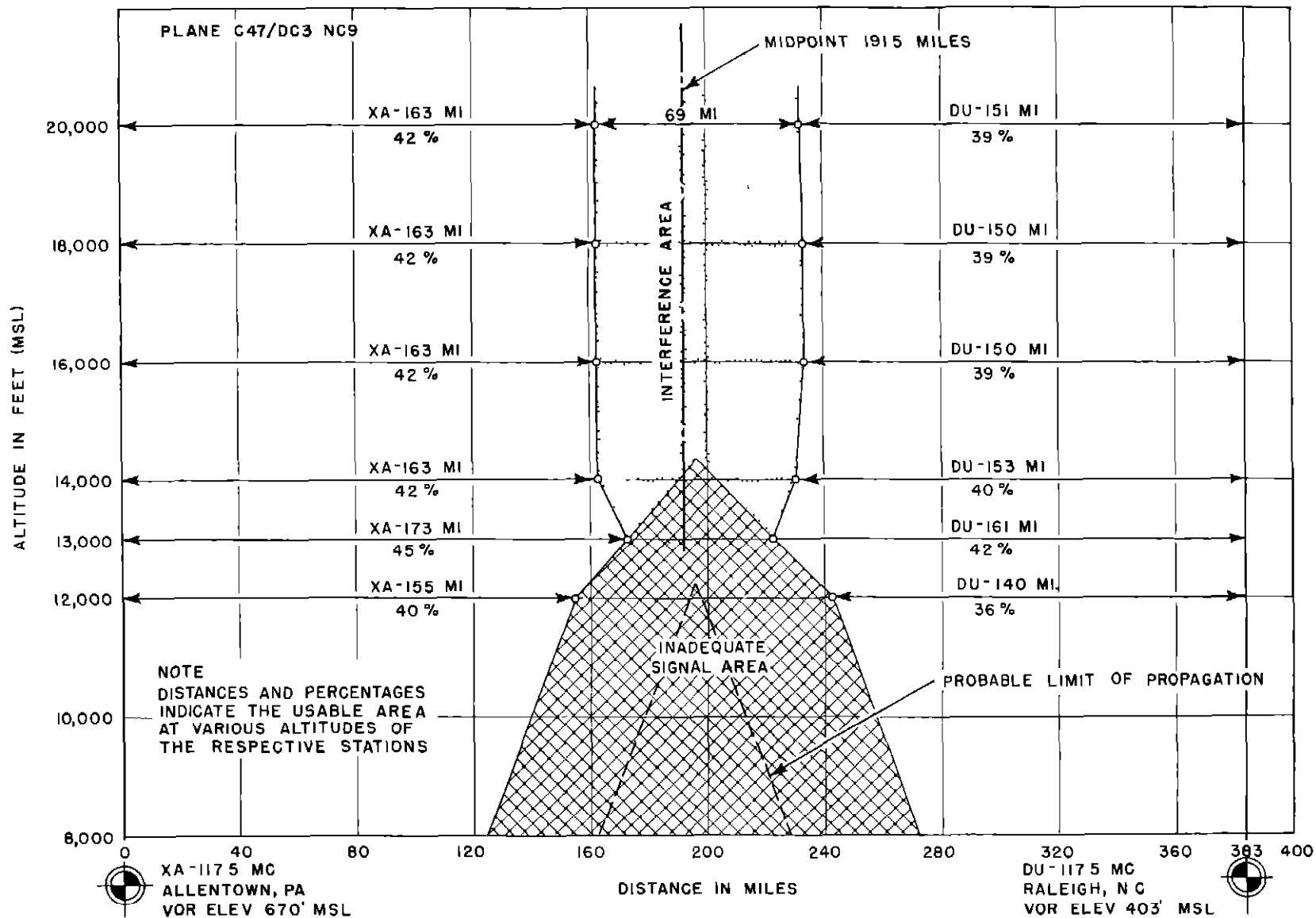


Fig 67 Interference Characteristics of Two Omnirange Facilities Operating on the Same Frequency

sists of a combination of severe audio heterodyning and variations of the course deviation indicator. Summarizing, when two omnirange stations are operated on the same frequency, the useful distance range at high altitudes is approximately 40 per cent of the spacing between the stations.

The investigation of adjacent frequency-channel interference was made using omnirange stations located at Raleigh, N C, and Spartanburg, S C. The Raleigh station was operated on a frequency of 117.4 Mc, and the Spartanburg station on a frequency of 117.5 Mc. The geographical separation was 192 miles. The information obtained in these flight tests, Fig. 68, indicates that from approximately 60 per cent at 6,000 feet to 75 per cent at 13,000 feet of the total distance is usable without interference. In this test it is important to note that the results obtained are dependent to a great extent on the selectivity characteristics of the receiving equipment. The use of an airline type receiver such as the Collins 51R would have provided vastly different results in the usable distance range.

Additional information concerning the co-channel interference problem was obtained by laboratory tests and is shown in Fig. 69. For these tests, simulated omnirange signals from two signal generators were fed to an airline type receiver and the ratio of the rf signal levels was varied. The phase of the variable phase signals were adjusted to cause the greatest interference on the indicators.

Power Frequency Variation

In some remote sections of the country where it may not be possible to obtain a standard commercial source of 60 cps power, it may be necessary to operate the station from local power, or perhaps, to utilize the emergency supply which is standard equipment at all CAA radio range stations. In some cases these sources of power do not maintain a constant frequency of 60 cps, and deviations as much as ± 2 cps may be experienced. At those stations where the power supply frequency variation exceeds ± 0.6 cps, a stabilized 60 cps tuning fork type generator and amplifier will be installed to supply power to the goniometer and subcarrier equipment.

In order to determine the errors caused by power supply frequency variation, a number of tests were conducted in which the goniometer and the subcarrier generator were operated

from a variable frequency power source. The variations in on-course indication were observed on two types of navigation receivers located approximately one-half mile from the station as the frequency of the power source to the goniometer and subcarrier generator was varied from 57 to 63 cps. Fig. 70 presents the maximum errors obtained with two types of receiving equipment under these conditions. Further tests were made by rotating the antenna array through an angle of 360° , in 20° steps for three values of power frequency. The results of these tests are shown in Fig. 71. The large errors shown in Fig. 70 for receiver No. 1 are due to the fact that no provision was made in the design of the 30 cps circuits of the receiver to minimize errors resulting from changes of frequency in the power supply at the range station. The errors observed using receiver No. 2 are appreciably smaller as a result of improved design of the 30 cps circuits.

CONCLUSIONS

As a result of several years of study and development, in addition to four years of operation of omnirange facilities, the following general conclusions have been reached:

- 1 The theoretical aspects of the phase comparison system for omnirange operation are sound.
- 2 Horizontal rather than vertical polarization provides steadier course indications.
- 3 A transmitter power rating of 200 w is adequate for line-of-sight operation to a distance of approximately 200 miles at an altitude of 20,000 feet, 100 miles at 5,000 feet, 63 miles at 2,000 feet, and 45 miles at 1,000 feet.
- 4 An accuracy of approximately $\pm 1.5^\circ$ may be realized on radial courses where the sites are free of serious reflecting objects. The accuracy figure is for the complete omnirange system, receivers, plus ground equipment.
- 5 Sites located on flat terrain with all obstacles such as large buildings, woods, power lines, etc., cleared to 1,000 feet, and all obstacles within 2,000 feet subtending a vertical angle of less than 2° have proven to be satisfactory. Nearby hills, higher than the site, reduce the distance range on radials passing over the hills.
- 6 Generation of sidebands by means of a

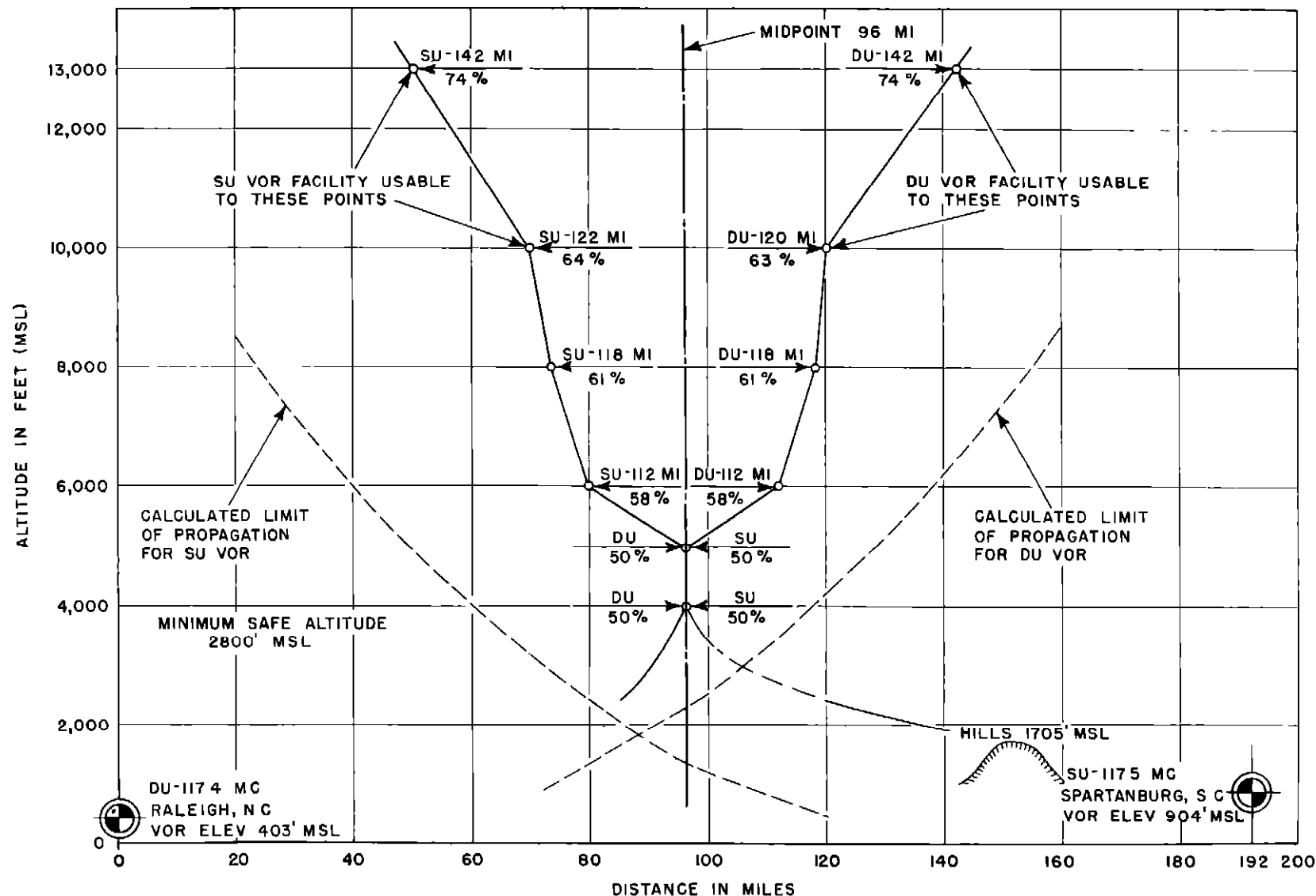


Fig 68 Adjacent Channel Interference Characteristics of Two Omnirange Facilities

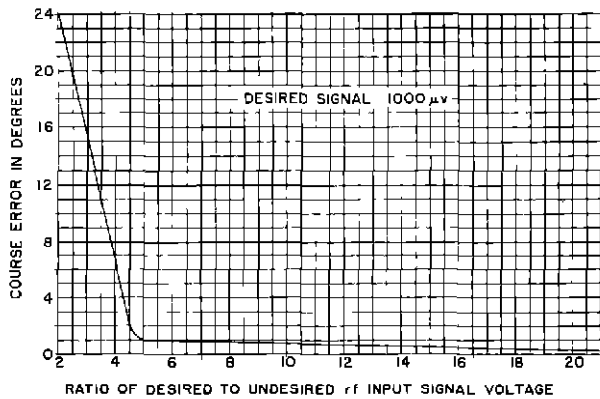


Fig 69 Course Error Versus Ratio of Desired to Undesired Signal Strength

rotating capacity goniometer was found more stable and reliable than methods using electronic sideband generators

7 For unattended operation, a monitor must be included as part of the ground equipment. This provides the maintenance personnel with continuous knowledge as to the status of the facility, and a useful tool for corrective maintenance. The monitor will show up a fault as soon as it occurs, and will further insure that the pilot receives only correct information.

8 Either automatic or manually operated indicating devices may be used to provide the pilot with navigational information. The latter type, however, define the range course more accurately.

9 Modulation factors of 30 per cent each are satisfactory for the reference and variable phase signals and the remaining 40 per cent is adequate for voice modulation and 1,020 cps tone identification.

10 Propeller modulation of received signals interferes with the omnirange courses under certain critical conditions of heading and propeller speed. A reduction in frequency from 60 to 30 cps, for the reference and vari-

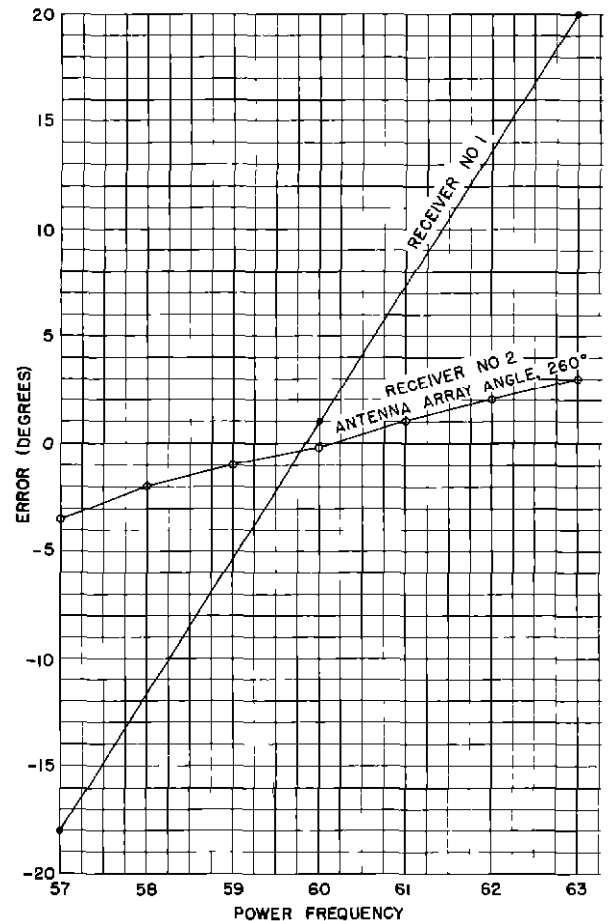


Fig 70 Course Error Versus Power Frequency

able phase signals, has minimized this interference.

As a result of this development and operational experience, the VHF omnirange has been adopted as one of the basic elements of the Common Civil-Military System, Transition Program, as recommended by the Radio Technical Commission for Aeronautics, Special Committee 31.

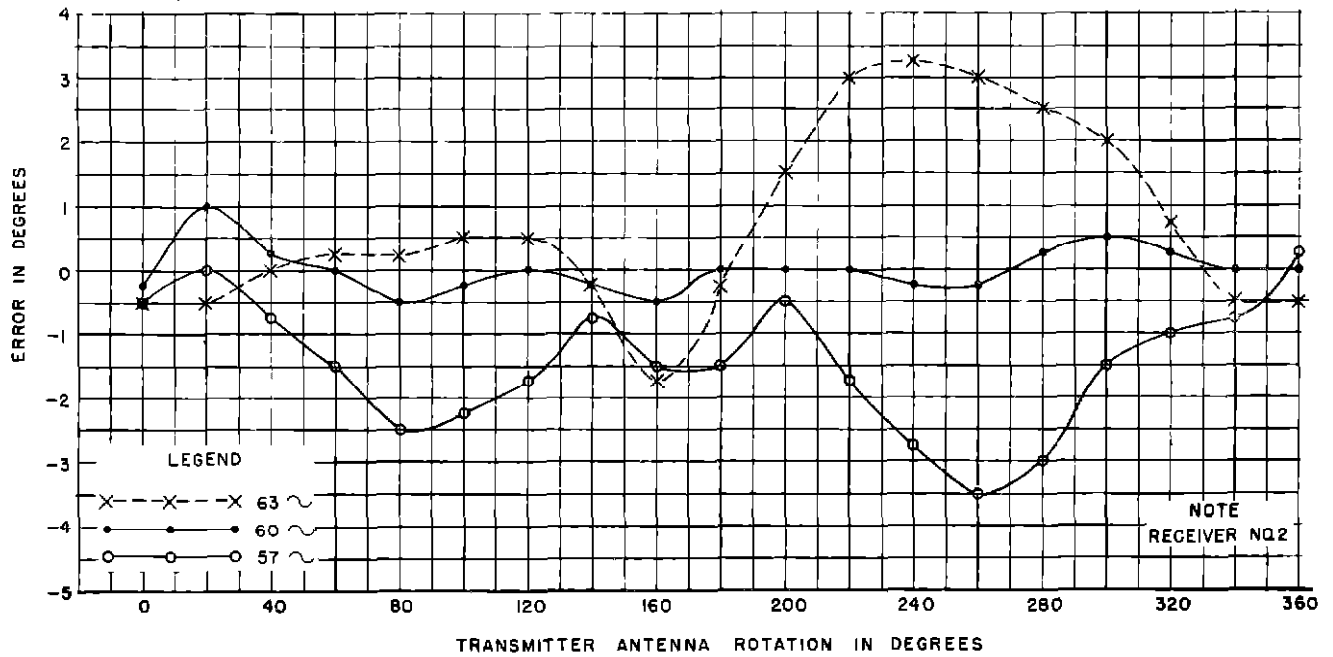


Fig 71 Calibration Error Curve Versus Power Frequency